EVALUATING THE MECHANISM OF OXALATE SYNTHESIS OF *FIBROPORIA RADICULOSA* ISOLATES ADAPTING TO COPPER-TOLERANCE

By

Katie Marie Jenkins

A Thesis
Submitted to the Faculty of
Mississippi State University
in Partial Fulfillment of the Requirements
for the Degree of Master of Science
in Forest Products
in the Department of Forest Products

Mississippi State, Mississippi

May 2012

EVALUATING THE MECHANISM OF OXALATE SYNTHESIS OF *FIBROPORIA RADICULOSA* ISOLATES ADAPTING TO COPPER-TOLERANCE

By

Katie Marie Jenkins

Approved:

Susan V. Diehl Professor Department of Forest Products (Director of Thesis)	M. Lynn Prewitt Assistant Research Professor Department of Forest Products (Committee Member)
Carol A. Clausen Adjunct Faculty Department of Forest Products Forest Products Laboratory Project Leader Durability and Wood Protection (Committee Member)	Kenneth O. Willeford Professor Department of Biochemistry, Molecular Biology, Entomology, and Plant Pathology (Committee Member)
Fredrick Green III Adjunct Faculty Department of Forest Products Forest Products Laboratory Microbiologist Durability and Wood Protection (Committee Member)	Tor P. Schultz Professor Department of Forest Products (Graduate Coordinator)
Rubin Shmulsky Department Head Department of Forest Products	George Hopper Dean College of Forest Resources

Name: Katie Marie Jenkins

Date of Degree: May 11, 2012

Institution: Mississippi State University

Major Field: Forest Products

Major Professor: Dr. Susan V. Diehl

Title of Study: EVALUATING THE MECHANISM OF OXALATE SYNTHESIS OF *FIBROPORIA RADICULOSA* ISOLATES ADAPTING TO COPPER-TOLERANCE

Pages in Study: 146

Candidate for Degree of Master of Science

Despite the drawbacks associated with tolerant organisms, copper is still used as the key component in current wood preservatives. Copper-tolerant fungi, like *Fibroporia radiculosa*, produce and accumulate high levels of oxalate in response to copper. The biosynthesis of oxalate has been connected to specific enzymes in the glyoxylate and tricarboxylic acid cycles. To gain insight on the mechanism of oxalate production, four *F. radiculosa* isolates undergoing decay of untreated and 1.2% ammoniacal copper citrate treated wood were evaluated for the differential expression of citrate synthase (CS), isocitrate lyase (ICL), glyoxylate dehydrogenase (GLOXDH), succinate/fumarate antiporter (ANTI), and a copper resistance-associated ATPase pump (ATPase). Samples were measured at 2, 4, 6, and 8 weeks and analyzed for oxalate and protein production, enzyme activities, and gene expression via RNA. ATPase pump expression was increased in the presence of copper, suggesting it functions in helping the fungus adapt to the copper-rich environment by pumping toxic copper ions out of the cell. When initial oxalate concentrations were low, ATPase expression was at its highest. As oxalate levels

increased ATPase pump activity decreased, suggesting that oxalate is binding the copper and rendering it immobile. Thus, there are fewer free copper ions moving into the cell and less need for ATPase expression. These results also found a connection in expression levels between CS, ANTI, ICL, and GLOXDH for the four isolates. This suggests the production of oxalate originates in the mictochondrial TCA cycle (CS), shunts to the glyoxysomal glyoxylate cycle (ANTI), moves through a portion of the glyoxylate cycle (ICL), and ultimately is made in the cytoplasm (GLOXDH).

DEDICATION

This research is dedicated to both of my grandfathers.

In loving memory of
Roland "Buddy" Jenkins,
October 13, 2005.

and

Joseph Lloyd Becnel, Sr.,
October 7, 2011.

ACKNOWLEDGEMENTS

The author wishes to extend her sincere gratitude to the numerous people who offered their support throughout the course of this study. I would like to personally thank Dr. Susan Diehl for her guidance, mentoring, and assistance in all aspects of my research. Expressed gratitude is given to Carol Clausen and Rick Green at the Forest Products Laboratory for their invaluable knowledge, guidance, and support over the course of this study. Special thanks are due to Dr. David Jones, Dr. Ken Willeford, Dr. Lynn Prewitt, and Amy Blodgett for their expertise, encouragement, and technical assistance. The undergraduate student workers, Mary Kate Mohammadi and Sarah Trautman, made invaluable contribution to the completion of this research. Finally, the author would like to thank Juliet Tang for her advice, expertise, and willingness to offer assistance, which provided immense value throughout the course of this study.

TABLE OF CONTENTS

Page

DEDICATION ii

ACKNOWLEDGEMENTS iii

LIST OF TABLES vii

LIST OF FIGURES x

I. LITERATURE REVIEW 1

Chemical and Physical Structure of Wood 1
Wood Biodeterioration 4
White-rot Decay 5
Brown-rot Decay 7
Copper-based Preservatives 9
Copper Tolerance 15
Significance of Oxalate 19
Role of Oxalate 20
Biosynthesis of Oxalate 22
Objectives of Research 25

II. MATERIALS AND METHODS 27

Preliminary Study One: Sequencing Analysis 27
Fungal Isolates 27
Media Preparation 27
DNA Extraction 27
PCR and Gel Electrophoresis 28
PCR Clean Up 29
Sequence Analysis 29
Preliminary Study Two: Oxalate Screening Analysis 30
Fungal Isolates 30
Test Wafer Preparation and Preservative Treatment 30
Decay Test 31
Decay Chamber Setup 31
Inoculation of Feeder Strips and Incubation 31

Sample Preparation 32
Oxalate Assay 32
Protein Assay 33
Evaluating the Role of Oxalate: Enzyme Analysis 33
Fungal Isolates 33
Test Wafer Preparation and Preservative Treatment 33
Decay Test 34
Decay Chamber Setup 34
Inoculation of Feeder Strips and Incubation 34
Sample Preparation 35
Oxalate Assay 35
Enzyme Assays 36
Fumarase Assay 36
Glyoxylate Dehydrogenase Assay 37
Isocitrate Lyase Assay 37
Malate Synthase Assay 37
Oxaloacetase Assay 37
Protein Assay 38
Evaluating the Role of Oxalate: Enzyme Gene Expression 38
RNA Extraction 38
cDNA Synthesis 39
Bio-Rad iQ iScript 39
Invitrogen SuperScript II Reverse Transcriptase 40
Primer Design 41
Real-Time qPCR 42
Evaluating the Role of Oxalate: The Effects of Copper Availability 43
Fungal Isolates 43
Test Block Preparation and Preservative Treatment 43
Decay Test 43
Decay Chamber Setup 43
Inoculation of Feeder Strips and Incubation 44
Sample Preparation 45
Oxalate Assay 45
Weight Loss 46

III. RESULTS AND DISCUSSION 47

Preliminary Study One: Sequencing Analysis Results 47
Sequence Analysis 47
Preliminary Study Two: Oxalate Screening Analysis 49
Oxalate Assay 49
Protein Assay 52
Evaluating the Role of Oxalate: Enzyme Analysis Results 54
Oxalate Assay 55
Protein Assay 61
Enzyme Assay 66

Evaluating the Role of Oxalate: Enzyme Gene Expression Results 74
RNA Quantification 74
cDNA Synthesis and Primer Design 76
Bio-Rad iQ iScript 76
Invitrogen SuperScript II Reverse Transcriptase 77
Expression Levels 79
Evaluating the Role of Oxalate: The Effects of Copper Availability 92
Oxalate Assay 92
Weight Loss 100

IV. CONCLUSIONS 108

REFERENCES 114

APPENDIX 120

LIST OF TABLES

TABLE		Page
Table 1.1	Copper-based Wood Preservatives.	13
Table 1.2	Intended Application for Copper-based Preservatives.	14
Table 1.3	Enzymes of the TCA and GLOX cycles thought to be involved in oxalate biosynthesis (Munir *et al.* 2001).	24
Table 2.1	Target gene, nucleotide sequence, and reference gene accession number for all oligonucleotide primers used for gene expression.	41
Table 3.1	Statistical (ANOVA) analysis of significant variation in oxalate production with respect to time. A, B, C, and D are all significantly different from each other.	56
Table 3.2	Statistical (ANOVA) analysis of significant variation in oxalate production with respect to isolate. A is significantly different than B.	58
Table 3.3	Statistical (ANOVA) analysis of significant variation in oxalate production with respect to treatment. A is significantly different than B.	59
Table 3.4	Statistical (ANOVA) analysis of significant variation in protein production with respect to time. A is significantly different than B.	62
Table 3.5	Statistical (ANOVA) analysis of significant variation in protein production with respect to isolate.	63
Table 3.6	Statistical (ANOVA) analysis of significant variation in oxalate production with respect to treatment. A is significantly different than B.	64
Table 3.7	Isocitrate lyase activity (IU/mg) of copper citrate treated and untreated test wafers exposed to L-11659-SP, FP-90848-T, TFFH 294, and L-9414-SP at weeks 2, 4, 6, and 8. ε = 16,800 $M^{-1}cm^{-1}$. Assay volume = 0.2 mL; enzyme volume = 0.01 mL.	67

Table 3.8 Glyoxylate dehydrogenase activity (IU/mg) of copper citrate treated and untreated test wafers exposed to L-11659-SP, FP-90848-T, TFFH 294, and L-9414-SP at weeks 2, 4, 6, and 8. ε = 19,600 $M^{-1}cm^{-1}$. Assay volume = 0.2 mL; enzyme volume = 0.01 mL. 69

Table 3.9 Statistical (ANOVA) analysis of significant variation in specific activity with respect to enzyme. A difference of 0.0564 between mean values indicates the minimum significant difference. 70

Table 3.10 Statistical (ANOVA) analysis of significant variation in specific activity with respect to time. A difference of 0.1049 between mean values indicates the minimum significant difference. 71

Table 3.11 Statistical (ANOVA) analysis of significant variation in specific activity with respect to isolate. A difference of 0.1048 between mean values indicates the minimum significant difference 71

Table 3.12 Statistical (ANOVA) analysis of significant variation in specific activity with respect to treatment. A difference of 0.057 between mean values indicates the minimum significant difference. 72

Table 3.13 Statistical (ANOVA) analysis of significant variation in oxalate production with respect to treatment. A is significantly different than B. 97

Table 3.14 Statistical (ANOVA) analysis of significant variation in oxalate production with respect to isolate. A difference of 0.0488 between mean values indicates the minimum significant difference.....97

Table 3.15 Statistical (ANOVA) analysis of significant variation in oxalate production with respect to time. A difference of 0.0489 between mean values indicates the minimum significant difference. 98

Table 3.16 Statistical (ANOVA) analysis of significant variation between treatments with respect to % weight loss. 104

Table 3.17 Statistical (ANOVA) analysis of significant variation in % weight loss with respect to isolate. A difference of 1.2703 between mean values indicates the minimum significant difference....105

Table 3.18 Statistical (ANOVA) analysis of significant variation in % weight loss with respect to time. A difference of 1.2731 between mean values indicates the minimum significant difference 105

Table A.1 Analysis of gene expression for ICL. Data analyzed by the comparative C_T method (Livak and Schmittgen 2001). 122

Table A.2 Analysis of gene expression for GLOXDH. Data analyzed by the comparative C_T method (Livak and Schmittgen 2001) 123

Table A.3 Analysis of gene expression for CS. Data analyzed by the comparative C_T method (Livak and Schmittgen 2001) 124

Table A.4 Analysis of gene expression for ANTI. Data analyzed by the comparative C_T method (Livak and Schmittgen 2001) 125

Table A.5 Analysis of gene expression for ATPase. Data analyzed by the comparative C_T method (Livak and Schmittgen 2001) 126

LIST OF FIGURES

FIGURE Page

Figure 1.1 Enzyme/ Enzyme pathways which may be utilized in some fungi to produce oxalate; [1-12] corresponding enzymes listed in Table 1.3. (A) the TCA cycle; (B) the GLOX cycle (Munir *et al.* 2001).....24

Figure 2.1 Decay chamber set-up including feeder strips and test wafers exposed to isolate, L-11659-SP.....32

Figure 2.2 Test wafers exposed to isolate, L-9414-SP, in an AWPA standard decay chamber 35

Figure 2.3 Variations on copper citrate (CC) – treated test blocks exposed to *F. radiculosa*. Bottle 1: untreated SYP; Bottle 2: CC treated SYP; Bottle 3: CC treated SYP on top of untreated SYP; Bottle 4: liquid CC on top of untreated SYP; Bottle 5: CC treated SYP adjacent to and in direct contact with untreated SYP. 45

Figure 3.1 Sequence distances based on percent identity and divergence of the fifteen *F. radiculosa* isolates. 48

Figure 3.2 Phylogenetic tree of *F. radiculosa* isolates based on sequence distances (nucleotide substitutions).....48

Figure 3.3 Oxalate concentration values (mg/mL) of fifteen *Fibroporia radiculosa* isolates exposed to amine copper (CA) and micronized copper quaternary (MCQ) test wafers for 2 and 4 weeks. 50

Figure 3.4 Protein concentration values (mg/mL) of fifteen *Fibroporia radiculosa* isolates exposed to amine copper (CA) and micronized copper quaternary (MCQ) test wafers for 2 and 4 weeks 52

Figure 3.5 Oxalate concentration values (mg/mL) of L-11659-SP (green), FP-90848-T (blue), TFFH 294 (red), and L-9414-SP (purple) exposed to copper citrate (CC) and untreated (UN) test wafers for 2, 4, 6, and 8 weeks. 55

Figure 3.6 Oxalate concentration values (mg/mL) for 2 weeks (green), 4 weeks (blue), 6 weeks (red) and 8 weeks (purple) for isolates L-11659-SP, FP-90848-T, TFFH 294, and L-9414-SP exposed to copper citrate (CC) and untreated (UN) test wafers. 57

Figure 3.7 Oxalate concentration values (mg/mL) of copper citrate treated and untreated test wafers exposed to L-11659-SP (green), FP-90848-T (blue), TFFH 294 (red), and L-9414-SP (purple) for weeks 2, 4, 6, and 8. 58

Figure 3.8 Protein concentration values (mg/mL) of L-11659-SP (green), FP-90848-T (blue), TFFH 294 (red), and L-9414-SP (purple) exposed to copper citrate (CC) and untreated (UN) test wafers for 2, 4, 6, and 8 weeks. 61

Figure 3.9 Protein concentration values (mg/mL) for 2 weeks (green), 4 weeks (blue), 6 weeks (red) and 8 weeks (purple) for isolates L-11659-SP, FP-90848-T, TFFH 294, and L-9414-SP exposed to copper citrate (CC) and untreated (UN) test wafers. 63

Figure 3.10 Protein concentration values (mg/mL) of copper citrate treated and untreated test wafers exposed to L-11659-SP (green), FP-90848-T (blue), TFFH 294 (red), and L-9414-SP (purple) for weeks 2, 4, 6, and 8. 64

Figure 3.11 Gel image of extracted RNA for gene expression analysis: Ladders are designated L; (A) wells are 1, rat brain RNA; 2 – 9, L-11659-SP w2-8; 10 – 12, FP-90848-T w2-4; CC treatment even wells; UN treatment odd wells; (B) wells are 1, rat brain RNA; 2 – 6, FP-90848-T w4-8; 7 – 12, L-9414-SP w2-6; UN treatment even wells, CC treatment odd wells; (C) wells are 1, rat brain RNA; 2 – 3, L-9414-SP w8; 4 – 11, TFFH 294 w2-8; CC treatment even wells; UN treatment odd wells; (D) wells are 1, L-11659-SP CC w2; 2 – 8, L-9414-SP w4-8 UN even wells, CC odd wells; 9 – 12, TFFH 294 UN wk2-8. 75

Figure 3.12 Gel image of the Bio-Rad iScript™ cDNA Synthesis protocol. Ladders are on the outer lanes. The four samples were amplified for all target regions; L-11659-SP, FP-90848-T, TFFH 294, and L-11659. Bottom row lanes: 1 – 4, 18S; 5 – 8, ICL; 9 – 12, GLOXDH. Top row lanes: 1 – 4, CS; 5 – 8, ANTI; 9-12, ATPase. 77

Figure 3.13 Gel image of the Invitrogen™ SuperScript™ II Reverse Transcriptase protocol. Ladders are on the outer lanes. The four samples were amplified for all target regions; L-11659-SP, FP-90848-T, TFFH 294, and L-11659. From left to right lanes: 1 – 4, 18S; 5 – 8, GLOXDH; 9 – 12, CS; 13 – 16, ANTI; 17 – 20, ATPase. Lane 21 is the non-template control (no band). 78

Figure 3.14 Isocitrate lyase expression levels of L-11659-SP (green), FP-90848-T (blue), TFFH 294 (red), and L-9414-SP (purple) exposed to copper citrate (CC) and untreated (UN) test wafers for 2, 4, 6, and 8 weeks. 80

Figure 3.15 Isocitrate lyase expression levels of L-11659-SP (green), FP-90848-T (blue), TFFH 294 (red), and L-9414-SP (purple) exposed to copper citrate (CC) and untreated (UN) test wafers for 2, 4, 6, and 8 weeks. 81

Figure 3.16 Glyoxylate dehydrogenase expression levels of L-11659-SP (green), FP-90848-T (blue), TFFH 294 (red), and L-9414-SP (purple) exposed to copper citrate (CC) and untreated (UN) test wafers for 2, 4, 6, and 8 weeks. 82

Figure 3.17 Glyoxylate dehydrogenase expression levels for 2 weeks (green), 4 weeks (blue), 6 weeks (red) and 8 weeks (purple) for isolates L-11659-SP, FP-90848-T, TFFH 294, and L-9414-SP exposed to copper citrate (CC) and untreated (UN) test wafers..... 83

Figure 3.18 Citrate synthase expression levels of L-11659-SP (green), FP-90848-T (blue), TFFH 294 (red), and L-9414-SP (purple) exposed to copper citrate (CC) and untreated (UN) test wafers for 2, 4, 6, and 8 weeks. 84

Figure 3.19 Citrate synthase expression levels for 2 weeks (green), 4 weeks (blue), 6 weeks (red) and 8 weeks (purple) for isolates L-11659-SP, FP-90848-T, TFFH 294, and L-9414-SP exposed to copper citrate (CC) and untreated (UN) test wafers..... 85

Figure 3.20 Antiporter expression levels of L-11659-SP (green), FP-90848-T (blue), TFFH 294 (red), and L-9414-SP (purple) exposed to copper citrate (CC) and untreated (UN) test wafers for 2, 4, 6, and 8 weeks. 86

Figure 3.21 Antiporter expression levels for 2 weeks (green), 4 weeks (blue), 6 weeks (red) and 8 weeks (purple) for isolates L-11659-SP, FP-90848-T, TFFH 294, and L-9414-SP exposed to copper citrate (CC) and untreated (UN) test wafers..... 87

Figure 3.22 ATPase pump expression levels of L-11659-SP (green), FP-90848-T (blue), TFFH 294 (red), and L-9414-SP (purple) exposed to copper citrate (CC) and untreated (UN) test wafers for 2, 4, 6, and 8 weeks. 88

Figure 3.23 ATPase pump expression levels for 2 weeks (green), 4 weeks (blue), 6 weeks (red) and 8 weeks (purple) for isolates L-11659-SP, FP-90848-T, TFFH 294, and L-9414-SP exposed to copper citrate (CC) and untreated (UN) test wafers.....89

Figure 3.24 Genes up-regulated in early decay; genes are in red. (A) TCA cycle; (B) GLOX cycle. Green box indicates TCA cycle in the mitochondria; orange box indicates GLOX cycle in the glyoxysome (Tang 2011). 90

Figure 3.25 Oxalate concentration values (mg/mL) of L-11659-SP exposed to UN (green), CC (blue), ST (red), LIQ (purple), and RP (orange) SYP blocks with respect to time.....93

Figure 3.26 Oxalate concentration values (mg/mL) of FP-90848-T exposed to UN (green), CC (blue), ST (red), LIQ (purple), and RP (orange) SYP blocks with respect to time. 94

Figure 3.27 Oxalate concentration values (mg/mL) of TFFH 294 exposed to UN (green), CC (blue), ST (red), LIQ (purple), and RP (orange) SYP blocks with respect to time. 95

Figure 3.28 Oxalate concentration values (mg/mL) of L-9414-SP exposed to UN (green), CC (blue), ST (red), LIQ (purple), and RP (orange) SYP blocks with respect to time. 96

Figure 3.29 Weight loss percentages of L-11659-SP exposed to UN (green), CC (blue), ST (red), LIQ (purple), and RP (orange) SYP blocks with respect to time. 100

Figure 3.30 Weight loss percentages of FP-90848-T exposed to UN (green), CC (blue), ST (red), LIQ (purple), and RP (orange) SYP blocks with respect to time. 101

Figure 3.31 Weight loss percentages of TFFH 294 exposed to UN (green), CC (blue), ST (red), LIQ (purple), and RP (orange) SYP blocks with respect to time. 102

Figure 3.32 Weight loss percentages of L-9414-SP exposed to UN (green), CC (blue), ST (red), LIQ (purple), and RP (orange) SYP blocks with respect to time. 103

Figure A.1 Sequence distances based on percent identity and divergence of the four *F. radiculosa* isolates. 121

Figure A.2 Phylogenetic tree of four *F. radiculosa* isolates based on sequence distances (nucleotide substitutions). 121

CHAPTER I

LITERATURE REVIEW

Chemical and Physical Structure of Wood

The chemical and physical structure of wood is a key component in the intricate process of wood degradation by microbial organisms. Wood has two basic domains: the void space and the woody cell wall. The void space, or lumen, helps to conduct water, while the cell wall establishes the environment within the cell (Wiedenhoeft 2010). The cell wall is composed of various layers: the middle lamella, the primary cell wall, and the secondary cell wall. Also within the cell wall, there are both primary and secondary components. The primary structural components, constituting the bulk of the cell wall, establish the chemical and physical nature of the cell wall. The secondary non-structural components give various characteristics to the wood (Panshin and deZeeuw 1980). Each of the structural and chemical components is essential to the structural utility of wood products in use today.

Primary or chemical components of the wood cell wall consist of 40-50 % cellulose, 20-35 % hemicelluloses, and 15-35 % lignin; each varying slightly based on wood species (Panshin and deZeeuw 1980). Cellulose functions as the main structural component providing strength in the cell wall and can exist as a primary and/or secondary structure. The primary structure consists of a generally linear, un-branched chain of β-

glucopyranose residues (5-7 μm) connected via a 1,4-β-glycosidic bond with every second residue rotated 180° forming a cellobiose (1.03 nm) residue. The secondary structure consists of long narrow sheets bundling together to form a crystalline structure (40 μm) with regions of ordered fibrils and semi-ordered fibrils (Henriksson 2009). Hemicellulose exists as mixtures of xylans or glucomannans in the cell wall based on the species of the wood. It helps form the structural integrity of the cell wall by closely associating with cellulose and binding the fibrils to lignin (Teleman 2009). Lignin exists as a three-dimensional matrix polymerized from varying percentages of three monomers: p-coumaryl alcohol, coniferyl alcohol, and/or sinapyl alcohol, based on wood species. Generally, lignin functions to provide rigidity to the cell wall, join cell wall components together, and make the cell wall hydrophobic (Henriksson 2009). In general, all layers of the cell wall are composed of cellulose fibrils surrounded by hemicellulose molecules organized in a ribbon-like structure, with lignin inhabiting the left over vacant spaces (Pereira *et al.* 2003).

Secondary cell wall components have no influence on structural associations in the wood. Instead, these components play a role in providing the wood with particular characteristics, like biological resistance, color, and odor (Panshin and deZeeuw 1980). These secondary components represent a very small portion of the wood and are typically found in very low quantities within a species. However, even in such low quantities, it is possible for these components to exist in a wide variety of different molecules (Pereira *et al.* 2003). Usually, these components consist of extraneous material, or extractives, and ash (Panshin and deZeeuw 1980). Extractives represent a wide range of organic compounds like, terpenoids, phenolic constituents, fats, and waxes. Terpenoids, derived

from isoprene (C_5H_8) units, consist of monoterpenoids (2 isoprene units), sesquiterpenoids (3 isoprene units), diterpenoids (4 isoprene units), triterpenoids (6 isoprene units), steroids, and polyterpenoids (> 8 isoprene units). Terpenoids are found in the resin of softwoods and exist in all forms; however, in hardwoods, only the higher terpenoids are found (Pereira *et al.* 2003; Sjöström 1993). The most common phenolic constituents are stilbenes, lignans, hydrolysable and condensed tannins, and flavonoids, and are commonly located in the heartwood and bark. These phenolic compounds contribute to protect the wood from microbial and fungicial attack (Sjöström 1993). Fats (esters of glycerol with long-chain fatty acids) and waxes (esters of long-chain alkanols with fatty acids) exist in small quantities and affect the permeability of the wood (Pereira *et al.* 2003). Inorganic components, like ash, make up approximately one percent of the dry weight and consist of various metals like, calcium, potassium, and magnesium, and metal salts such as, carbonates, silicates, and phosphates (Sjöström 1993). Additionally, the presence of secondary cell wall components is also related to permeability and certain physical properties, like specific gravity, hardness, and strength (Panshin and deZeeuw 1980).

The distribution, orientation, and proportion of chemical components largely vary for each of the wood cell wall layers. The primary function of the middle lamella is to join neighboring cells together. Because of this, the middle lamella is composed mostly of lignin, which allows adherence of these neighboring cells. The primary cell wall, usually undistinguishable from the middle lamella, is a thin layer characterized by a random, unorganized arrangement of cellulose fibrils. It has high lignin concentrations and low cellulose concentrations (Pereira *et al.* 2003). The secondary cell wall (high in

cellulose concentrations) is composed of three layers: S1, S2, and S3, and are distinguished by the change in cellulose fibril angles. The thin S1 layer cellulose fibrils are laid relatively horizontally (50°-70°). Cellulose fibrils in the thick S2 layer are almost perpendicular (5°-30°) to that of the S1 layer. The S2 layer, because of its thickness and fibril orientation, has the greatest affect on the strength properties of the wood. The S3 cellulose fibrils are oriented similar to the S1 layer (> 70°). Because of the "Z" orientation of cellulose fibrils within the S1, S2, and S3 layers, the secondary cell wall is largely responsible for the strength properties of wood (Panshin and deZeeuw 1980; Sjöström 1993; Wiedenhoeft 2010).

Wood Biodeterioration

Decay can be defined as the deterioration of the wood cell wall by some biological manner, resulting in a loss of strength properties. Wood is easily susceptible to a variety of biological agents because of its porous-like nature. Certain biological agents like, bacteria, fungi, insects, and mold have the potential to cause severe deterioration of various wood-based materials. One of the most detrimental organisms causing wood deterioration are the decay fungi because they can initiate severe cell degradation by consuming the structural materials within wood. When attacked by decay fungi, the wood results in a loss of physical and mechanical properties brought upon by a softening or weakening of the wood itself. Fungal growth depends on a variety of factors: a food source (breakdown of cell wall components), water (wood fiber saturation point above

30%), favorable temperature (between 20-32 °C), sufficient oxygen, and an acidic environment (pH: 2-6) (Shmulsky and Jones 2011; Clausen 2010).

Fungal decay can be classified into two major types: brown-rot and white-rot. Typically, brown-rot and white-rot fungi belong to the Basidiomycota family. Both brown-rot and white-rot fungi attack wood cells via hyphael growth through bordered pits and secrete enzymatic and non-enzymatic metabolites to obtain nutrients from the wood cell walls. Brown-rot fungi commonly attack coniferous (softwood) species, while white-rot fungi are more common to the hardwood species. These two types of decay fungi breakdown and utilize wood components by two uniquely different mechanisms. Brown-rot fungi have both enzymatic and non-enzymatic mechanisms to remove the cellulose and hemicellulose components leaving the wood a dry, crumbly, powdery, lignin-rich brown mass. White-rot fungi can uniformly or selectively remove the lignin, cellulose, and hemicellulose leaving the wood in a bleached, stringy, spongy mass. The white-rot fungi can have both cellulolytic and lignin-degrading enzymes while the brown-rot fungi only posses the cellulolytic enzymes (Goodell *et al.* 2008). Both brown-rot and white rot organisms reduce the pH of the wood during colonization and incipient decay, but it has been shown that brown-rot organisms can drive the pH lower than the white-rot organisms can (Green *et al.* 1991; Goodell 2003).

White-rot Decay

White-rot fungi are one of the few organisms to cause complete degradation of the wood structure and all wood cell wall components (Nilsson 2009). Wood decay by white-rot fungi is extremely variable and can be classified by the way cell wall components that are broken down. White-rot organisms utilize a simultaneous (non-

selective) decay mechanism to breakdown cellulose, hemicellulose, and lignin at a uniform rate within the wood. This type of decay starts by the erosion of the lumen followed by extensive degradation of all cell wall components then finally degradation of the middle lamella (Messner *et al.* 2003). Selective decay breaks down hemicellulose and lignin and leaves the cellulose relatively un-degraded. In this type of decay, the degraded wood has certain areas that appear more fibrous due to the destruction of lignin and hemicellulose. Typically, simultaneous white-rot decay is the most common form of white-rot decay in wood products. Certain species of white-rot fungi are capable of performing both simultaneous and selective decay mechanisms at the same time on the same piece of wood (Goodell *et al.* 2008; Messner *et al.* 2003).

White-rot fungi decay wood enzymatically by utilizing certain mechanisms to oxidize and mineralize cellulose, hemicellulose, and lignin. Cellulose is hydrolyzed at the β-1,4-glycosidic linkage producing carbon and energy sources for cellulotic microorganisms (Pérez *et al.* 2002). To degrade cellulose, white-rot fungi produce endoglucanases, cellobiohydrolases (exoglucanases), and β-glucosidases, which actively degrade the crystalline cellulose. Endoglucanases hydrolyze internal bonds in both amorphous and crystalline regions, which release newly formed terminal ends. Cellobiohydrolases efficiently breakdown crystalline cellulose and degrade chains generated by endoglucanases. β-glucosidases break the bonds between cellobiose units. Complete degradation of hemicellulose to monomeric sugars and acetic acid is achieved by a variety of hydrolytic enzymes including, xylanases, xylosidase, esterases, glucuronidases, and arabinofuranosidase (Pérez *et al.* 2002; Goodell *et al.* 2008). Xylanases cleave xylan and generate oligosaccharides, while xylosidases attack those

oligosaccharides to generate xylose. Esterases, glucuronosidases, and arabinofuranosidases act as accessory enzymes and aid in the hydrolysis of xylans and mannans (Pérez *et al.* 2002). The main lignin degrading enzymes produced by white-rot fungi are lignin peroxidase, manganese peroxidase and laccase. Lignin peroxidase can degrade phenolic and non-phenolic lignin, while manganese peroxidase and laccase can only degrade phenolic lignin (Li 2003). Lignin peroxidase cannot penetrate the cell wall and is limited to the exposed components on the cell wall surface. In the presence of hydrogen peroxide, lignin peroxidase produces a veratryl alcohol radical that can penetrate into the cell wall to access intracellular components. Manganese peroxidase oxidizes Mn^{2+} to Mn^{3+}, which can diffuse into the cell wall and degrade phenolic lignin compounds. Laccase uses oxygen as an oxidizing reagent to degrade phenolic lignin compounds (Goodell *et al.* 2008).

Brown-Rot Decay

The largest threat to the destruction of coniferous wood in service is the result of brown-rot fungi (Goodell 2003). These organisms are capable of utilizing two different methods to decay wood: a non-enzymatic and an enzymatic mechanism. In the initial stages of decay, brown-rot fungi must first attack the hemicelluloses before accessing the cellulose. This initial step is critical for the organism to establish itself in the wood (Green and Highley 1997). Following hemicellulose degradation, cellulose is rapidly depolymerized and results in strength loss of the wood at a very early stage. During its attack on the cellulose and hemicellulose, it is hypothesized that the brown-rot fungi chemically modify the lignin via demethoxylation and demethylation; however, these organisms are not capable of fully depolymerizing lignin in the process. The

modification of lignin is carried out through an enzymatic mechanism (Nilsson 2009; Xu and Goodell 2001).

The hyphae produced by the brown-rot fungi can secrete both enzymatic and low molecular weight metabolites, channel them into the cell wall, and actively breakdown its components (Nilsson 2009). Typically, the Fenton reaction is associated with early stages of decay and must occur away from the fungal hyphae to avoid the produced reactive oxygen species from destroying the hyphae. In non-enzymatic decay, brown-rot fungi produce low molecular agents that are responsible for cell wall depolymerization by free radical production ($^{\cdot}OH$) via the Fenton reaction ($Fe^{2+} + H_2O_2 \rightarrow Fe^{3+} + {}^{\cdot}OH + OH^-$). Extracellular hydrogen peroxide (H_2O_2) reacts with ferrous iron (Fe^{2+}) creating hydroxyl radicals ($^{\cdot}OH$) that are able to diffuse through the cell wall and degrade hemicellulose (Xu and Goodell 2001). For the Fenton reaction to occur, brown-rot fungi require certain mechanisms to solubilize iron from iron oxides, to reduce Fe^{3+} to Fe^{2+}, and to produce H_2O_2 (Arantes *et al.* 2009).

Several mechanisms have been proposed for the production of Fenton reagents; however, the production of these reagents mainly relies on certain metabolites, like oxalate, and low molecular weight compounds with the capability to reduce Fe^{3+}. It has been shown that brown-rot fungi produce phenolate-type low molecular weight compounds with the ability to reduce Fe^{3+} and promote $^{\cdot}OH$ production. Metabolites produced by brown-rot fungi, like oxalate, have the potential to obtain iron from iron-oxide complexes by creating a pH gradient between the fungal environment and the cell wall. Once iron is obtained, it forms an iron-oxalate complex, which can diffuse into the cell wall (Arantes *et al.* 2009). Little cell wall material is metabolized in the early stages

of decay by brown-rot fungi (Goodell *et al.* 2008). Initial attack by brown-rot fungi is localized in the S2 layer of the cell wall then moves throughout the S1 and S3 layers as it progresses (Nilsson 2009). The S3 layer remains untouched until late stages of decay and the porosity of this layer is relatively unchanged (Green and Highley 1997).

In the enzymatic mechanism, brown-rot fungi produce endoglucans and exoglucanases to cleave the β-1,4- glucosidic linkages between cellulose monomers and β-glucosidases to hydrolyze the cellobiose units but lack cellobiohydrolase and exoglucans. To breakdown hemicellulose, these organisms utilize endoxylanases and β-xylosidases. *Coniophora puteana* is the only known brown-rot fungus capable of producing cellobiohydrolase and cellobiose dehydrogenase. Because these extracellular enzymes are too large to penetrate the wood cell wall, it has been established that cellulose degradation mainly occurs via a non-enzymatic mechanism in initial decay by brown-rot fungi (Green and Highley 1997; Xu and Goodell 2001; Goodell 2003).

Copper-based Preservatives

Naturally durable wood products have the ability to resist attack by various biological agents, whereas, a majority of current wood species used in forest products that will be in contact with the environment are non-resistant to decay. Because of the high biodegradability of these products, preventative measures to protect the wood are needed. Pressure treatment with wood preservatives is the most common form of protection for wood products. The use of preservative treatments significantly extends the service life of wood-based products. Protection is dependent upon penetration and

retention levels of the various chemicals within the wood (Shupe *et al.* 2008). The effectiveness of wood preservatives depends on sufficient protection against a variable range of wood-inhabiting organisms, low environmental impact, and low mammalian toxicity (Lebow 2004; Shmulsky and Jones 2011).

Current commercial preservatives in use today are classified as oil-based or water-borne formulations and generally have broad-spectrum toxicity against various organisms. The basic difference between the two is the type of liquid (oil or water) used to transport the toxic chemical into the wood (Shmulsky and Jones 2011; Shupe *et al.* 2008). The most common types of oil-based preservatives are creosote, copper oxine, copper naphthenate, and pentachlorophenol. Wood treated with preservatives that use volatile solvent carriers have the potential to cause shrinking upon moisture loss after the treating process. Less-volatile oils, like creosote, protect from weathering, but could have negative influences on cleanliness, odor, color, paintability, gluability, and fire resistance. Wood treated with oil-based preservatives is not recommended for residences, enclosed structures, or regular contact with humans (Shupe *et al.* 2008). Water-borne preservatives are applied as aqueous solutions or use water as the carrier and become chemically "fixed" and stabilized within the wood (Lebow 2010). Common uses for wood treated with water-borne preservatives are residential, construction, and other various products intended for use outdoors. Most water-borne preservatives utilize copper (II) and are the most common form of protection for softwood species used mainly in residential applications. Problems associated with water-borne preservatives include drying and shrinking of treated wood, increased risk of corrosion, inability to

treat hardwood species, and the lack of water repellency (Lebow 2010; Shupe *et al.* 2008).

Between the late 1970s and 2004, the most commonly used wood preservative was a water-borne preservative, chromated copper arsenate (CCA), because it was economical and provided broad-range protection against various types of deterioration (Lebow 2010). Three main formulations (CCA-A, CCA-B, and CCA-C) have been successful in providing long-term protection of treated wood products; however of the three formulations, CCA-C achieves greater efficacy against wood-inhabiting organisms and resistance against leaching. CCA-C active components consist of 47.5% chromium trioxide, 34% arsenic pentoxide, and 18.5% copper oxide (Lebow 2010). CCA-C is efficacious because copper provides protection against fungi, arsenic provides protection against copper-tolerant fungi and termites, and chromium fixes the copper and arsenic into the wood (Freeman and McIntyre 2008). In 2004, due to voluntary label changes, the Environmental Protection Agency (EPA) restricted the use of CCA to industrial applications (Lebow 2004; Lebow *et al.* 2004; Freeman and McIntyre 2008; Lebow 2010). Because of this restriction, the American Wood Preservers' Association (AWPA) continues to standardize a variety of chromium and arsenic-free formulations, which utilize copper as the primary ingredient (Lebow 2004).

Today, copper is the primary component used to protect wood for residential applications because it exhibits algaecide, bactericide, fungicide, insecticide, and moldicide properties (Freeman and McIntyre 2008). Unlike the majority of organic molecules, copper possesses efficacy against a wide variety of wood-inhabiting organisms including the decay fungi. Other advantages of using copper as a primary

component of protection include the capacity to easily create a variety of formulations, the ability to easily analyze and assess penetration levels, and it has been shown to slow photodegradation by UV radiation and water. The use of copper as the primary form of protection can pose certain problems including tolerance, corrosivity, and aquatic toxicity. Tolerant organisms have the ability to grow and thrive in the presence of high concentrations of toxic metals, specifically copper. Due to the threat of tolerant organisms, copper-formulations are usually combined with an organic co-biocide for further protection. Typically, common copper co-biocides used are quaternary components and azoles (Shupe *et al.* 2008).

The restriction of CCA – treated wood in the residential market led to the development of several alternative preservative treatments utilized by the industry today. Table 1 outlines these alternative copper-based preservatives, categorizes them based on formulation, and details the percentage of components found in each preservative (Lebow 2004; Lebow *et al.* 2004; Freeman and McIntyre 2008; Lebow 2010).

Table 1.1 Copper-based Wood Preservatives

Preservative	***Formulation Type***	***Proportion of Components***
Acid Copper Chromate (ACC)	Water-borne	31.8% Copper oxide 68.2% Chromium trioxide
Alkaline Copper Quat (ACQ-A)	Water-borne	50% Copper oxide 50% Didecythyl ammonium chloride
Alkaline Copper Quat (ACQ-B)	Water-borne	67% Copper oxide 33% Didecythyl ammonium chloride
Alkaline Copper Quat (ACQ-C)	Water-borne	67% Copper oxide 33% Alkylbenzyldimethyl ammonium chloride
Alkaline Copper Quat (ACQ-D)	Water-borne	67% Copper oxide 33% Didecythyl ammonium chloride
Ammoniacal Copper Citrate (CC)	Water-borne	62% Copper oxide 38% Citric acid
Copper Azole (CBA-A)	Water-borne	49% Copper 49% Boric acid 2% Tebuconazole
Copper Azole (CA-B)	Water-borne	96% Copper 4% Tebuconazole
Copper Azole (CA-C)	Water-borne	96% Copper 2% Tebuconazole 2% Propiconazole
Copper bis (dimethyldithiocarbamate) (CDDC)	Water-borne	17-29% Copper oxide 71-83% Sodium dimethyldithio-carbamate
Copper Naphthenate (CuN-W)	Water-borne	Reaction product of copper salts and naphthenic acid
Copper Naphthenate (CuNap)	Oil-borne	Dissolved in alkanolamine/ammonia in water
Copper Xyligen (Copper HDO) (CX-A)	Water-borne	61.5% Copper oxide 14% Bis-(N-cyclohexyl-diazenium dioxy) copper 24.5% Boric acid
Oxine Copper (Copper-8-quinolinolate)	Oil-borne	10% Copper-8-quinolinolate 10% Nickel-2-ethylhexanoate 80% Inert ingredients

In recent years, water-borne micronized copper formulations have emerged as an alternative formulated preservative. The micronized particles are produced by the mechanical grinding of copper in water-borne or oil-borne compounds and are aided by a dispersal agent. This process results in approximately 90 percent of the copper particles being less than 1000 nm in size. Typically, polymeric dispersants are used as the dispersing agents and allow the attachment of particles to the surface of the wood as well as maintain distance between the particles. Micronized particles are believed to be

"fixed" into the wood by strong adhesion between the dispersant and wood fiber (Freeman and McIntyre 2008). Micronized formulations in use today contain a smaller percentage of copper and are considered more environmentally favorable. The variety of copper-based wood preservatives continues to increase as a result of various biocidal properties demonstrated by copper; however, the formulations need to be used in the capacity intended.

In the early 2000s, AWPA developed a guideline to classify preservatives appropriately. The Use Category System (UCS) standards detail specific uses, retention levels, penetration requirements, and severity of deterioration. Use Category 1 (UC-1), the lowest category, is used when the wood is intended for interior construction and is completely protected from the elements. UC-2 is intended for interior construction and is exposed to occasional dampness. UC-3 is intended for above ground use, while UC-4 is intended for in-ground contact of exterior applications. UC-5 is used for wood in contact with seawater (Lebow 2004; Lebow *et al.* 2004). Table 2 provides information about the intended application for each of the copper-based preservatives listed above (Lebow 2006).

Table 1.2 Intended Application for Copper-based Preservatives

Preservative	***Application***
Acid Copper Chromate (ACC)	Direct contact with the ground
Alkaline Copper Quat (ACQ-A – ACQ-B)	Direct contact with the ground
Ammoniacal Copper Citrate (CC)	Direct contact with the ground
Copper Azole (CBA-A – CA-C)	Direct contact with the ground
Copper bis(dimethyldithiocarbamate) (CDDC)	Direct contact with the ground
Copper Naphthenate (CuN-W, CuN)	Direct contact with the ground
Copper Xyligen (Copper HDO) (CX-A)	Direct contact with the ground
Oxine Copper (Copper-8-quinolinolate)	Above ground, fully exposed to the weather

Extensive testing is required to accurately evaluate these properties. AWPA Standards require that testing be conducted when evaluating both new and existing preservative formulations. Testing protocols include, but is not limited to, laboratory leaching tests which evaluates how quickly a treatment is utilized; laboratory decay tests which exposes the wood to aggressive fungal decay organisms or termites; field stake evaluation which exposes the wood to the natural environment; above-ground field tests which compares deterioration between untreated wood and preservative treated wood; and corrosion, treatability, and strength testing (Lebow 2010).

The use of copper as a primary component for the development of wood preservatives continues to prevail despite the ability of tolerant organisms to circumvent copper toxicity. Organic co-biocides are included to inhibit tolerant fungi; however, these co-biocides are not always effective (Freeman and McIntyre 2008). There has been some research into the development of preservatives that lack copper or other heavy metals. These particular formulations rely on combinations of organic fungicides and insecticides, and could possibly create alternative problems such as the breakdown of the preservative by non-wood degrading organisms (Lebow 2006). To develop preservatives that are effective in stopping all forms of biological attack, it is clear that additional research into the mechanism of copper – tolerance is needed.

Copper Tolerance

The risks associated with using copper as a primary treating agent is the possibility for organisms, specifically fungi, to tolerate or successfully resist the toxic effect. These organisms are able to survive in less – than ideal growth conditions by

evolving adaptation mechanisms (DeGroot and Woodward 1999; Hall 2002). Green and Clausen (2003) defined tolerance as the relative ability of an organism to grow and thrive when subjected to an unfavorable environmental factor or toxin. Specifically, copper tolerance is defined as the ability of an organism to grow and thrive in the presence of copper ions (Hastrup *et al.* 2005). In comparison to other organisms, fungi have the possibility to be extremely tolerant of toxic metals in high concentrations (Freeman and McIntyre 2008). Copper-tolerant fungi have the ability to decay copper treated wood in which the concentration of copper is higher than 1.6 mM/l (Gadd 1993). These particular organisms can detoxify copper in copper-treated wood, which enables toleration of environments containing high concentrations of toxic metals (Hastrup *et al.* 2005).

Fungicides require certain characteristics like high uptake levels and numerous active sites to be effective. In fungal cells, initial uptake of copper by ion exchange is followed by permeation throughout the cell, and eventually leads to accumulation aided by unspecific reactions within cell constituents (Somers 1963). Affinity, distribution, and accumulation vary with species. Numerous characteristics make copper an ideal fungicide. Excess copper causes damage through the oxidation of proteins, enzymes, and lipids, which can lead to the interference of certain enzymatic processes. It can also inhibit intracellular enzymes responsible for the destruction of lignocellulosic materials, interrupt transport of nutrients in and out of the cell by binding to the cell wall, and cause denaturation of proteins and enzymes which eventually leads to cell death (Freeman and McIntyre 2008).

Tolerance is particularly variable with respect to preservative formulations, fungal species, and even fungal isolates (Hastrup *et al.* 2005; Freeman and McIntyre 2008). The

majority of copper-tolerant fungi is classified as brown-rot basidiomycetes and is found in the genera *Fibroporia (Antrodia), Postia, Serpula, Laetiporus, Meruliporia, Gloeophyllum, Tyromyces,* and *Wolfiporia* (DeGroot and Woodward 1999; Green and Clausen 2005; Arango *et al.* 2009; Clausen and Jenkins 2011; Schilling and Inda 2011). Studies utilizing copper naphthenate were not successful in preventing attack by tolerant organisms (Sutter *et al.* 1983). However, oxine copper has been shown to provide exceptional protection against tolerant fungi. Clausen and Green (2003) showed the inability of *Postia placenta, Wolfiporia cocos*, *Meruliporia incrassata*, and *Antrodia vaillantii* to produce specific metabolites, which aid in the breakdown process when exposed to oxine copper. DeGroot and Woodward (1999) used *Serpula lacrymans* in agar plate assays against CCA and agar block tests against copper napthenate and determined a difference in tolerance of the isolates in relation to the two preservatives. Treatments with ammoniacal copper citrate exposed to *Serpula lacrymans* have also shown variation in breakdown ability (Freeman and McIntyre 2008). Collet (1992) found that isolates of *Antrodia vaillantii* varied drastically in their tolerance to copper (Green and Clausen 2003). Pohleven and Humar (2002) conducted studies on Norway spruce with preservatives used in the European market and observed variability of copper tolerance when exposed to *Antrodia spp.* (Green and Clausen 2005). Because of the high variability associated with tolerance, it is apparent that these organisms must employ numerous mechanisms to overcome preservative treatments.

There are many theories attributed to the mechanism of copper tolerance. Clausen and Green (2003) stated that the "interaction of a number of diverse factors such as growth rate, pH, oxalic acid production, and decay capacity all contribute to copper

tolerance". The mechanism of tolerance associated with copper-tolerant fungi has most commonly been connected to the production of oxalate (Green and Clausen 2003, 2005; Hastrup *et al.* 2006; Freeman and McIntyre 2008; Arango *et al.* 2009; Shilling and Inda 2011). High extracellular accumulation of oxalate initiates the precipitation of copper into the insoluble form of oxalate (copper oxalate crystals), and renders the copper ion inert (Green and Clausen 2003). These organisms have the ability to immobilize copper by precipitating copper oxalate (DeGroot and Woodward 1999). Both copper oxalate and calcium oxalate crystals are present in decayed wood treated with copper-based preservatives (Freeman and McIntyre 2008). Another important factor related to copper tolerance is the presence of a low pH environment, which is also stimulated by oxalate production (Green and Clausen 2005). Choi *et al.* (2002) showed spores from copper-tolerant organisms did not germinate in the presence of copper because the spores lack the ability to actively produce oxalate (Freeman and McIntyre 2008). Thus, oxalate accumulation and precipitation of copper oxalate crystals plays an important role in the mechanism of copper tolerance (Clausen and Green 2003).

It has been demonstrated that in a low pH environment, copper oxalate crystal formation, and the production and accumulation of oxalate are not the only mechanisms of copper tolerance in these organisms (Clausen *et al.* 2008). Alternative mechanisms have been documented and include the trapping of metal ions by cell wall constituents, altering ion uptake when membrane permeability of copper is low, extracellular precipitation or chelation by metabolites, or complexing of metallothioneins and phytochelatins intracellularly (Freeman and McIntyre 2008). In the presence of copper, fungal reactions prompt the formation of a thicker cell wall and an increased extracellular

mucilaginous material (hyphal sheath). Copper treated Scots pine exposed to *Coriolus versicolor* and *Gloeophyllum trabeum* demonstrated increased *N*-acetyl glucosamine production correlating to the amount of chitin present, which is indicative of thicker cell wall development. Experiments on *Trametes versicolor* in culture media containing increased copper concentrations showed an increase production of extracellular mucilaginous material leading to an increased tolerance to copper (Vesentini *et al*. 2006; Freeman and McIntyre 2008).

Because these copper-tolerant organisms have the ability to overcome the preventative measures in use today, it is critical that these mechanisms be investigated. Knowing the exact mechanisms, organisms involved, and specific requirements would give insight into the physiological intricacies of copper tolerance.

Significance of Oxalate

The production of oxalate ($C_2O_4^{2-}$) occurs in large quantities by numerous classes of fungi. Oxalate aids in establishing colonization and performs critical roles in fungal metabolism (Dutton and Evans 1996). Also, oxalate assists in cleaving hemicellulose side-chains, eventually depolymerizing hemicellulose and cellulose, which causes significant strength loss in wood (Green *et al.* 1991). It is believed that oxalate is a metabolic byproduct of incomplete glucose oxidation via malate in the tricarboxylic acid (TCA) cycle or glyoxylate in the glyoxylate (GLOX) cycle (Schilling and Jellison 2005; Hastrup *et al.* 2006). The majority of brown-rot fungi produce oxalate in detectable amounts; however, its production is limited in white-rot fungi due to the existence of oxalate decarboxylase (Hastrup *et al*. 2006). Intracellular oxalate decarboxylase breaks

down oxalate to carbon dioxide and formate, and is not present in brown-rot organisms (Espejo and Agosin 1991; Hastrup *et al.* 2006). Without oxalate decarboxylase, wood low in carbon and nitrogen has the potential to generate oxalate instead of carbon dioxide from the TCA and GLOX cycles (Dutton and Evans 1996; Schilling and Jellison 2005). Without oxalate decarboxylase or other alternative regulation mechanisms, oxalate has the potential to accumulate as a function of fungal respiration (Schilling and Jellison 2005).

Role of Oxalate

Oxalate functions in a number of unique ways in brown rot fungi. It has been theorized that oxalate functions in iron reduction, acid hydrolysis of cellulose, detoxifying metals, and chelating calcium from pit membranes (Schilling and Jellison 2005). Specifically in brown-rot fungi, oxalate functions to rapidly lower pH in the immediate environment, initiate depolymerization of hemicellulose side-chains, and precipitate calcium oxalate (Hastrup *et al.* 2006). Oxalate also functions as a chelator to remove iron from iron-oxide complexes in the lumen. Another theorized, yet to be confirmed function of oxalate is to reduce the pH near the hyphae, which creates a pH differential between the fungal environment and the wood cell wall. The combination of removing iron from iron-oxide complexes and reducing the pH allows metal reduction away from the organism protecting it from oxidative damage (Arantes *et al*. 2009).

In the non-enzymatic decay mechanism utilized by brown-rot fungi, it has been theorized that oxalate and other low molecular weight mediators aid in the reduction of Fe^{3+}. This reduction of Fe^{3+} promotes the generation of hydroxyl radicals via the Fenton reaction. Schmidt *et al.* (1981) demonstrated that oxalate has the ability to increase the

activity of Fenton-based degradation by reducing Fe^{3+} to Fe^{2+}. However, the reactivity of Fe^{3+} is dependent upon the pH and concentration of oxalate in the surrounding areas. It is possible that high oxalate concentrations could form extremely stable iron-oxalate complexes, which would delay Fenton-based degradation (Arantes *et al.* 2009).

Initially, brown-rot basidiomycetes produce oxalate in large amounts; however levels of accumulation and function vary based on genus and species. Some brown-rot basidiomycetes produce oxalate for initial decay but do not accumulate significant levels during the decay process. Other brown-rot basidiomycetes utilize oxalate throughout the decay process resulting in normal levels of accumulation (Goodell 2003). Typically, oxalate produced by these organisms exists as a dihydrate calcium oxalate crystals and is persistent throughout the growth stage (Dutton and Evans 1996; Goodell 2003). Calcium ions which are released during decay can precipitate oxalate to form calcium oxalate crystals (Hastrup *et al.* 2006). The formation of calcium oxalate crystals plays a crucial role in regulating the pH of the environment and facilitating the occurrence of the lower pH environments typically observed (Goodell 2003).

Undecayed wood has a pH that varies between 3 and 6. Brown-rot fungi lower the pH of the environment (between pH of 1-3) following initial colonization, because cellulolytic activity is inhibited in higher pH environments. The majority of brown-rot fungi initiate pH reduction through the production of oxalate. The pH reduction is critical in the function of extracellular enzymes used by the fungi to degrade the wood (Goodell 2003). Green *et al.* (1991) demonstrated that oxalate functions to depolymerize cellulose over a range of pH levels from 1.5 to 2.5. They also showed that low pH levels are responsible for high strength loss in the initial stages of decay. This rapid drop in pH,

seen in the initial decay stage, has been proposed to serve as an important factor in the decay process (Green *et al.* 1991). Management of pH levels and the development of pH gradients between the hyphae and wood cell wall occur as copper oxalate crystals are solubilized. It is possible that brown-rot fungi regulate pH by utilizing the crystalline and acid forms of oxalate in certain environments (Goodell 2003).

Oxalate is a metabolic byproduct of the decay process, and is also a major factor that leads to the tolerance of copper based preservatives. The presence of copper stimulates a rapid production of oxalate, and then the copper is inactivated by the excess oxalate (Green and Clausen 2005). The production of oxalate tends to vary with the type of copper treatment and fungal species (Arango *et al.* 2009). Most brown-rot fungi produce oxalate routinely; however, copper-tolerant fungi produce it in much higher quantities as an induced response to copper. Green and Clausen (2005) found that copper-tolerant fungi produce 2-17 times more oxalate in copper citrate – treated blocks compared to untreated controls. They also found that at week four copper stimulated 66-93% more oxalate production when compared to untreated controls (Green and Clausen 2005). Because oxalate plays a significant role in the decay process of copper-tolerant fungi, a certain mechanism must be utilized for its production.

Biosynthesis of Oxalate

Several pathways have been proposed for the biosynthesis of oxalate in brown-rot fungi; however, in recent years, many researchers have linked it to the tricarboxylic acid (TCA) and glyoxylate (GLOX) cycles (Dutton and Evans 1996; Munir *et al*. 2000; Munir *et al.* 2001; Yoon *et al.* 2002). Both the TCA and GLOX cycles produce extracellular oxalate. The TCA cycle is localized in the mitochondria while the GLOX cycle takes

place in the glyoxysome (Dutton and Evans 1996). There are four key enzymes involved in the synthesis of oxalate, namely isocitrate lyase, malate synthase, gloxylate dehydrogenase, and oxaloacetase. Isocitrate lyase serves as a vital enzyme in the production of oxalate (Munir *et al.* 2001). Both glyoxylate dehydrogenase and oxaloacetase lead to the direct production of oxalate within the TCA and GLOX cycles (Munir *et al.* 2001; Yoon *et al.* 2002).

Munir *et al.* (2001) investigated the role of oxalic acid biosynthesis in the copper-tolerant fungus, *Tyromyces palustris*. This study hypothesized that 1 M of glucose is converted to 2 M of oxalate rather than producing the traditional carbon dioxide from the TCA cycle. They further suggested that oxalate production was coupled with energy production, and proposed the overall oxidation of 2 M of acetyl-CoA, yielding 2 M oxalic acid, generating a net amount of 4 NADHs and 2 ATPS (Munir *et al.* 2001). Figure 1.1 shows the proposed biosynthesis of oxalate from glucose in the TCA and GLOX cycles as suggested by Munir *et al.* (2001). Table 1.3 details the twelve enzymes required for each of the reactions from Figure 1.1 (Munir *et al.* 2001).

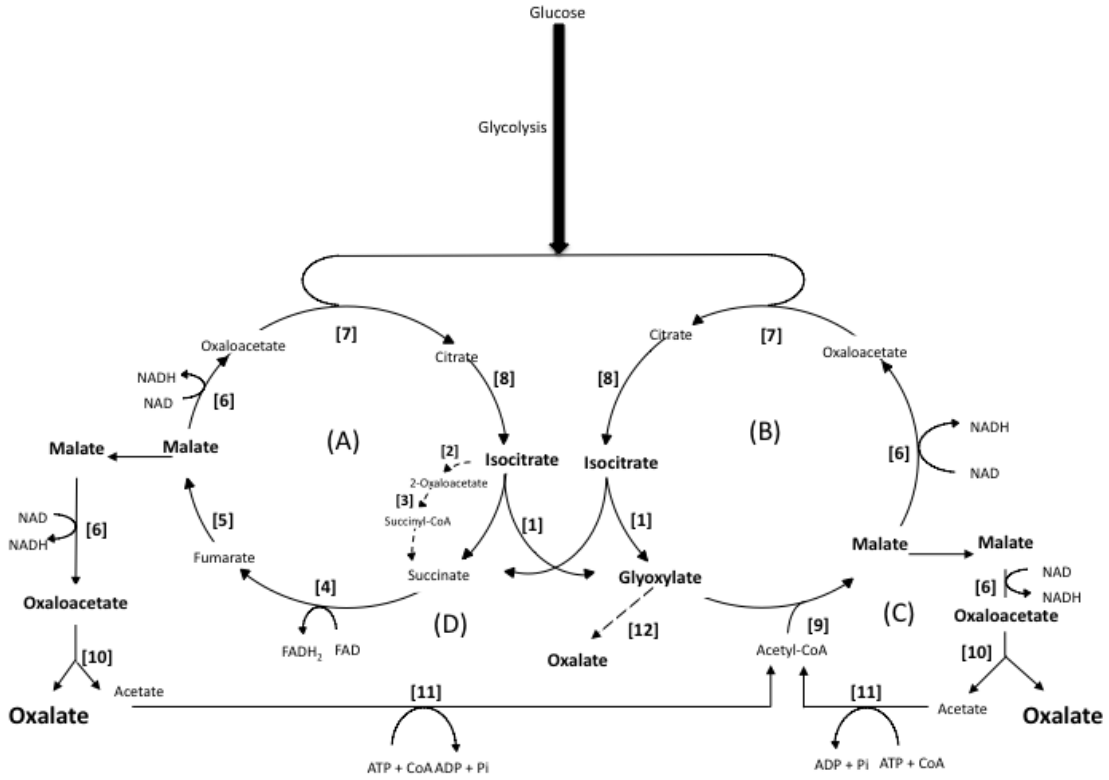

Figure 1.1 Enzyme/ Enzyme pathways which may be utilized in some fungi to produce oxalate; [1-12] corresponding enzymes listed in Table 1.3. (A) the TCA cycle; (B) the GLOX cycle (Munir *et al.* 2001).

Table 1.3 Enzymes of the TCA and GLOX cycles thought to be involved in oxalate biosynthesis (Munir *et al.* 2001).

NUMBER	ENZYME
1	Isocitrate lyase
2	Isocitrate dehydrogenase
3	2-Oxoglutarate dehydrogenase
4	Succinate dehydrogenase
5	Fumarase
6	Malate dehydrogenase
7	Citrate synthase
8	Aconitase
9	Malate synthase
10	Oxaloacetase
11	Acetyl-CoA synthease
12	glyoxylate dehydrogenase

Using the Munir *et al.* (2001) study as a model (Figure 1.1, Table 1.3), it was hypothesized that there are three unique pathways for oxalate production. One pathway produces oxalate utilizing the TCA cycle only; another produces oxalate from the GLOX cycle only; and the third switches from the TCA to the GLOX cycle to produces oxalate. In the TCA cycle, fumarate is synthesized to malate via fumarase. Malate is then converted to oxaloacetate via malate dehydrogenase; then, this leads to the production of oxalate by oxaloacetase. Within the GLOX cycle, glyoxylate is converted to malate via malate synthase. Malate is then converted to oxaloacetate by malate dehydrogenase and that is converted to oxalate via oxaloacetase. In the third potential pathway, isocitrate is synthesized in the TCA cycle and then produces glyoxylate utilized by the GLOX cycle via isocitrate lyase. Glyoxylate is then converted directly to oxalate via glyoxylate dehydrogenase. Therefore, using *F. radiculosa*, each of these enzymatic pathways were evaluated in relation to oxalate production.

Objectives of Research

Many studies have been conducted on oxalate production; however, little is known about the mechanism utilized by copper-tolerant fungi. A better understanding of this mechanism is crucial in developing alternative methods to decrease problems caused by these particular organisms. The purpose of this study was to gain insight into the biosynthesis of oxalate by which the brown-rot decay fungus, *Fibroporia radiculosa*, regulates tolerance of copper-treated wood. Specific objectives of this study are as follows:

1. Assess the variation of oxalate production of fifteen *F. radiculosa* isolates exposed to copper-treated wood.
2. Evaluate select *F. radiculosa* isolates undergoing decay of untreated and copper-treated wood for enzyme activity in relation to oxalate production.
3. Examine select *F. radiculosa* isolates undergoing decay of untreated and copper-treated wood for the differential expression of genes associated with oxalate production.
4. Propose a potential pathway involved in the production of oxalate.
5. Determine the effect of alternative applications of ammoniacal copper citrate in relation to oxalate production of the select *F. radiculosa* isolates.

CHAPTER II

MATERIALS AND METHODS

Preliminary Study One: Sequencing Analysis Results

Fungal Isolates

Fifteen isolates of *Fibroporia radiculosa* were obtained from the USDA Forest Products Laboratory in Madison, WI. Specific isolates used for this analysis include: Baxter-31, HHB-6386-SP, FP-103272-T, FP-105309-R, FP-105780-SP, FP-90848-T, L-12451-SP, L-7878-SP, L-9318-SP, L-9414-SP, L-11659-SP, L-12617-SP, MJL-630-SP, RLG-7629-SP, and TFFH 294.

Media Preparation

All isolates were maintained on 2% malt agar (BD, Fisher Scientific, Pittsburg, PA) media plates. Six mm plugs were placed in 100 mL of 2% Malt Broth (BD, Fisher Scientific, Pittsburg, PA) and grown for approximately 2 weeks in stationary culture. Once mats of fungal mycelium were visible, contents of the flasks were filtered using Whatman™ filter paper (Fisher). Mycelial mats were stored at -20°C until processed for DNA.

DNA Extraction

DNA extractions were carried out using the NucleoSpin® Plant II Kit (Machery-Nagel). Each 50 mg fungal tissue sample was placed in a 2 mL screw-top tube with two

5 mm glass beads, 500 μl CTAB lysis buffer (2% cis-trimethyl ammonium boric acid, 100 mM Tris, 20 mM Na_2EDTA, 1.4 M NaCl, and 1% polyvinylpyrolidine), 17 μl of RNase A, and 17 μl of Proteinase K. Samples were homogenized using a bead mill for three minutes twice at maximum speed, and incubated at 60°C for one hour. The mixture was transferred to a NucleoSpin® filter column and centrifuged for five minutes at 11,000 x g. The flow through was transferred to a second NucleoSpin® filter column and mixed with 850 μl binding buffer (550 μl PC), and centrifuged for one minute at 11,000 x g. The filter was washed with 400 μl of wash buffer 1, and centrifuged for one minute at 11,000 x g. The filter was washed a second and third time with 700 μl and 200 μl of PW2, respectively. The filter was dried by centrifugation for two minutes at 13,000 x g. DNA was eluted with 75 μl of 70°C elution buffer (PE), incubated at room temperature for five minutes, and centrifuged at 8,000 x g for one minute. DNA concentration (ng/μl) was determined using a NanoDrop 1000 spectrophotometer (Thermo Scientific, Waltham, MA).

Polymerase Chain Reaction (PCR) and Gel Electrophoresis

The ITS region was amplified for the extracted DNA using a nonspecific forward primer: 5'-CTTGGTCATTTAGAGGAAGTAA-3' (Gardes and Bruns, 1993) and a nonspecific reverse primer: 5'-TCCTCCGCTTATTGATATGC-3' (White *et al.* 1990). Fungal DNA amplification was carried out using an Eppendorff® Mastercycler with the following settings: an initial hot start at 98°C for two minutes (DNA template only), melting at 95°C for 45 seconds, annealing at 52°C for 45 seconds, and extension at 72°C for two minutes, and final extension at 72°C for 10 minutes for 35 cycles. After the initial

hot start, a master mix containing 10 mM reaction buffer, 25 mM MgCl, 10 mM deoxynucleotide triphosphates (dNTPs), 10 mg/ml Bovine Serum Albumin (BSA), deionized water, and 5 units/μl Taq polymerase was added to each sample.

An 8 μl sample of amplified DNA was added to 2 μl of loading dye (50 mM EDTA, 30% glycerol, 0.25% bromophenol blue, 0.25% xylene cyanol) and loaded into a 2% agarose gel to assess successful amplification of the ITS region.

PCR Clean Up

Successfully amplified PCR products were filtered with the NucleoSpin® Extract II (Machery-Nagel) kit to remove residual PCR reagents. Sample products were loaded onto a filter column and centrifuged for one minute at 11,000 x g. The membrane was washed with 600 μl of NT3 and centrifuged for one minute at 11,000 x g. The filter was dried by centrifugation for two minutes at 11,000 x g. Purified PCR products were eluted with 20 μl of 70°C elution buffer (NE) incubated at room temperature for five minutes, and centrifuged at 11,000 x g for one minute. Samples were then visualized on a 2% agarose gel and base pair size was determined.

Sequence Analysis

Up to 10 μl of purified PCR products (33 ng – 64 ng) with 8 μl of DTCS Quick Start Master Mix (Beckman Coulter®) and 2 μl forward primer and reverse primer, respectively, were prepped for sequencing using an Eppendorff® Mastercycler with the following settings: 96°C for 20 seconds, 50°C for 20 seconds, and 60°C for four minutes, for 30 cycles. Immediately following the amplification reaction, 5 μl of stop solution (2 μl of 3 M Sodium Acetate, pH 5.2, 2 μl of 100 mM Na_2EDTA, pH 8, 1 μl of 20 mg/mL

glycogen) was added to each reaction tube. A 60 μl aliquot of cold 65% ethanol was also added and the samples were centrifuged for 15 minutes at 4°C and 14,000 x g. The supernatant was removed and the pellet was washed twice with 200 μl of cold 70% ethanol and centrifuged for 2 minutes at 4°C and 14,000 x g. After the second wash, the samples were air-dried and resuspended in 40 μl of sample loading solution. Samples were loaded into a sequencing plate, capped with one drop of mineral oil, and sequenced with CEQ 8000 Genetic Analysis System (Beckman Coulter®). Sequences were processed using the CEQ sequencing analysis software and MegAlign (Lasergene®) was used to determine match identities.

Preliminary Study Two: Oxalate Screening Analysis

Fungal Isolates

Isolates used for this analysis include: Baxter-31, HHB-6386-SP, FP-103272-T, FP-105309-R, FP-105780-SP, FP-90848-T, L-12451-SP, L-7878-SP, L-9318-SP, L-9414-SP, L-11659-SP, L-12617-SP, MJL-630-SP, RLG-7629-SP, and TFFH 294. All isolates were maintained on 2% malt agar (BD, Fisher Scientific, Pittsburg, PA) media plates.

Test Wafer Preparation and Preservative Treatments

Two sets of southern yellow pine (SYP) wafers measuring 24 mm x 18 mm x 5 mm (t x r x l) were vacuum treated with micronized copper quaternary ammonia compound (MCQ) and amine copper (CA), respectively. SYP test wafers were autoclaved for 20 minutes at 16 psi at 122°C prior to exposure to prevent contamination.

Decay Test

Decay Chamber Setup

A modified version of the AWPA soil-block test (Standard E22-09) was used for this study (AWPA 2010). Decay chambers consisted of round plastic containers 110 mm in diameter and 80 mm in depth with matching lids. The lids were punctured and a cotton plug was inserted to facilitate gas exchange while maintaining sterile conditions. Chambers were filled with 75 mL sterile deionized water initially followed by 150 g of soil (Dorman Lake test site), which was sifted to remove unwanted debris prior to use. Two SYP feeder strips measuring 65 mm x 20 mm x 3 mm (t x r x l) were placed directly on the soil surface in each container with approximately a 1 cm gap between them. Chambers were sealed and autoclaved for sterility for 40 minutes at 16 psi and 122°C. After sterilization, chambers were placed under a laminar flow hood and allowed to cool before inoculation.

Inoculation of Feeder Strips and Incubation

Sterile containers were inoculated aseptically with approximately 6 mm plugs of actively growing mycelia. Four mycelia plugs from each of the 15 isolates were placed in each container adjacent to the SYP feeder strips and in contact with the soil surface, respectively. Containers were sealed and incubated at 26.7°C for 2 weeks to allow initial colonization of the feeder strips.

After the 2-week colonization period, two MCQ and two CA treated SYP test wafers were placed directly on top of the colonized SYP feeder strips per one container (Figure 2.1). Ten milliliters of sterile deionized water was added to each container prior to being sealed. All containers were incubated at 26.7°C for 4 weeks.

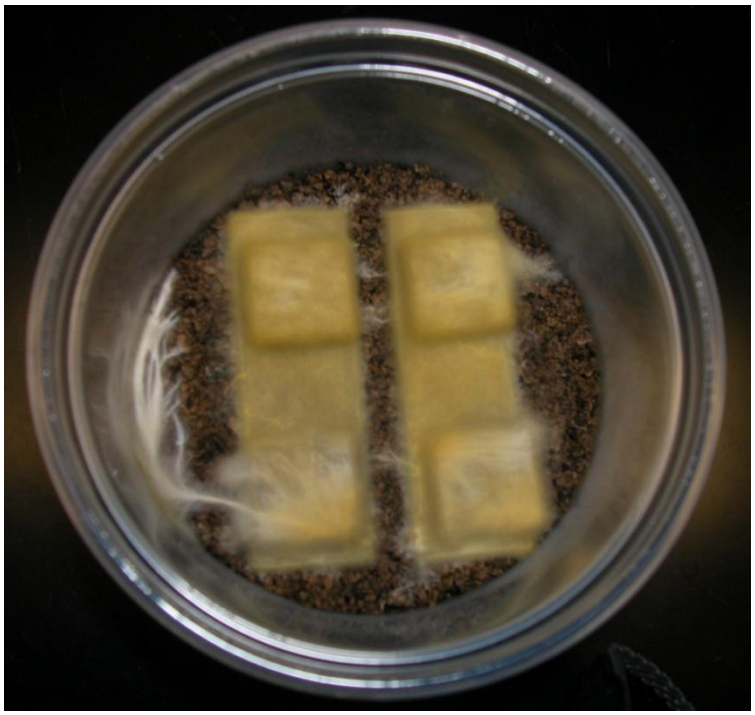

Figure 2.1 Decay chamber set-up including feeder strips and test wafers exposed to isolate, L-11659-SP.

Sample Preparation

SYP test wafers were removed from incubation at weeks 2 and 4, and were gently brushed free of surface mycelia. Each wafer was placed separately in a 50 mL disposable sterile centrifuge tubes (Fisherbrand®), three milliliters of 0.1 M phosphate buffer pH 7.0 (62 mL 0.1 M Na_2HPO_4 and 38 mL 0.1 M KH_2PO_4) was added, and the tubes were shaken for 2 hours. After agitation, one milliliter of liquid was stored at -20°C for oxalate and protein analysis.

Oxalate Assay

Ten µl of sample solution and oxalate standards were placed in 96-well polystyrene microplates (Costar®, Corning, NY), respectively. Two-hundred µl of Reagent A (oxalate oxidase reagent) and 20 µl Reagent B (3-methyl-2-benzothiazoline

hydrazone reagent) were added to each well (Trinity Biotech Co., Wicklow, Ireland). The 96-well plate was gently shaken and incubated at room temperature for five minutes. Concentration (mg/ml) was measured spectrophotometrically at 560 nm using an Epoch Microplate Spectrophotometer (BioTek®, Winooski, VT).

Protein Assay

Oxalate concentration was normalized based on total protein concentration according to the Bradford Protein Assay protocol. The dye reagent (Bio-Rad Laboratories) was diluted with four parts deionized water and 200 μl was added to 10 μl sample solution in the 96-well microplate. The plate was incubated at room temperature for five minutes before absorbance (concentration (mg/ml)) was measured at 595 nm.

Evaluating the Role of Oxalate: Enzyme Analysis Results

Fungal Isolates

Isolates used for this analysis include: FP-90848-T, L-9414-SP, L-11659-SP, and TFFH 294. All isolates were maintained on 2% Malt agar (BD, Fisher Scientific, Pittsburg, PA) media plates.

Test Wafer Preparation and Preservative Treatments

Test wafers (SYP) measuring 70 mm x 22 mm x 4 mm (t x r x l) were vacuum treated with 1.2% ammoniacal copper citrate for 40 minutes at 172 kPa. Untreated wafers served as controls. All SYP test wafers were autoclaved for 20 minutes at 16 psi at 122°C prior to exposure to prevent contamination.

Decay Test

Decay Chamber Setup

The same modified version of the AWPA soil-block test (Standard E22-09) used in Preliminary Study Two was also used for this study (AWPA 2010).

Inoculation of Feeder Strips and Incubation

Sterile containers were inoculated aseptically with approximately 6mm plugs of actively growing mycelia. Six mycelia plugs from the 4 isolates were placed in each container adjacent to the SYP feeder strips and in contact with the soil surface, respectively. Containers were sealed and incubated at 26.7°C for 2 weeks to allow initial colonization of the feeder strips.

After the 2-week colonization period, two SYP test wafers (copper citrate and untreated, respectively) were placed directly on top of the colonized SYP feeder strips per container (Figure 2.2). Ten milliliters of sterile deionized water was added to each container prior to being sealed. All containers were incubated at 26.7°C for 8 weeks.

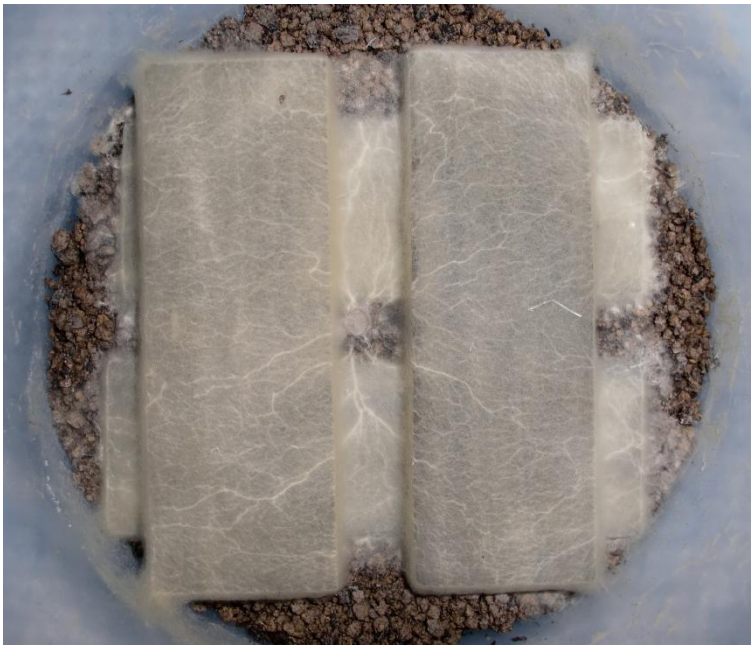

Figure 2.2 Test wafers exposed to isolate, L-9414-SP, in an AWPA standard decay chamber.

Sample Preparation

Untreated and 1.2% copper citrate treated SYP wafers exposed to the four isolates were harvested at weeks 2, 4, 6, and 8. Blocks were rasped into sawdust-like material and approximately 0.2 g of sawdust was placed into 2 mL tubes containing two 5 mm glass beads. The 2 mL tubes were dropped in liquid nitrogen to flash freeze any enzymatic activity the samples contained at the time and stored at -80°C until processed.

Oxalate Assay

To determine oxalate concentration, 1.5 mL of cold 0.1 M phosphate buffer was added to each sample and homogenized for three minutes by a bead mill. After centrifuging to remove unwanted debris, the crude homogenate was placed directly on ice for processing. Concentration was analyzed spectrophotometrically by the Biotek Epoch 96-well plate reader at 560 nm using oxalate reagents from Trinity Biotech.

Enzyme Assays

To determine enzyme activity, one sample of sawdust was removed from the freezer and placed directly on ice. A 1.5 mL aliquot of cold buffer, specific to the assay protocol, was added to each tube and homogenized for three minutes by a bead mill, and immediately returned to ice. Tubes were centrifuged for two and a half minutes at 12,000 RCF at 4°C, the supernatant was placed into a clean 1.5 mL tube, and tubes were re-centrifuged to remove any residual debris. The crude homogenate was aliquoted into 0.5 mL tubes and placed directly on ice for processing. Extras were stored at -80°C.

Fumarase, glyoxylate dehydrogenase, isocitrate lyase, malate synthase, and oxaloacetase were assayed with an Epoch Microplate Spectrophotometer according to the specific wavelength for each enzyme. Assay protocols were modified for 96-well plate volumes, and samples were measured in triplicate. To determine activity, absorbance values were measured every 15 seconds for a 2 minute period and the change in absorbance/minute (ΔA/min) was calculated from these values. Varying amounts of enzyme filtrate (crude homogenate) were used for each sample. Concentration was normalized based on total protein values. Total protein (mg), total units (IU), and specific activity (IU/mg) were calculated for test samples showing detectable activity.

Fumarase Assay

Fumarase activity was determined based on the protocol outlined by Bergmeyer *et al.* (Sigma-Aldrich 1998). Potassium phosphate buffer (100 mM pH 7.6) was added to each sawdust sample before homogenization. Total assay volume (200 μl) contained final concentrations of 50 mM $_{L}$-malic acid and enzyme filtrate. ΔA/min was measured at 240 nm at 25°C. Enzyme activity was indicated by an increase in ΔA/min over time.

Glyoxylate Dehydrogenase Assay

Glyoxylate dehydrogenase activity was determined based on the protocol outlined by Tokimatsu *et al.* (1998). Potassium phosphate buffer (35 mM pH 8.0) was added to each sawdust sample before homogenization. Total assay volume (200 μl) contained final concentrations of 32 mM glyoxylate, 0.16 mM cytochrome *c*, and enzyme filtrate. ΔA/min was measured at 550 nm at 30°C. Enzyme activity was indicated by an increase in ΔA/min over time.

Isocitrate Lyase Assay

Isocitrate lyase activity was determined based on the protocol outlined by Chell *et al.* (Sigma-Aldrich 1996a). Imidazole buffer (50 mM pH 6.8) was added to each sawdust sample before homogenization. Total assay volume (200 μl) contained final concentrations of 50 mM $MgCl_2$, 10 mM EDTA, 40 mM phenylhydrazine HCl, 10 mM $_{DL}$-isocitrate, and enzyme filtrate. ΔA/min was measured at 324 nm at 30°C. Enzyme activity was indicated by an increase in ΔA/min over time.

Malate Synthase Assay

Malate synthase activity was determined based on the protocol outlined by Silverstein and Chell *et al.* (Sigma-Aldrich, 1996b). Imidazole buffer (50 mM pH 8.0) was added to each sawdust sample before homogenization. Total assay volume (200 μl) contained final concentrations of 100 mM $MgCl_2$, 2.5 mM acetyl CoA, 10 mM glyoxylic acid, 2 mM DTNB (prepared in 95% ethanol), and enzyme filtrate. ΔA/min was measured at 240 nm at 30°C. Enzyme activity was indicated by an increase in ΔA/min over time.

Oxaloacetase Assay

Oxaloacetase activity was determined based on the protocol outlined by Akamatsu *et al.* (1992). Potassium phosphate buffer (0.1 M pH 7.6) was added to each sawdust sample before homogenization. Total assay volume (200 μl) contained final concentrations of 0.2 M imidazole buffer, 1 mM oxaloacetic acid, and enzyme filtrate. ΔA/min was measured at 255 nm at 30°C. Enzyme activity was indicated by a decrease in ΔA/min over time.

Protein Assay

Oxalate and enzyme concentrations were normalized based on total protein concentration according to the Bradford Protein Assay protocol as previously described.

Evaluating the Role of Oxalate: Gene Expression Results

RNA Extraction

RNA was isolated using the Ambion® RNAqueous™ Kit (Ambion, Austin, TX) with an added DNase I (Promega, Madison, WI) digestion step to remove unwanted genomic DNA contaminants. For each test sample, five tubes containing 0.2 g sawdust were placed on ice and each received 1 mL denaturation buffer. Tubes were homogenized using a bead mill for three minutes, incubated on ice for three minutes, then homogenized again for three minutes. After homogenization, tubes were centrifuged at 10,000 RCF for two minutes and the supernatant was transferred into new 2.0 mL tubes free of debris. The clarified supernatant was pooled and centrifuged again to remove any residual debris. An equal volume of 64% ethanol was added to each sample and mixed

by pipetting. A 700 μl aliquot of the supernatant/ethanol mixture was added to a filter column and centrifuged at 10,000 RCF for 30 seconds. The filtrate was discarded and this step was repeated until all of the supernatant/ethanol mixture was passed through the filter. Following this step, 500 μl of Wash Solution #1 was added to the filter column and centrifuged at 10,000 RCF for 30 seconds and the flow-through was discarded. In a new tube, DNase I digestion was prepared by adding 40 μl DNase-free water, 5 μl DNase I 10x Buffer, and 5 μl DNase I enzyme. The digestion mixture was gently mixed and 50 μl was added directly to each filter and incubated at room temperature for 15 minutes. After incubation, the filter was washed twice with 500 μl of Wash Solution #2/3 and centrifuged at 10,000 RCF for 30 seconds, discarding the flow-through. The filter was centrifuged again at 10,000 RCF for 2 minutes to dry the membrane and remove any residual ethanol. The filter was placed in a new collection tube and RNA was eluted by two aliquots of 40 μl and 10 μl of 70°C Elution Solution. The filters were incubated at room temperature for one minute before being centrifuged at 10,000 RCF for one minute. Following elution, RNA was kept on ice at all times. RNA was quantified by a NanoDrop 1000 spectrophotometer (Thermo Scientific, Waltham, MA), and quality was determined by Experion™ chip electrophoresis (RNA StdSens Analysis Kit, Bio-Rad; Hercules, CA). All RNA was stored at -80°C.

cDNA Synthesis

Bio-Rad iQ™ iScript™

RNA was synthesized to first strand cDNA by the iScript™ cDNA Synthesis Kit (Bio-Rad, Hercules, CA). For each sample, 4 μl of 5x iScript™ reaction mix and 15 μl of

RNA template (0.20 μg) and nuclease-free water were added to a 0.2 mL tube and heated for 2 minutes at 70°C and immediately returned to ice. One μl of iScript™ reverse transcriptase was added to each reaction and the protocol was performed using an Eppendorff® Mastercycler with the following settings: incubation at 25°C for 5 minutes, incubation at 42°C for 30 minutes, and incubation at 85°C for 5 minutes.

Invitrogen™ SuperScript™ II Reverse Transcriptase

RNA was also synthesized to first strand cDNA by the Invitrogen™ SuperScript™ II Reverse Transcriptase Kit (Carlsbad, CA). For each sample, 1 μl of Oligo(dT)$_{12-18}$ primer, 1 μl of 10 mM dNTP mix, and 10 μl of RNA template (1 μg) and nuclease-free water were added to a 0.2 mL tube and heated for 5 minutes at 65°C then immediately returned to ice. Four μl of 5x First-Strand Buffer, 2 μl of 0.1 M DTT, and 1 μl SUPERaseIn™ was added to the reaction mix and incubated at 25°C for 10 minutes. Following incubation, 1 μl of SuperScript™ II RT was added to each reaction and mixed by pipetting gently up and down. cDNA synthesis was carried out using an Eppendorff® Mastercycler with the following settings: incubation at 42°C for 90 minutes and incubation at 85°C for 5 minutes. Non-template controls (no RNA template added to the reaction mixture) were also included.

Reverse transcriptase free controls were prepared by adding 1 μl of Oligo(dT)$_{12-18}$ primer, 1 μl of 10 mM dNTP mix, and 10 μl of RNA template (1 μg) and nuclease-free water to a 0.2 mL tube and heated for 5 minutes at 65°C then immediately returned to ice. Four μl of 5x First-Strand Buffer, 2 μl of 0.1 M DTT, and 1 μl SUPERaseIn™ was added to the reaction mix and incubated at 25°C for 10 minutes. cDNA synthesis was carried

out using an Eppendorff® Mastercycler with the following settings: incubation at 42°C for 90 minutes and incubation at 85°C for 5 minutes.

Primer Design

Expression levels of six specific genes were examined for the copper citrate and untreated test samples across all time points using real-time qPCR. Gene-specific primers were designed utilizing gene and coding (CDS) sequences of *F. radiculosa* TFFH 294 obtained from Dr. Juliet Tang. CDS sequences for isocitrate lyase (ICL), glyoxylate dehydrogenase (GLOXDH), citrate synthase (CS), succinate/fumarate antiporter (ANTI), and the copper resistance-associated ATPase pump (ATPase) were matched against gene sequences for the respective genes. Target regions spanning at least one intron were determined by Lasergene MegAlign (DNASTAR, Madison, WI). Forward and reverse primer pairs were designed for these target regions to have at least 50% GC content, no 3' complementarity, and uniquely specific for the desired region. Sequences used for real-time qPCR are listed in Table 2.1. Actin (HK) was used as the housekeeping gene.

Table 2.1 Target gene, nucleotide sequence, and reference gene accession number for all oligonucleotide primers used for gene expression.

Target Gene	Primer Sequence		Accession Number
HK	Forward	5'-GTGATGGTTGGTATGGGTCAGAAGG	XP_003026150.1
	Reverse	5'-GAAGCTCGTTGTAGAAAGTGTGATGC	
ICL	Forward	5'-CAGTACTGCATCCAGCACGAACGAGC	BAD93181.1
	Reverse	5'-CGTGACTCTGCTTGCTTGCGGTCGTG	
GLOXDH	Forward	5'-CGATGCGATCACGACAAACCTGCGCC	BAH29964.1
	Reverse	5'-CGAGGAACTTCTGCCGCCGCTTCTC	
CS	Forward	5'-CATCCTATGAGCCAATTCAGTTTGGC	EGN99006.1
	Reverse	5'-CCATGCAGTCTTCGAATACCGGCTTC	
ANTI	Forward	5'-CAAGGGATGGCTAGCAGACAAGGAG	EGO00768.1
	Reverse	5'-GCCGAATCTTCACAACCTCCATGGGC	
ATPase	Forward	5'-GCGCTGCGTCGTGGCTATGGTTGGCG	XP_002473512.1
	Reverse	5'-CCGATACAAGGATGAACGCGGCGCTG	

Primer pairs were screened by conventional PCR to insure correct regions were amplified. Only a small sample set (all four isolates, one time point, one treatment) was screened to conserve reagents. Sample reactions contained 10 μl of iQ™ Supermix, 0.5 μl forward primer, 0.5 μl reverse primer, 8 μl nuclease-free water, and 1 μl cDNA template (Bio-Rad, Hercules, CA). The reaction protocol included an initial denaturation at 95°C for 3 minutes, followed by 40 cycles of a 15 second 95°C denaturation, 30 second annealing at 65°C, 30 second 72°C extension, and a final extension at 72°C for 5 minutes. Both non-template controls (NTC) and RT-free controls were also included. A 2 μl sample of amplified product and 6 μl running buffer was added to 2 μl of loading dye (50 mM EDTA, 30% glycerol, 0.25% bromophenol blue, 0.25% xylene cyanol) and loaded into a 2% agarose gel to visualize successful amplification of the target regions.

Real-Time qPCR

To determine gene expression, Reverse Transcriptase Quantitative Polymerase Chain Reaction (RT-qPCR) was monitored in real time for the six genes in question. RT-qPCR reactions were carried out in an iCycler iQ™ 96 well PCR plates with Microseal® 'B' Film using an iQ™ 5 Real-Time PCR Detection System (Bio-Rad, Hercules, CA). Two genes of interest were performed on one plate and all samples were measured in triplicate. The 20 μl reactions contained 10 μl 2x iQ™ SYBR® Green Supermix (Bio-Rad, Hercules, CA), 8 μl sterile molecular grade water, 0.5μl of both forward and reverse primers (10 μM), and 1 μl cDNA template. The reaction protocol included an initial denaturation at 95°C for 3 minutes, followed by 40 cycles of a 15 second 95°C denaturation, 30 second annealing at 65°C, and a 30 second 72°C extension. A melt curve analysis of the resulting PCR product was performed immediately following the amplification and consisted of a 1 minute incubation at 95°C followed by a 1 minute annealing at 55°C prior to 81 cycles of 10 seconds with temperatures increase 0.5°C each cycle. Following amplification, threshold (C_T) values were calculated and normalized against expression data for the HK gene using the $2^{-\Delta\Delta C}{}_T$ method.

Evaluating the Role of Oxalate: The Effects of Copper Results

Fungal Isolates

Isolates used for this analysis include: FP-90848-T, L-9414-SP, L-11659-SP, and TFFH 294. All isolates were maintained on 2% Malt agar (BD, Fisher Scientific, Pittsburg, PA) media plates.

Test Block Preparation and Preservative Treatments

Test blocks (SYP) measuring 10 mm^3 were vacuum treated with 1.2% ammoniacal copper citrate. Untreated blocks served as controls. Both treated and untreated blocks were conditioned at 27°C and 70% relative humidity (RH) for 2 weeks. Following conditioning, all blocks were steam-sterilized for 20 minutes at at 122°C prior to exposure to prevent contamination.

Decay Test

Decay Chamber Setup

A modified version of the AWPA soil-block test (Standard E10-09) was used for this study (AWPA 2009). Decay chambers consisted of 16 oz. glass culture bottles with metal screw cap lids. The glass bottles were filled with soil (according to Standard E10-09) and an SYP feeder strip measuring 34 mm x 28 mm x 3 mm. Bottles were capped and autoclaved for sterility for 40 minutes at 16 psi and 122°C. After sterilization, chambers were placed under a laminar flow hood and allowed to cool before inoculation.

Inoculation of Feeder Strips and Incubation

Sterile bottles were inoculated aseptically with approximately 6 mm plugs of actively growing mycelia. Four mycelia plugs from each isolate were placed in each jar adjacent to the SYP feeder strips and in contact with the soil surface, respectively. Containers were capped and incubated at 27°C and 70% RH for 2 weeks to allow initial colonization of the feeder strips.

After the 2-week colonization period, five variations of copper citrate – treated test blocks were placed directly on top of the colonized SYP feeder strips to assess the difference in oxalate production when exposed to the four isolates. Variation 1 included

untreated SYP blocks to serve as primary controls. Variation 2 included 1.2% ammoniacal copper citrate blocks to serve as the secondary controls. Variation 3 included 1.2% ammoniacal copper citrate blocks placed directly on top of untreated blocks, which were in contact with the feeder strips. Variation 4 included 100 μl of 1.2% ammoniacal copper citrate added directly on top of untreated blocks. Variation 5 included untreated blocks that were adjacent to in direct contact with 1.2% ammoniacal copper citrate blocks; the copper treated blocks were introduced every two weeks (Figure 2.3). For variations 3, 4, and 5 untreated blocks were assayed for oxalate production. All containers were incubated at 27°C and 70% RH for 8 weeks; with the exception of Variation 5, which only ran for 6 weeks.

Figure 2.3 Variations on copper citrate (CC) – treated test blocks exposed to *F. radiculosa*. Bottle 1: untreated SYP; Bottle 2: CC treated SYP; Bottle 3: CC treated SYP on top of untreated SYP; Bottle 4: liquid CC on top of untreated SYP; Bottle 5: CC treated SYP adjacent to and in direct contact with untreated SYP.

Sample Preparation

Six SYP test blocks were removed from test bottles after 2, 4, 6, and 8 weeks of incubation and were gently brushed free of surface mycelia. Blocks that were tested for

oxalate production were untreated blocks (variation 1), 1.2% ammoniacal copper citrate blocks (variation 2), untreated blocks (variation 3), 100 μl of 1.2% ammoniacal copper citrate added to untreated blocks (variation 4), and untreated blocks exposed to 1.2% ammoniacal copper citrate blocks every two weeks. Appropriate blocks were placed separately in a 50 mL disposable sterile centrifuge tubes, three milliliters of 0.1 M phosphate buffer pH 7.0 was added, and the tubes were shaken for 2 hours. After agitation, one milliliter of liquid was removed and stored at -20°C for oxalate analysis.

Oxalate Assay

Concentration was analyzed (triplicate) spectrophotometrically by the Biotek Epoch 96-well plate reader at 560 nm using oxalate reagents from Trinity Biotech as described previously.

Weight Loss

Initial weights of all test blocks were recorded prior to inoculation. After oxalate concentration was determined, exposed test blocks were oven-dried overnight at 60°C and weights were recorded the following day. Test blocks were reconditioned to initial conditions (27°C 70% RH) for two weeks prior to reweighing. Weight loss (%) was calculated to determine the decay capacity of the samples with respect to treatment and time.

CHAPTER III

RESULTS AND DISCUSSION

Preliminary Study One: Sequencing Analysis Results

Sequence Analysis

The purpose of preliminary study one was to evaluate the differences, if any, by sequencing the ITS region of the fifteen *F. radiculosa* isolates. Pure culture tissue samples were successful in generating pure DNA ($A_{260/280}$ = 1.8) for all fifteen isolates. PCR amplification was successful and showed one major band for each of the fifteen isolates on the 2% agarose gel. The ITS region was sequenced for each isolate and the sequences were aligned by Clustal W in MegAlign (Lasergene®). Sequence distances (percent identity and divergence) were calculated for the fifteen different isolates (Figure 3.1). To the right of the black diagonal line in Figure 3.1 are percent identities of the fifteen sequences aligned against each other. To the left of the black diagonal line in Figure 3.1 is the divergence of the fifteen sequences aligned against each other. The evolutionary relationships between the fifteen isolates are represented in Figure 3.2.

Percent Identity

Divergence

	1	2	3	4	5	6	7	8	9	10	11	12	13	14	15		
1		99.5	98.8	76.9	94.1	78.6	99.4	68.8	83.2	96.7	90.0	99.1	99.5	82.2	97.0	1	TFFH 294.seq
2	0.5		99.4	94.5	100.0	94.6	99.8	79.3	97.5	97.1	94.1	100.0	100.0	97.7	99.5	2	Baxter-31.seq
3	1.3	0.6		99.4	99.4	99.4	99.4	87.3	99.4	99.1	96.9	99.4	99.4	99.4	99.4	3	FP-90848-T.seq
4	27.2	5.5	0.3		79.9	74.9	88.3	69.6	76.6	91.9	86.5	88.1	95.6	80.3	89.4	4	FP-103272-T.seq
5	6.1	0.0	0.6	23.1		81.1	99.1	70.8	85.7	97.1	90.3	99.1	100.0	84.5	97.2	5	FP-105309-R.seq
6	25.2	5.6	0.6	29.6	21.7		89.8	65.9	77.0	93.6	92.3	85.0	95.1	76.8	90.1	6	FP-105780-SP.seq
7	0.7	0.2	0.6	12.3	0.9	11.0		76.3	92.6	96.8	90.1	99.8	99.7	94.1	97.3	7	HHB-6386-SP.seq
8	40.3	24.1	13.9	38.3	36.7	44.8	28.6		67.2	78.3	73.9	72.7	79.6	68.7	76.7	8	L-7878-SP.seq
9	18.9	2.3	0.6	27.5	15.8	26.9	7.6	42.9		95.5	89.5	92.0	98.4	83.5	94.1	9	L-9318-SP.seq
10	3.4	2.9	0.9	8.3	2.9	6.7	3.3	25.6	4.4		91.9	97.1	97.3	96.0	96.9	10	L-9414-SP.seq
11	10.7	6.2	3.2	14.5	10.4	8.1	10.7	32.0	11.1	8.6		90.5	94.7	88.1	91.5	11	L-11659-SP.seq
12	0.9	0.0	0.6	12.6	1.0	16.7	0.2	33.7	8.3	2.9	10.2		100.0	91.1	97.4	12	L-12451-SP.seq
13	0.5	0.0	0.6	4.3	0.0	5.1	0.3	23.5	1.4	2.7	5.5	0.0		98.6	99.8	13	L-12617-SP.seq
14	20.4	2.3	0.6	22.4	17.4	27.5	6.1	40.4	18.5	4.2	13.0	9.5	1.4		94.9	14	MJL-630-SP.seq
15	3.1	0.5	0.6	11.0	2.8	10.6	2.8	27.7	6.0	3.2	9.0	2.6	0.2	5.3		15	RLG-7629-SP.seq
	1	2	3	4	5	6	7	8	9	10	11	12	13	14	15		

Figure 3.1 Sequence distances based on percent identity and divergence of the fifteen *F. radiculosa* isolates.

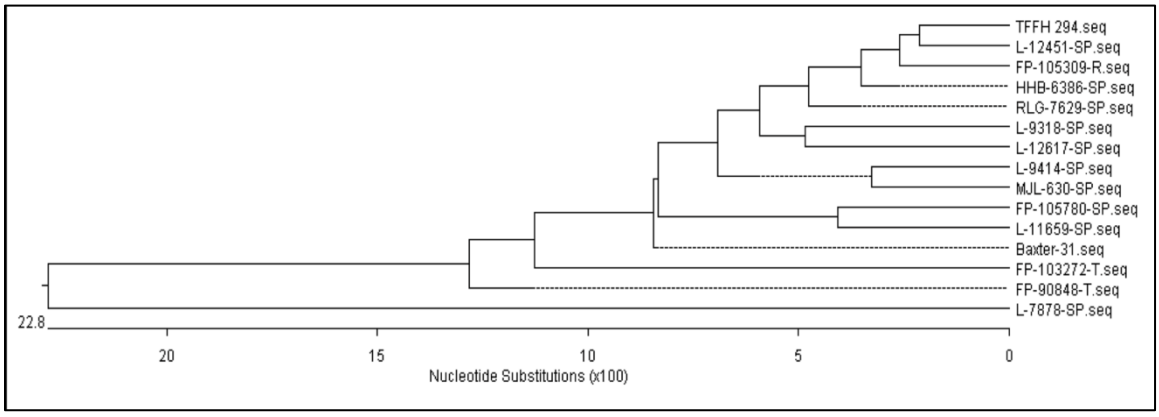

Figure 3.2 Phylogenetic tree of *F. radiculosa* isolates based on sequence distances (nucleotide substitutions).

The phylogenetic analysis of the fifteen isolates showed some variability in the ITS region. Connection at the same branch indicated two isolates were closely related in comparison to the other isolates (Figure 3.2). Overall, L-7878-SP had the highest difference in nucleotide sequences (Figure 3.2) when compared to the other fourteen isolates. The lowest percent identity match (Figure 3.1) was between FP-105780-SP and

L-7878-SP. NCBI nucleotide blast indicated that this isolate was not *Fibroporia radiculosa*.

Preliminary Study Two: Oxalate Screening Results

The purpose of preliminary study two was to determine the variation of oxalate production for the fifteen *F. radiculosa* isolates. All isolates were exposed to amine copper (CA) and micronized copper quaternary (MCQ) treated SYP wafers for a four week period. Oxalate and protein production was analyzed at two and four weeks for all samples. Concentration values depicted in the figures are the average of four biological replicates. Following the evaluation, TFFH 294 and three other isolates were chosen for enzyme analysis and gene expression based on growth capability and oxalate production.

Oxalate Assay

Results clearly indicate all isolates have the ability to produce oxalate when exposed to CA and MCQ treated SYP wafers at 2 and 4 weeks. Figure 3.3 shows the variation of oxalate concentration (mg/mL) at weeks 2 (dark) and 4 (light) for CA (blue) and MCQ (green) treated SYP wafers with respect to each isolate.

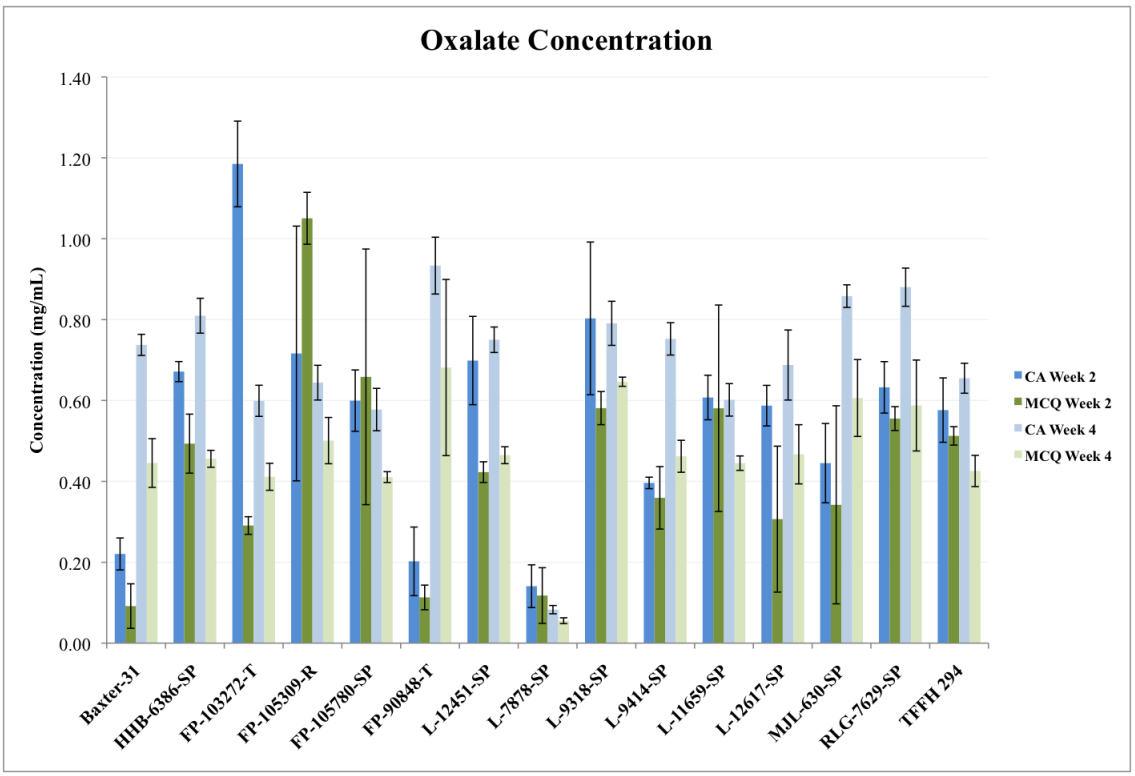

Figure 3.3 Oxalate concentration values (mg/mL) of fifteen *Fibroporia radiculosa* isolates exposed to amine copper (CA) and micronized copper quaternary (MCQ) test wafers for 2 and 4 weeks.

Overall, highest oxalate concentration was seen in FP-103272-T at week 2 on CA treated wood (1.185 mg/mL) and in FP-105309-R at week 2 on MCQ treated wood (1.050 mg/mL). At week 4 the highest oxalate concentration was seen in FP-90848-T for both CA and MCQ treated wood (0.933 mg/ml and 0.681 mg/mL, respectively). The lowest oxalate concentration for both time points was seen in L-7878-SP for both CA and MCQ treated wood. With the exception of L-7878-SP, isolates produced similar amounts of oxalate for the two treatments and time points. It is possible that the lack of high oxalate production by L-7878-SP was an indication that this organism is not copper tolerant. ANOVA analysis was performed to determine significant difference between isolates. At

the 0.05 level (Tukey's mean separation), it was found that the isolates (excluding L-7878-SP) were not significantly different from each other at both time points.

To degrade the wood cell wall components efficiently, the presence of a low pH environment appears essential. Theoretically, oxalate aids in developing the pH gradient between the fungal hyphae and the wood cell wall by precipitating calcium-oxalate crystals. This precipitation of oxalate crystals functions to drive the pH of the environment lower to allow degradation by cellulolytic enzymes (Goodell 2003; Hastrup *et al.* 2006). In the presence of copper, high oxalate accumulation initiates the precipitation of copper-oxalate crystals, which render the copper ion inert (DeGroot and Woodward 1999; Green and Clausen 2003). The formation of copper-oxalate crystals is stimulated by a low pH environment (Green and Clausen 2005). As expected, oxalate is present in the initial stages of decay; however, concentration fluctuates with respect to isolate (Figure 3.3). This fluctuation could be attributed to the organism's ability to adapt to the presence of copper within the respective test wafer or an indication of inhibition by the amine and quaternary components in the treatments. It is possible that some isolates take longer than others to acclimate to their environment in the presence of CA and/or MCQ treated wood (FP-90848-T week 4). The fluctuation could also be due to the individual isolate's ability to synthesize oxalate in the presence of the two different copper treatments. For example, FP-103272-T produced much higher concentrations of oxalate when exposed to CA at week 2 than when exposed to MCQ at week 2 (Figure 3.3). The organisms' differing capability to grow in the presence of a co – biocide most likely accounts for the differences in oxalate production between the fifteen isolates.

Protein Assay

Figure 3.4 shows the variation of protein concentration (mg/mL) at weeks 2 (dark) and 4 (light) for CA (blue) and MCQ (green) treated SYP wafers with respect to the isolate.

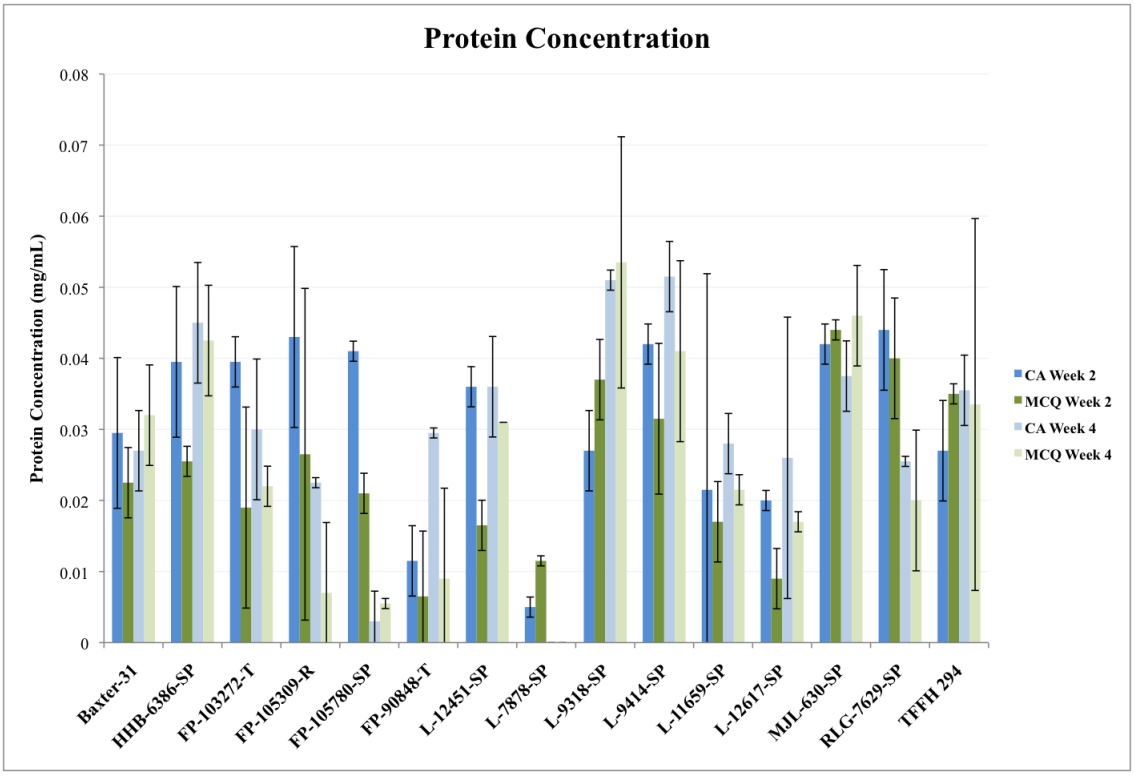

Figure 3.4 Protein concentration values (mg/mL) of fifteen *Fibroporia radiculosa* isolates exposed to amine copper (CA) and micronized copper quaternary (MCQ) test wafers for 2 and 4 weeks.

Overall, highest protein concentration was observed in L-9318-SP for both CA and MCQ treated wood at week 4. Like oxalate production, the isolates produced similar amounts of protein for the two treatments and time points. Again, L-7878-SP produced very low protein concentrations for both treatments and time points, which are most likely attributed to its poor growth on CA and MCQ, treated wood. ANOVA analysis (P =

0.05) indicated no significant difference between isolates, excluding L-7878-SP, with respect to protein production.

Protein concentration is a reflection of the active growth of a particular test fungus. An elevation in protein concentration can be directly correlated to an increase in the growth of the organism at a given time point. It can also be related to how well the organism can adapt to a particular substrate. Because protein concentration is a reflection of active growth, it can be assumed that the protein concentration might also be a reflection of how well the organism produces metabolites like oxalate. For this study, oxalate concentration might be directly compared between isolates by evaluating the protein concentration in the test samples. If an isolate produced low protein but high oxalate, the actual oxalate production for that particular isolate would be much higher in comparison to the other isolates. For example, FP-90848-T produced very low protein concentration for CA and MCQ treated wood at week 4 when compared to the other isolates (Figure 3.4). This low protein production actually means that FP-90848-T produced preferentially higher oxalate than documented (Figure 3.3), as well as much higher oxalate in comparison to the other isolates. The same holds true for high protein production and low oxalate production. For example, Baxter-31 produced relatively high protein for CA and MCQ treated wood at week 2 in comparison to the other isolates (Figure 3.4). This high protein actually means that Baxter-31 produced even lower oxalate values than documented (Figure 3.3). In reality, Baxter-31 produced very low oxalate at week 2 and FP-90848-T produced very high oxalate at week 4 in comparison to the other isolates. Measuring protein is extremely important in determining and understanding certain comparisons between isolates, treatments, and time.

Due to the lack of significant variation in oxalate and protein production between isolates, excluding L-7878-SP, other factors were examined before determining which three isolates (TFFH 294 automatically chosen) would be used for enzyme analysis and gene expression. ANOVA analysis indicated there was significant variation between CA and MCQ treated samples with respect to oxalate production, as well as significant variation between the two time points with respect to oxalate production. Although statistically there were no differences between isolates there were differences in trends between some isolates. Based on the results of this study, L-11659-SP, FP-90848-T, L-9414-SP, and TFFH 294 were used to determine enzyme activity and gene expression in relation to oxalate production.

Evaluating the Role of Oxalate: Enzyme Analysis Results

The purpose of this study was to evaluate potential factors involved in the production of oxalate within L-11659-SP, FP-98048-T, TFFH 294, and L-9414-SP when undergoing decay of 1.2% copper citrate (CC) treated and untreated (UN) SYP wafers. Test samples were analyzed for oxalate and enzyme activity for five enzymes thought to be involved in the production of oxalate. In order to determine the specific activity of each enzyme, protein concentration was also determined. Concentration values illustrated in the next series of figures are the average of four biological replicates. Based on oxalate production and enzyme activity results, only certain enzymes from this study were evaluated for the differential expression of genes.

Oxalate Assay

Overall, oxalate production reached its highest level at week 6 for all isolates when exposed both CC and UN treated wood. Lowest production of oxalate was at week 2 for all isolates exposed to both CC and UN treated wood. Figure 3.5 shows the variation of oxalate concentration (mg/mL) for each time point for each of the four isolates for both CC and UN treatments. Dark colors (green, blue, red, and purple) represent CC treatment and light colors represent UN treatment.

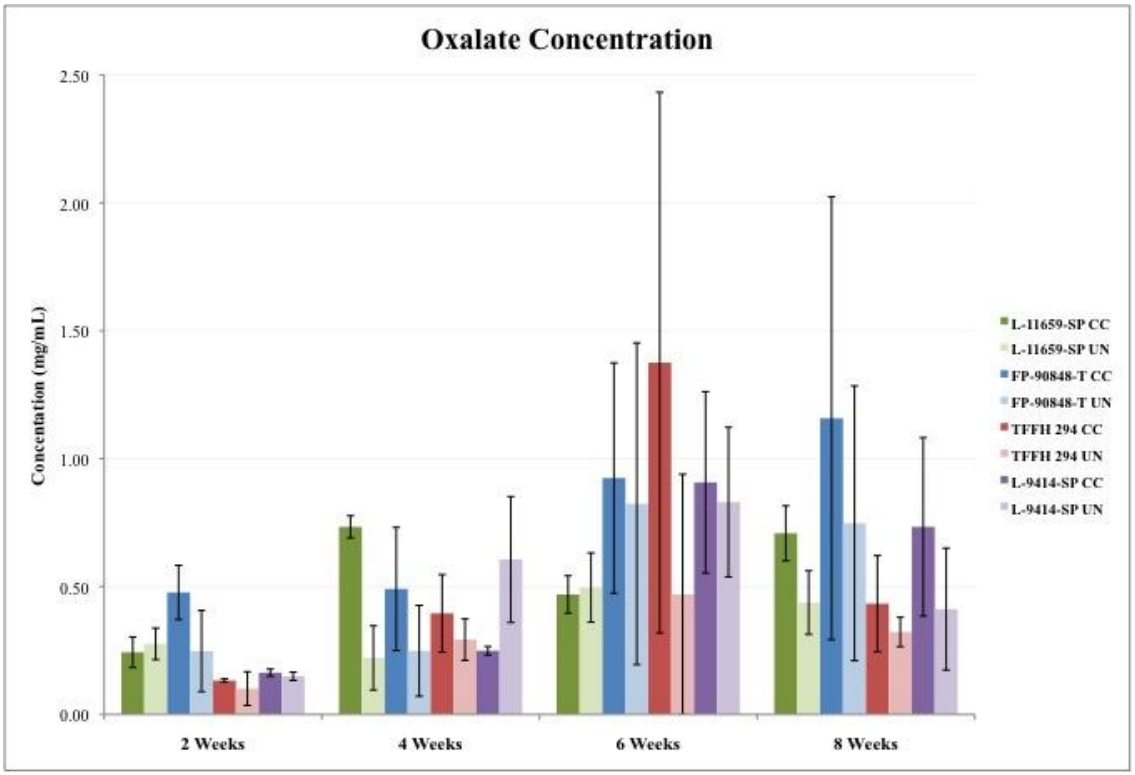

Figure 3.5 Oxalate concentration values (mg/mL) of L-11659-SP (green), FP-90848-T (blue), TFFH 294 (red), and L-9414-SP (purple) exposed to copper citrate (CC) and untreated (UN) test wafers for 2, 4, 6, and 8 weeks.

ANOVA analysis (P = 0.05) indicated a significant difference between all four time points with respect to oxalate production. Table 3.1 details the variation between the

time points; a difference of 0.1457 between mean values signifies the minimum significant difference.

Table 3.1 Statistical (ANOVA) analysis of significant variation in oxalate production with respect to time. A, B, C, and D are all significantly different from each other.

Tukey's Grouping	Time	Mean
A	6 weeks	0.78656
B	8 weeks	0.61895
C	4 weeks	0.38863
D	2 weeks	0.22376

The highest overall producer of oxalate was FP-90848-T. Figure 3.6 shows the variation of oxalate concentration (mg/mL) for each isolate exposed to both CC and UN treatments for the four time points. Dark colors (green, blue, red, and purple) represent CC treatment and light colors represent UN treatment.

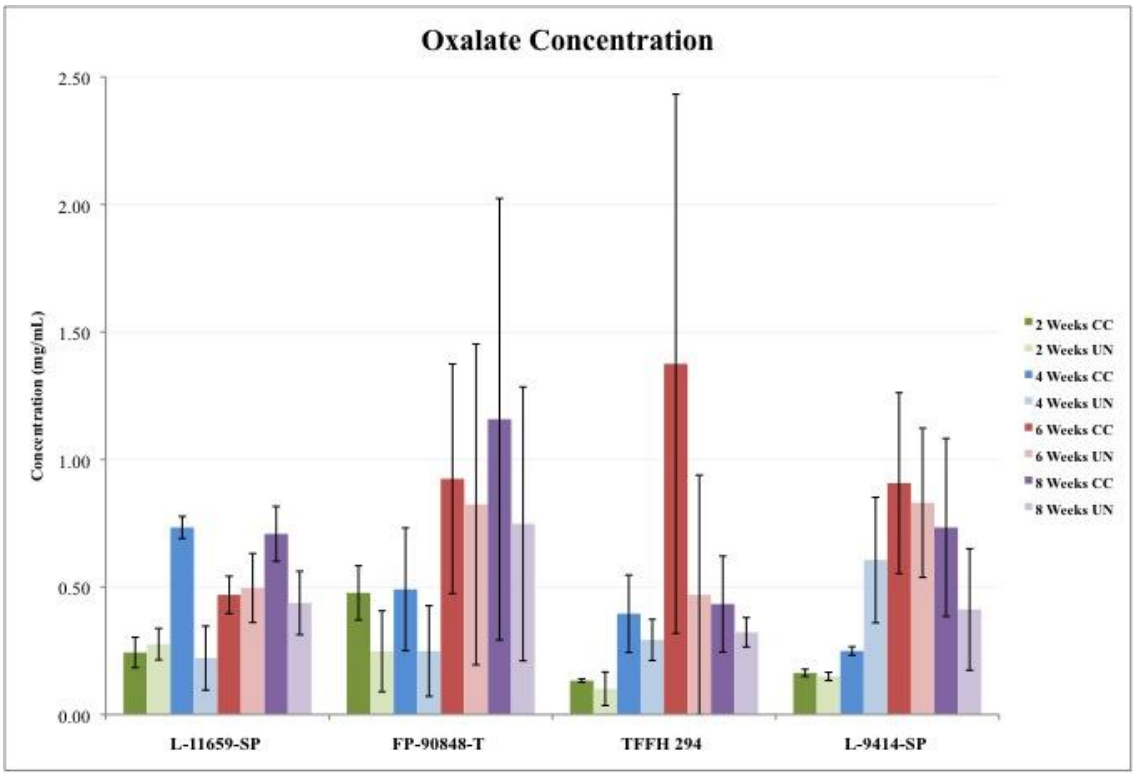

Figure 3.6 Oxalate concentration values (mg/mL) for 2 weeks (green), 4 weeks (blue), 6 weeks (red) and 8 weeks (purple) for isolates L-11659-SP, FP-90848-T, TFFH 294, and L-9414-SP exposed to copper citrate (CC) and untreated (UN) test wafers.

ANOVA analysis (P = 0.05) indicated significantly more oxalate was produced by FP-90848-T compared to L-11659-SP and TFFH 294; however, there was not a significant difference between FP-90848-T and L-9414-SP. L-11659-SP, TFFH 294, and L-9414-SP were not significantly different from each other. Table 3.2 details the variation between isolates with respect to oxalate production; a difference of 0.1449 between mean values signifies the minimum significant difference.

Table 3.2 Statistical (ANOVA) analysis of significant variation in oxalate production with respect to isolate. A is significantly different than B.

Tukey's Grouping		Isolate	Mean
	A	FP-90848-T	0.78656
B	A	L-9414-SP	0.61895
B		L-11659-SP	0.38863
B		TFFH 294	0.22376

Figure 3.7 shows CC treated wood facilitates the production of higher oxalate concentration (mg/mL) values overall. TFFH 294 at week 6 exposed to CC treated wood had the overall highest oxalate concentration value (1.375 mg/mL). L-9414-SP exposed to UN wood had higher oxalate concentration values than when exposed to CC treated wood at weeks 2, 4, and 6.

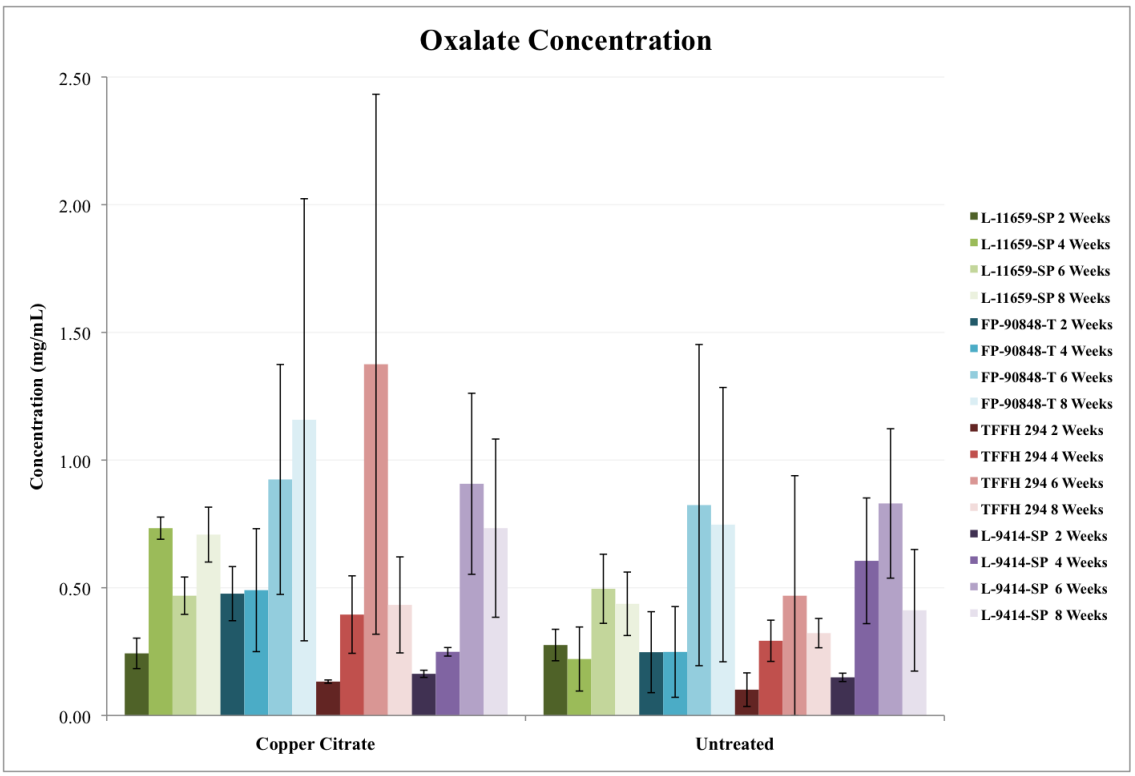

Figure 3.7 Oxalate concentration values (mg/mL) of copper citrate treated and untreated test wafers exposed to L-11659-SP (green), FP-90848-T (blue), TFFH 294 (red), and L-9414-SP (purple) for weeks 2, 4, 6, and 8.

ANOVA analysis (P = 0.05) indicated a significant difference between the two treatments with respect to oxalate production. Table 3.3 details the variation between treatments; a difference of 0.0779 between mean values signifies the minimum significant difference.

Table 3.3 Statistical (ANOVA) analysis of significant variation in oxalate production with respect to treatment. A is significantly different than B.

Tukey's Grouping	Treatment	Mean
A	Copper Citrate	0.59463
B	Untreated	0.40426

Oxalate concentration produced by the four isolates exposed to both treatments was significantly higher at week 6 (Table 3.1). FP-90848-T generated significantly higher amounts of oxalate for both CC and UN treatments over the eight week period (Table 3.2). TFFH 294 produced the lowest oxalate concentration when compared to the other three isolates over the course of the study (Table 3.2). Overall, the CC treatment stimulated significantly higher amounts of oxalate than the UN controls (Table 3.3).

Oxalate is a critical component of decay by brown-rot fungi because of its ability to establish the organism within a particular woddy environment. Because oxalate is crucial in allowing the organism to survive a certain environment, production should be higher in the initial stages of decay. Overall, accumulated oxalate increased from weeks 2 through 6 and then dropped at week 8 (Figure 3.5). It is possible that these isolates are accumulating high oxalate concentrations at week 6 because that is the time point in which oxalate is most needed. The slight drop in oxalate production at week 8 could be perceived as the time point to which the organism is beginning to establish itself in that environment and no longer needs oxalate in high quantities. It should be noted that oxalate in too high a concentration could be toxic to the fungus.

An organism will react to a particular environment as needed. In untreated wood, the production of oxalate is still necessary to reduce the pH of the surrounding environment. High levels of oxalate should not be required in untreated wood because the organism does not need to overcome any extraneous chemicals. Brown-rot fungi have evolved a mechanism to bypass the toxic effect of copper by increasing oxalate production in the presence of a copper-rich environment. In copper-treated wood, the organism stimulates higher amounts of oxalate in order to tie-up the copper ions

(DeGroot and Woodward 1999; Green and Clausen 2003). Overall, oxalate production is higher in copper citrate treated wood when compared to untreated wood (Figure 3.7; Table 3.3). Because oxalate production in CC treated wood is higher than the UN controls, it can be deduced that copper is in fact stimulating the production of oxalate in these four isolates. But, the response of an individual organisms' ability to produce higher amounts of oxalate on CC treated wood varied with respect to time and isolate.

Biologically, all organisms are unique; therefore, it is evident that different isolates will react differently to the same environment at a given time point. Interestingly, only FP-90848-T and TFFH 294 showed higher oxalate production in CC treated wood at all four time points when compared to the UN controls (Figure 3.6). At week 2, FP-90848-T showed higher oxalate accumulation in CC treated wood when compared to the UN controls (Figure 3.5). By week 4, FP-11659-SP showed higher oxalate production in CC treated wood than the UN controls (Figure 3.5). In TFFH 294, week 6 showed much higher oxalate production in CC treated wood than the UN controls (Figure 3.5). However, L-9414-SP did not show higher oxalate production on CC treated wood until week 8 (Figure 3.5). This could be attributed to the metabolism of the specific isolate and its ability to initiate specific mechanisms to overcome copper in that environment. The different responses of the four isolates could also suggest a variation in the active growth of an individual organism in response to the copper-rich environment.

Protein Assay

Unlike the oxalate levels, protein accumulation reached its highest cumulative level at week 8 for all isolates when exposed to both CC and UN treated wood with the

exception of FP-90848-T (highest at week 6). Lowest protein concentration (mg/mL) was at week 2 for all isolates exposed to both CC and UN treated wood. Figure 3.8 shows the variation of protein concentration at each time point for all four isolates exposed to both CC and UN treatments. Dark colors (green, blue, red, and purple) represent CC treatment and light colors represent UN treatment.

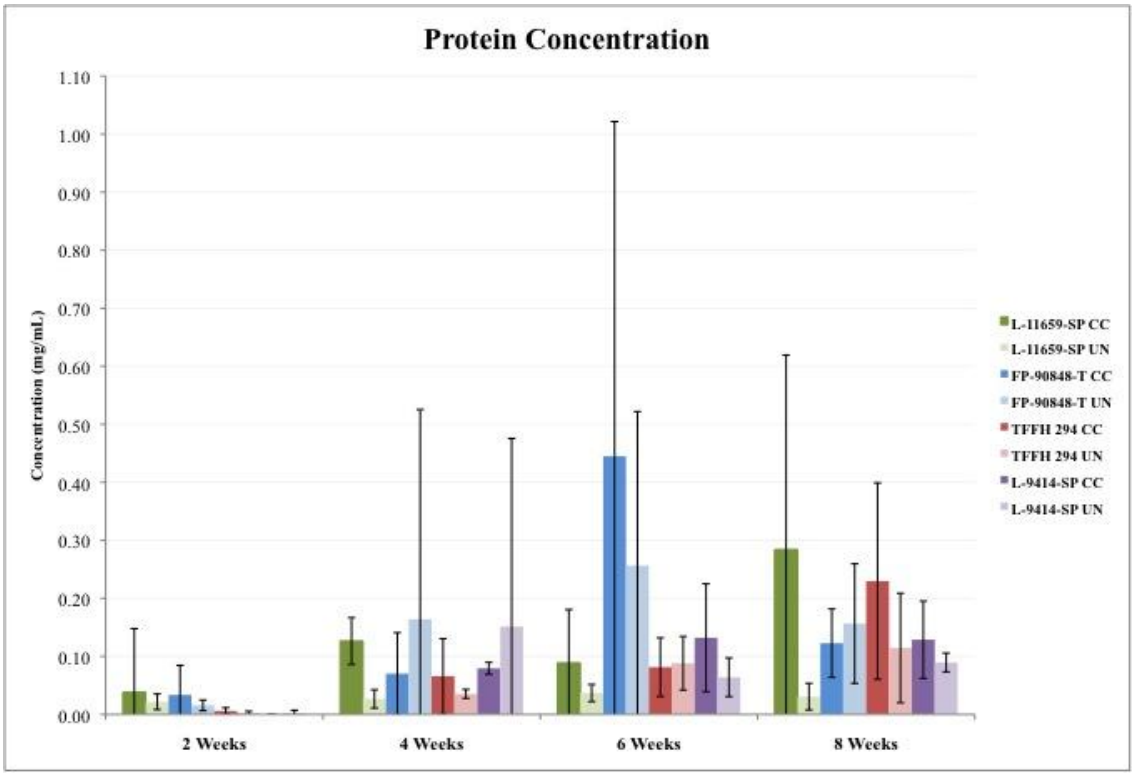

Figure 3.8 Protein concentration values (mg/mL) of L-11659-SP (green), FP-90848-T (blue), TFFH 294 (red), and L-9414-SP (purple) exposed to copper citrate (CC) and untreated (UN) test wafers for 2, 4, 6, and 8 weeks.

ANOVA analysis (P = 0.05) indicated that significantly less protein was produced at week 2 than the other three time points. Weeks 4, 6, and 8 were not significantly different from each other. Table 3.4 details the variation between the time points; a difference of 0.0819 between mean values signifies the minimum significant difference.

Table 3.4 Statistical (ANOVA) analysis of significant variation in protein production with respect to time. A is significantly different than B.

Tukey's Grouping	Time	Mean
A	6 weeks	0.14565
A	8 weeks	0.13539
A	4 weeks	0.10653
B	2 weeks	0.01860

The highest overall protein producer was FP-90848-T. Figure 3.9 shows the variation of protein concentration (mg/mL) for each isolate exposed to both CC and UN treatments for the four time points. Dark colors (green, blue, red, and purple) represent CC treatment and light colors represent UN treatment.

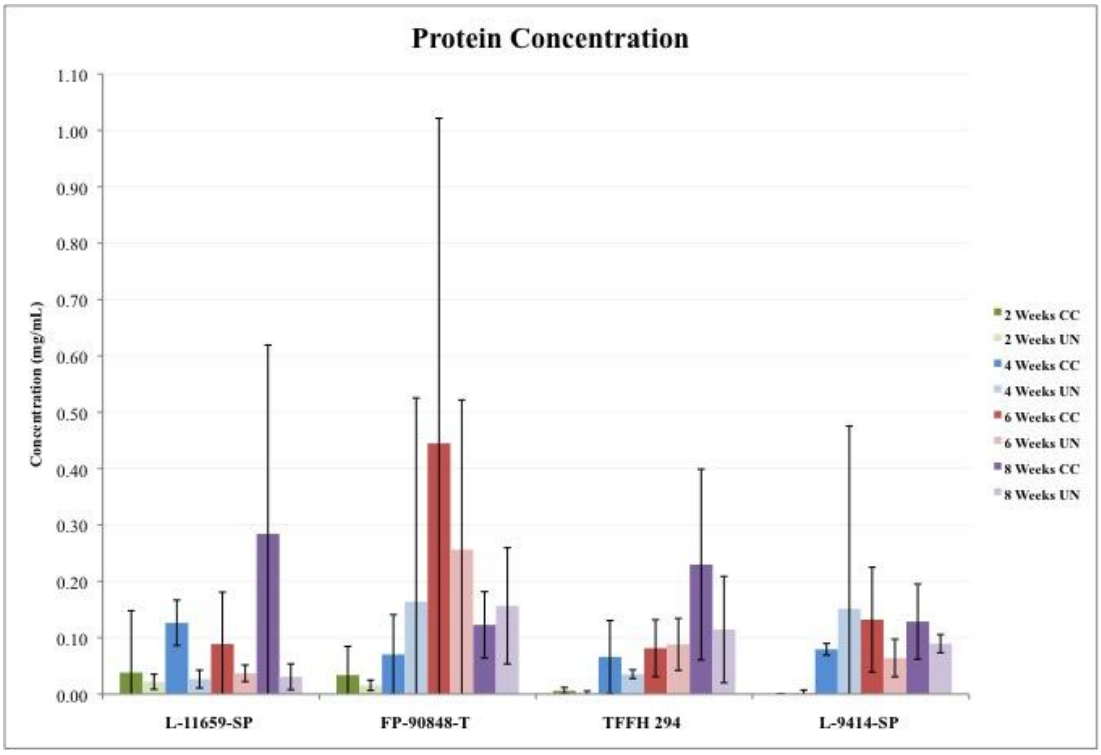

Figure 3.9 Protein concentration values (mg/mL) for 2 weeks (green), 4 weeks (blue), 6 weeks (red) and 8 weeks (purple) for isolates L-11659-SP, FP-90848-T, TFFH 294, and L-9414-SP exposed to copper citrate (CC) and untreated (UN) test wafers.

ANOVA analysis (P = 0.05) indicated no significant difference between isolates with respect to protein concentration. Table 3.5 details the variation between isolates; a difference of 0.0928 between mean values signifies the minimum significant difference.

Table 3.5 Statistical (ANOVA) analysis of significant variation in protein production with respect to isolate.

Tukey's Grouping	Isolate	Mean
A	FP-90848-T	0.14698
A	L-11659-SP	0.08710
A	TFFH 294	0.08484
A	L-9414-SP	0.07677

Figure 3.10 shows protein concentration (mg/mL) values with respect to CC treated and UN wood. For the most part, isolates on CC treated wood produced more protein than UN samples.

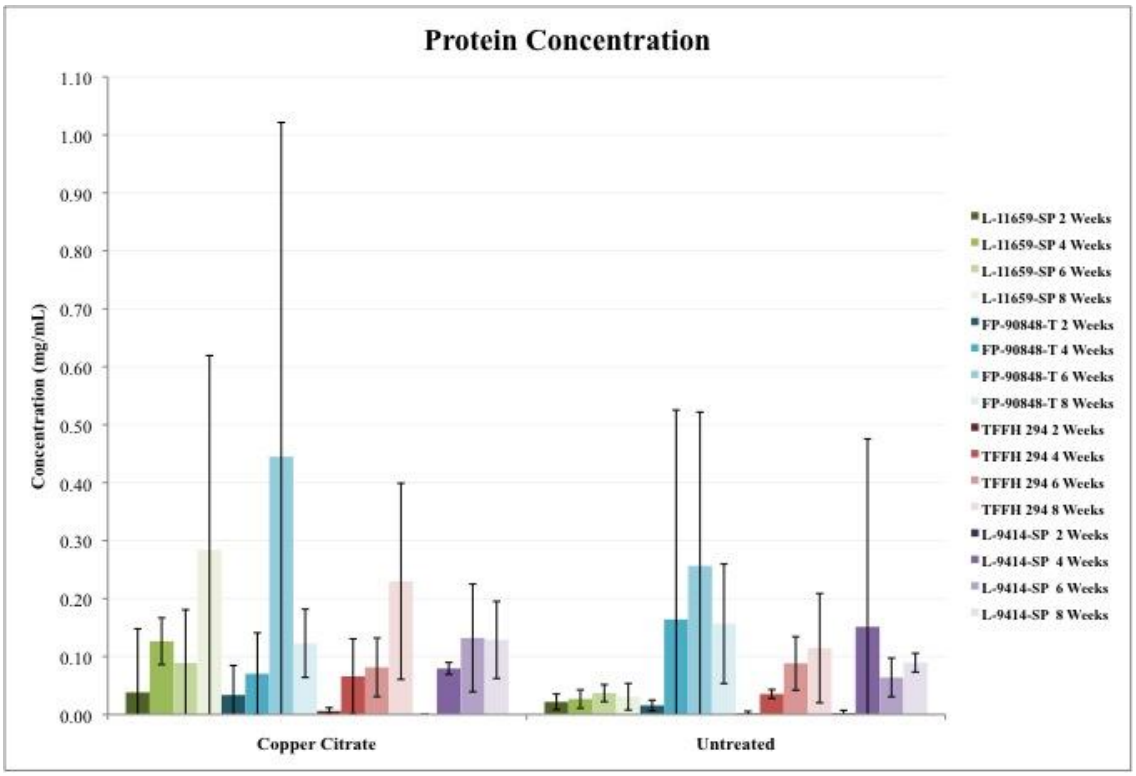

Figure 3.10 Protein concentration values (mg/mL) of copper citrate treated and untreated test wafers exposed to L-11659-SP (green), FP-90848-T (blue), TFFH 294 (red), and L-9414-SP (purple) for weeks 2, 4, 6, and 8.

ANOVA analysis (P = 0.05) indicated a significant difference between the two treatments with respect to protein production. Table 3.6 details the variation between treatments; a difference of 0.0430 between mean values signifies the minimum significant difference.

Table 3.6 Statistical (ANOVA) analysis of significant variation in oxalate production with respect to treatment. A is significantly different than B.

Tukey's Grouping	Treatment	Mean
A	Copper Citrate	0.13296
B	Untreated	0.07398

Protein concentration was significantly lower at week 2 over the course of the study (Table 3.4). FP-90848-T generated the highest protein concentration; however, the concentration was not significantly different when compared to the other three isolates (Table 3.5). It is important to note that there are differences in the amount of protein production by each isolate in comparison to the amount of oxalate production. For oxalate, the highest to lowest concentration by isolate is FP-90848-T, L-9414-SP, L-11659-SP, and TFFH 294 (Table 3.2). However, for protein, the highest to lowest concentration by isolate is FP-90848-T, L-11659-SP, TFFH 294, and L-9414-SP (Table 3.5). Like oxalate concentration, isolates exposed to the CC treatment generated significantly higher protein concentration than the UN controls (Table 3.6).

Since protein concentration is directly related to active growth, it can be assumed that higher protein production indicates better growth. Elevated protein production can also be a reflection of the amount of work it takes to overcome an unfavorable environment. In both CC and UN treated wood at week 2, isolates produced significantly less protein than the other three time points (Figure 3.8; Table 3.4). This indicates that at week 2 the fungi were just beginning to establish themselves on the wood. Theoretically, the organism could be producing only the specific proteins which aid in helping it adapt to the surrounding environment. The CC treatment showed significantly higher protein production than the UN controls (Figure 3.10; Table 3.6). The increased protein production seen in the CC treatment would suggest that these four isolates may need to produce more proteins to bypass the copper ions and obtain nutrients for growth. It could also indicate that detoxifying copper utilizes different metabolites, enzymes, and more energy. Variation in the amount of oxalate produced (Table 3.2) compared to the amount

of protein produced (Table 3.5) suggests L-11659-SP generated lower oxalate than documented, while L-9414-SP generated higher oxalate than documented.

Enzyme Assay

The change in absorbance per minute (ΔA/min) was plotted against the measured crude homogenate values (10µl, 25µl, 40µl, and 55µl) forming a linear relationship, which was used to determined the slope of the best fit line ($\Delta A/min_{sample}$) for each test sample. The $\Delta A/min_{sample}$ was used to calculate total units (IU) for enzymes showing detectable activity. Protein concentration values were used to determine total protein (mg) for each test sample. The total units (IU) and total protein (mg) were used to calculate specific activity (µmol min^{-1} mg^{-1}) for isocitrate lyase (Table 3.7) and glyoxylate dehydrogenase (Table 3.8). The four isolates are reported by treatment and time point in each of the tables.

Table 3.7 Isocitrate lyase activity (IU/mg) of copper citrate treated and untreated test wafers exposed to L-11659-SP, FP-90848-T, TFFH 294, and L-9414-SP at weeks 2, 4, 6, and 8. ε = 16,800 $M^{-1}cm^{-1}$. Assay volume = 0.2 mL; enzyme volume = 0.01 mL.

Isolate	Treatment	Time Point	Total Protein (mg)	Total Units (IU)	Specific Activity (IU/mg)
L-11659-SP	CC	Week 2	6.0500	0.0860	0.0142
L-11659-SP	CC	Week 4	1.3667	0.0917	0.0671
L-11659-SP	CC	Week 6	5.6000	0.0616	0.0110
L-11659-SP	CC	Week 8	7.8750	0.0988	0.0125
L-11659-SP	UN	Week 2	4.8250	0.0848	0.0176
L-11659-SP	UN	Week 4	2.9333	0.0976	0.0333
L-11659-SP	UN	Week 6	3.5500	0.0628	0.0177
L-11659-SP	UN	Week 8	5.1917	0.0637	0.0123
FP-90848-T	CC	Week 2	1.2250	0.1970	0.1608
FP-90848-T	CC	Week 4	1.1917	0.1827	0.1533
FP-90848-T	CC	Week 6	5.5250	0.1217	0.0220
FP-90848-T	CC	Week 8	7.8889	0.1360	0.0172
FP-90848-T	UN	Week 2	3.2500	0.1991	0.0613
FP-90848-T	UN	Week 4	3.3750	0.1455	0.0431
FP-90848-T	UN	Week 6	4.5250	0.0863	0.0191
FP-90848-T	UN	Week 8	8.1778	0.0664	0.0081
TFFH 294	CC	Week 2	1.2833	0.2568	0.2001
TFFH 294	CC	Week 4	2.9250	0.1574	0.0538
TFFH 294	CC	Week 6	8.9833	0.1506	0.0168
TFFH 294	CC	Week 8	11.1583	0.1557	0.0139
TFFH 294	UN	Week 2	1.0542	0.1929	0.1829
TFFH 294	UN	Week 4	5.7889	0.1455	0.0251
TFFH 294	UN	Week 6	10.3750	0.1268	0.0122
TFFH 294	UN	Week 8	10.5500	0.1045	0.0099
L-9414-SP	CC	Week 2	0.1000	0.0851	0.8512
L-9414-SP	CC	Week 4	1.9889	0.1956	0.0984
L-9414-SP	CC	Week 6	3.0667	0.1405	0.0458
L-9414-SP	CC	Week 8	5.2417	0.1185	0.0226
L-9414-SP	UN	Week 2	0.1750	0.1970	1.1259
L-9414-SP	UN	Week 4	2.0833	0.1438	0.0690
L-9414-SP	UN	Week 6	4.6833	0.1568	0.0335
L-9414-SP	UN	Week 8	5.9833	0.1595	0.0267

For L-11659-SP, the highest ICL activity (0.0671 IU/mg) occurred when exposed to the CC treatment at week 4. There are minimal differences in ICL activity between CC and UN treatments. The CC treatment produced higher ICL activity levels than the UN controls at weeks 4 and 8 when exposed to this isolate. FP-90848-T produced highest ICL activity (0.1608 IU/mg) when exposed to CC at week 2. Both weeks 2 and 4 stimulated much higher ICL activity than the later weeks. The CC treatment generated higher ICL activity levels than the UN controls for all time points when exposed to this isolate. TFFH 294 stimulated highest ICL activity (0.2001 IU/mg) when exposed to CC at week 2. Again, the CC treatment produced higher ICL activity than the UN controls for all time points when exposed to this isolate. L-9414-SP exposed to UN at week 2 produced the highest ICL activity (1.1259 IU/mg) of all the isolates. Weeks 4, 8, and 8 stimulated higher ICL activity when exposed to the CC treatment for this isolate.

L-11659-SP stimulated lowest ICL activity values when compared to the other three isolates. Highest ICL activity for each of the isolates was seen at week 2; week 4 also produced much higher activity values than the later weeks. When comparing all four isolates, the CC treatment only stimulated higher ICL activity at weeks 4 and 6.

Table 3.8 Glyoxylate dehydrogenase activity (IU/mg) of copper citrate treated and untreated test wafers exposed to L-11659-SP, FP-90848-T, TFFH 294, and L-9414-SP at weeks 2, 4, 6, and 8. ε = 19,600 $M^{-1}cm^{-1}$. Assay volume = 0.2 mL; enzyme volume = 0.01 mL.

Isolate	Treatment	Time Point	Total Protein (mg)	Total Units (IU)	Specific Activity (IU/mg)
L-11659-SP	CC	Week 2	2.4167	0.0133	0.0055
L-11659-SP	CC	Week 4	4.5000	0.0272	0.0060
L-11659-SP	CC	Week 6	6.1500	0.0283	0.0046
L-11659-SP	CC	Week 8	6.4445	0.0224	0.0035
L-11659-SP	UN	Week 2	4.2583	0.0156	0.0037
L-11659-SP	UN	Week 4	3.4222	0.0259	0.0076
L-11659-SP	UN	Week 6	3.5250	0.0247	0.0070
L-11659-SP	UN	Week 8	2.1722	0.0133	0.0061
FP-90848-T	CC	Week 2	3.1667	0.0304	0.0096
FP-90848-T	CC	Week 4	2.9167	0.0311	0.0107
FP-90848-T	CC	Week 6	11.0000	0.0622	0.0057
FP-90848-T	CC	Week 8	3.6222	0.0510	0.0141
FP-90848-T	UN	Week 2	1.5375	0.0263	0.0171
FP-90848-T	UN	Week 4	5.0333	0.0224	0.0045
FP-90848-T	UN	Week 6	6.2833	0.0416	0.0066
FP-90848-T	UN	Week 8	5.8222	0.0490	0.0084
TFFH 294	CC	Week 2	0.9500	0.0115	0.0121
TFFH 294	CC	Week 4	3.9250	0.0349	0.0089
TFFH 294	CC	Week 6	6.1444	0.0747	0.0122
TFFH 294	CC	Week 8	6.9583	0.0357	0.0051
TFFH 294	UN	Week 2	0.2583	0.0140	0.0543
TFFH 294	UN	Week 4	4.6167	0.0385	0.0083
TFFH 294	UN	Week 6	7.6333	0.0321	0.0042
TFFH 294	UN	Week 8	7.9083	0.0508	0.0064
L-9414-SP	CC	Week 2	0.1000	0.0151	0.1510
L-9414-SP	CC	Week 4	4.0556	0.0395	0.0097
L-9414-SP	CC	Week 6	6.9833	0.0556	0.0080
L-9414-SP	CC	Week 8	11.0083	0.0622	0.0057
L-9414-SP	UN	Week 2	0.1375	0.0232	0.1688
L-9414-SP	UN	Week 4	0.3189	0.0259	0.0811
L-9414-SP	UN	Week 6	5.8667	0.0492	0.0084
L-9414-SP	UN	Week 8	5.4222	0.0135	0.0025

L-11659-SP produced highest GLOXDH activity (0.0076 IU/mg) when exposed to UN at week 4. Like the ICL activity, there are minimal differences in GLOXDH activity between CC and UN treatments. The UN controls produced higher ICL activity levels than the CC treatment at weeks 4, 6, and 8 when exposed to this isolate. FP-90848-T produced highest GLOXDH activity (0.0171 IU/mg) when exposed to UN at week 2. The CC treatment generated higher GLOXDH activity levels than the UN controls at weeks 4 and 8 when exposed to this isolate. TFFH 294 stimulated highest GLOXDH activity (0.0543 IU/mg) when exposed to UN at week 2. The CC treatment produced higher GLOXDH activity than the UN controls at weeks 4 and 6 when exposed to this isolate. L-9414-SP exposed to UN at week 2 produced the highest GLOXDH activity (0.1688 IU/mg). Only week 8 stimulated higher GLOXDH activity when exposed to the CC treatment for this isolate.

Like ICL activity, L-11659-SP stimulated lowest GLOXDH activity values when compared to the other three isolates. Highest GLOXDH activity for each of the isolates was seen at week 2 and continued to decrease with respect to time.

ANOVA analysis ($P = 0.05$) indicated a significant difference between the two enzymes with respect to specific activity. ICL produced much higher activity than GLOXDH for each of the isolates exposed to both CC and UN treatments. Table 3.9 details the variation between enzymes.

Table 3.9 Statistical (ANOVA) analysis of significant variation in specific activity with respect to enzyme. A difference of 0.0564 between mean values indicates the minimum significant difference.

Tukey's Grouping	Enzyme	Mean
A	ICL	0.15862
B	GLOXDH	0.02659

ANOVA analysis (P = 0.05) indicated a significant difference between week 2 and the other three time points with respect to specific activity. Week 2 produced much higher activity levels for both ICL and GLOXDH. Table 3.10 details the variation between time.

Table 3.10 Statistical (ANOVA) analysis of significant variation in specific activity with respect to time. A difference of 0.1049 between mean values indicates the minimum significant difference.

Tukey's Grouping	Time	Mean
A	2 Weeks	0.24205
B	4 Weeks	0.06571
B	6 Weeks	0.04862
B	8 Weeks	0.01187

ANOVA analysis (P = 0.05) indicated a significant difference between L-9414-SP and the other three isolates with respect to specific activity. Both ICL and GLOXDH total activity levels were highest in L-9414-SP. Table 3.11 details the variation between isolate.

Table 3.11 Statistical (ANOVA) analysis of significant variation in specific activity with respect to isolate. A difference of 0.1048 between mean values indicates the minimum significant difference.

Tukey's Grouping	Isolate	Mean
A	L-9414-SP	0.25306
B	FP-90848-T	0.05347
B	TFFH 294	0.05178
B	L-11659-SP	0.01587

ANOVA analysis (P = 0.05) indicated no significant difference between the two treatments with respect to specific activity. Table 3.12 details the variation between treatments.

Table 3.12 Statistical (ANOVA) analysis of significant variation in specific activity with respect to treatment. A difference of 0.057 between mean values indicates the minimum significant difference.

Tukey's Grouping	Treatment	Mean
A	Untreated	0.09705
A	Copper Citrate	0.08866

There was no detectable enzymatic activity for fumarase, malate synthase, and oxaloacetase for all isolates exposed to both treatments. However, all samples tested for fumarase, malate synthase, and oxaloacetase activity increased in protein concentration over the 8 week period. Measurable protein could be an indication of the production of proteins unrelated to these three enzymes.

Specific activity details the proclivity of an enzyme. The activity of an enzyme is dependent on the amount of total protein in the sample and indicates how efficiently it can convert substrate to product under the given conditions. For this study, the specific activity of ICL and GLOXDH was determined using the change in absorbance per minute

(ΔA/min) and the protein concentration of the crude-homogenate in each of the test samples. Because the crude-homogenate was used to measure protein concentration, the specific enzyme was not the only measurable protein in the crude-homogenate mixture. It is highly likely that the protein assay measured a variety of proteins and metabolites present in the crude-homogenate sample. This could explain the low specific activity values for both ICL and GLOXDH. It could also explain why FUM, MS, and OAA had undetectable activity (ΔA/min). If other metabolites and proteins were present in the crude-homogenate, it is possible that they could have interfered with FUM, MS, and OAA detection. Theoretically, all five enzymes should have been detected because they are important components in the TCA and GLOX cycles (Figure 1.1). However, because only ICL and GLOXDH showed activity (ΔA/min), it is probable that FUM, MS, and OAA were undetectable because they existed in low quantities.

ICL is a central enzyme in the production of oxalate (Munir *et al.* 2001). In this study, ICL production was significantly higher than GLOXDH production for the four isolates (Table 3.9). In theory, ICL production should be higher because it feeds into both the TCA and GLOX cycles (Figure 1.1). In the TCA cycle, ICL converts isocitrate to glyoxylate. ICL is also found in the GLOX cycle and again converts isocitrate to glyoxylate. For all four isolates, ICL activity was highest at week 2 for both CC and UN treated wood. Because ICL generates glyoxylate, it would make sense for it to be highly produced at the earlier time points. In all four isolates, oxalate production was significantly lower at week 2 (Table 3.1). If ICL is a central enzyme in oxalate production, it would need time to convert enough glyoxylate before oxalate levels start increasing. At week 4, the CC treatment generated higher ICL activity than the UN

controls. The CC treatment started generating higher oxalate production when compared to the UN controls at week 8 (Figure 3.5). This could also be a reflection of the amount of time needed by the fungus to overcome initial exposure to copper and start efficiently generating oxalate in higher quantities.

GLOXDH has been linked to the direct production of oxalate (Munir *et al.* 2001; Yoon *et al.* 2002). The GLOX cycle produces glyoxylate which leaves the cycle to be acted on by GLOXDH to produce oxalate (Figure 1.1). GLOXDH is expressed significantly lower than ICL (Table 3.9), which makes sense because GLOXDH is only found in the GLOX cycle. Theoretically, if GLOXDH is a key factor in the biosynthesis of oxalate it should reflect the same patterns in both oxalate production and enzyme activity for the four isolates. It is important to note that the differences between the CC and UN treatments in oxalate production (Figure 3.6) correlate to the differences between the CC and UN treatments in GLOXDH activity (Table 3.8) for FP-90848-T, TFFH 294, and L-9414-SP.

Evaluating the Role of Oxalate: Gene Expression Analysis Results

The purpose of this study was to determine expression levels of specific genes within L-11659-SP, FP-98048-T, TFFH 294, and L-9414-SP undergoing decay of 1.2% copper citrate (CC) treated and untreated (UN) SYP wafers. Extracted RNA from each test sample was converted to cDNA, which was used to evaluate expression levels of five genes thought to be involved in oxalate production. Fold change was determined for all samples using TFFH 294 exposed to untreated controls at week 4 as the endogenous control.

RNA Quantification

After the samples were successfully extracted for RNA, the quantity and quality was evaluated by Experion™ chip electrophoresis. Figure 3.11 shows the integrity of RNA for the 32 samples used for gene expression. Because of poor quality and RNA degradation, several samples had to be re-extracted and can be seen in Figure 3.11D. After re-extraction, samples did not demonstrate RNA degradation.

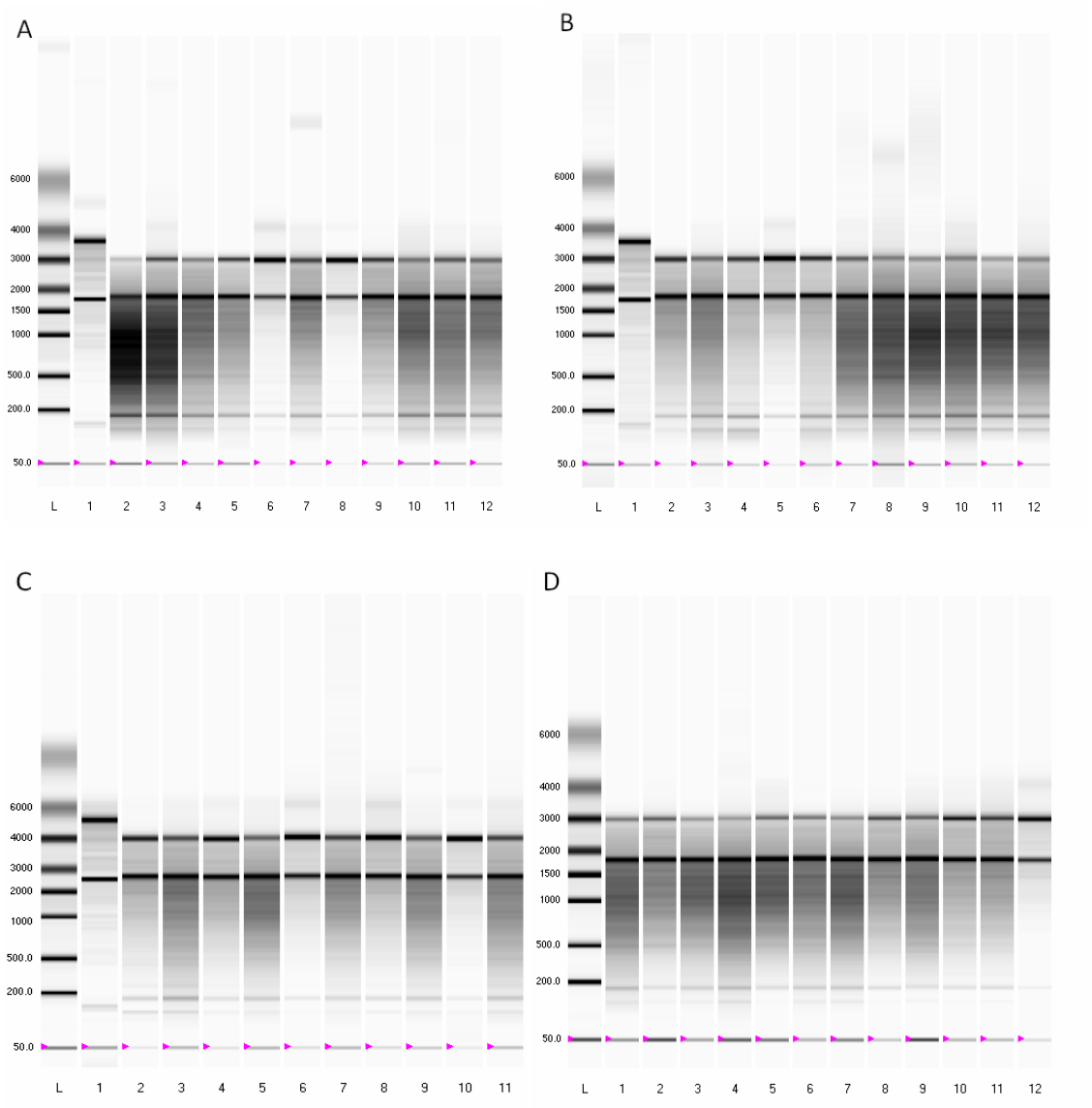

Figure 3.11 Gel image of extracted RNA for gene expression analysis: Ladders are designated L; (A) wells are 1, rat brain RNA; 2 – 9, L-11659-SP w2-8; 10 – 12, FP-90848-T w2-4; CC treatment even wells; UN treatment odd wells; (B) wells are 1, rat brain RNA; 2 – 6, FP-90848-T w4-8; 7 – 12, L-9414-SP w2-6; UN treatment even wells, CC treatment odd wells; (C) wells are 1, rat brain RNA; 2 – 3, L-9414-SP w8; 4 – 11, TFFH 294 w2-8; CC treatment even wells; UN treatment odd wells; (D) wells are 1, L-11659-SP CC w2; 2 – 8, L-9414-SP w4-8 UN even wells, CC odd wells; 9 – 12, TFFH 294 UN wk2-8.

cDNA Synthesis and Primer Design

Two cDNA synthesis protocols (iScript™ cDNA Synthesis and Invitrogen™ SuperScript™ II Reverse Transcriptase) were performed on the 32 samples used for gene expression. To determine the more efficient protocol, a conventional PCR amplification of cDNA from a small sample set (L-11659-SP, FP-90848-T, TFFH 294, and L-9414-SP; CC week 2) was carried out to verify if the target regions were being actively produced by all four isolates. Target regions in question were isocitrate lyase (ICL), glyoxylate dehydrogenase (GLOXDH), citrate synthase (CS), succinate/fumarate antiporter (ANTI), and the copper resistance-associated ATPase pump (ATPase). Gel electrophoresis of the amplified PCR products demonstrated that the four samples generated appropriate base-pair length bands for each of the target regions in question.

Bio-Rad iQ™ iScript™

RNA was synthesized to first strand cDNA by the Bio-Rad iScript™ cDNA Synthesis protocol for the four samples. Amplified PCR products for ICL, GLOXDH, CS, ANTI, and ATPase target regions can be seen in Figure 3.12. Multiple bands are seen for all five target regions. Based on the size of the band, the second band is the result of DNA contamination of an intron due to inefficient priming.

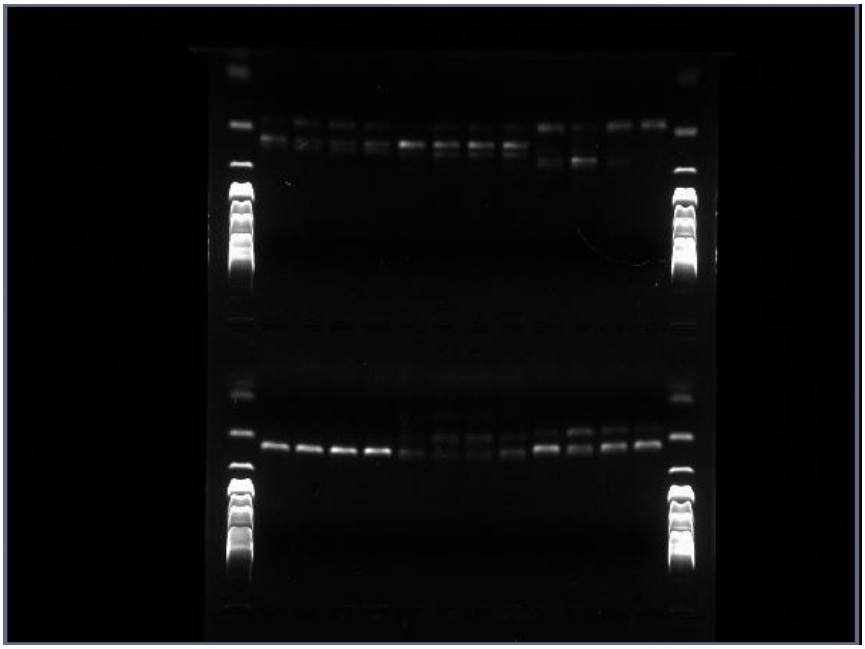

Figure 3.12 Gel image of the Bio-Rad iScript™ cDNA Synthesis protocol. Ladders are on the outer lanes. The four samples were amplified for all target regions; L-11659-SP, FP-90848-T, TFFH 294, and L-9414-SP. Bottom row lanes: 1 – 4, 18S; 5 – 8, ICL; 9 – 12, GLOXDH. Top row lanes: 1 – 4, CS; 5 – 8, ANTI; 9-12, ATPase.

Invitrogen SuperScript™ II Reverse Transcriptase

RNA was synthesized to first strand cDNA by the Invitrogen™ SuperScript™ II Reverse Transcriptase protocol for the four samples. Amplified PCR products for ICL, GLOXDH, CS, ANTI, and ATPase target regions can be seen in Figure 3.13. Multiple bands were not seen for the majority of the target regions (exception L-9414-SP CS) with this cDNA synthesis protocol. The ICL region was not pictured in this gel; however, it showed no double band for the four samples.

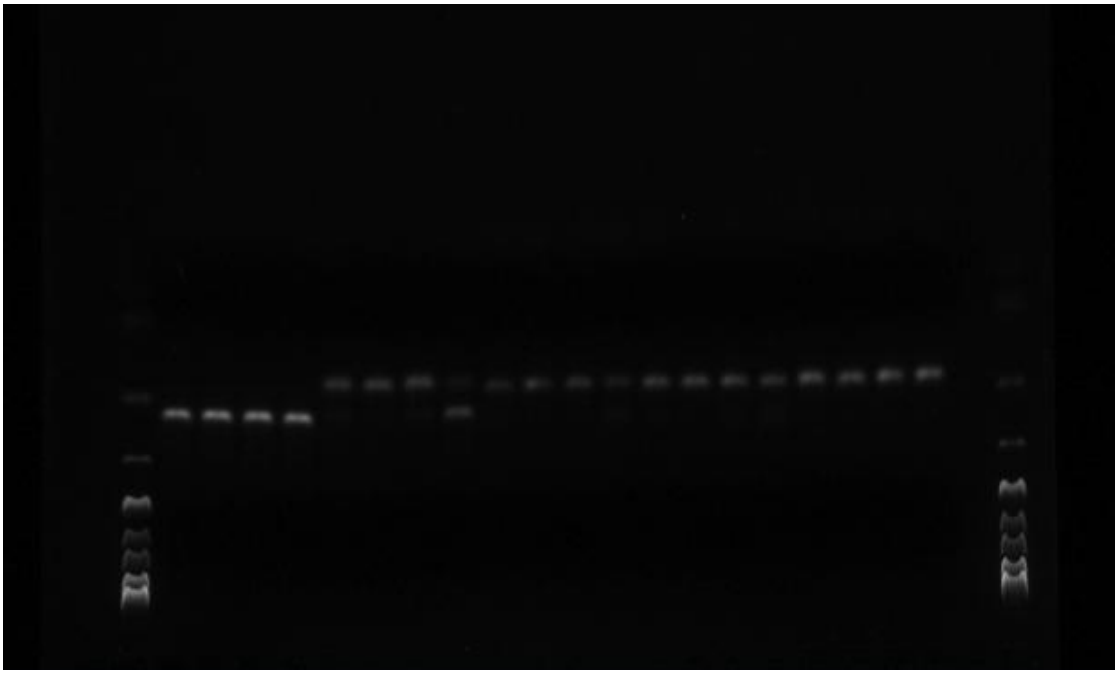

Figure 3.13 Gel image of the Invitrogen™ SuperScript™ II Reverse Transcriptase protocol. Ladders are on the outer lanes. The four samples were amplified for all target regions; L-11659-SP, FP-90848-T, TFFH 294, and L-9419-SP. From left to right lanes: 1 – 4, 18S; 5 – 8, GLOXDH; 9 – 12, CS; 13 – 16, ANTI; 17 – 20, ATPase. Lane 21 is the non-template control (no band).

The Bio-Rad iScript™ cDNA Synthesis protocol uses both random hexamers and oligo dT primers to generate cDNA synthesis. Random hexamers target random points in the sequence to initiate cDNA synthesis, while oligo dT primers target the 3' poly A sequence to begin cDNA synthesis. The Invitrogen™ SuperScript™ II Reverse Transcriptase protocol only uses oligo dT primers to generate cDNA synthesis. Inefficiency of the Bio-Rad protocol could be a result of the use of random hexamers, which could have a higher probability of amplifying DNA contaminates when used in combination with the five target primers designed for this study. It is evident that the Invitrogen™ protocol produced target regions that were not contaminated by DNA

(Figure 3.13). For these reasons, cDNA synthesized by the Invitrogen™ SuperScript™ II Reverse Transcriptase protocol was used to measure expression levels of ICL, GLOXDH, CS, ANTI, and ATPase.

Expression Levels

Real-time qPCR was used to analyze C_T values of the test samples for ICL, GLOXDH, CS, ANTI, and ATPase genes. Using the actin (HK) mean C_T, average replicate C_T values were normalized for all plates. Normalized C_T values were used to calculate the mean fold change ($2^{-\Delta\Delta C_T}$) in expression of the five genes using the comparative C_T method (Livak and Schmittgen 2001). TFFH 294 exposed to UN controls at week 4 was used as the endogenous control for all calculations. In the subsequent graphs, the expression level for the endogenous control is set at 1. If the other isolates/time points expression levels are above 1, expression is increased by a certain factor, which results in a higher gene production for the respective sample. If expression levels are below 1, expression is decreased, which results in a lower gene production for the respective sample.

Relative changes in ICL expression for each isolate with respect to time can be seen in Figure 3.14 and 3.15. Dark colors (green, blue, red, and purple) represent CC treatment and light colors represent UN treatment (Figure 3.14). In general, there was not a large variation in fold change values between treatment, isolate, and time for ICL with respect to the endogenous control. L-9414-SP exposed to CC at week 2 had the highest fold change difference (5.352) when compared to the other three isolates. The CC treatment generated higher fold change differences when compared to the UN controls for TFFH 294 and L-9414-SP at week 2 and L-11659-SP at week 6.

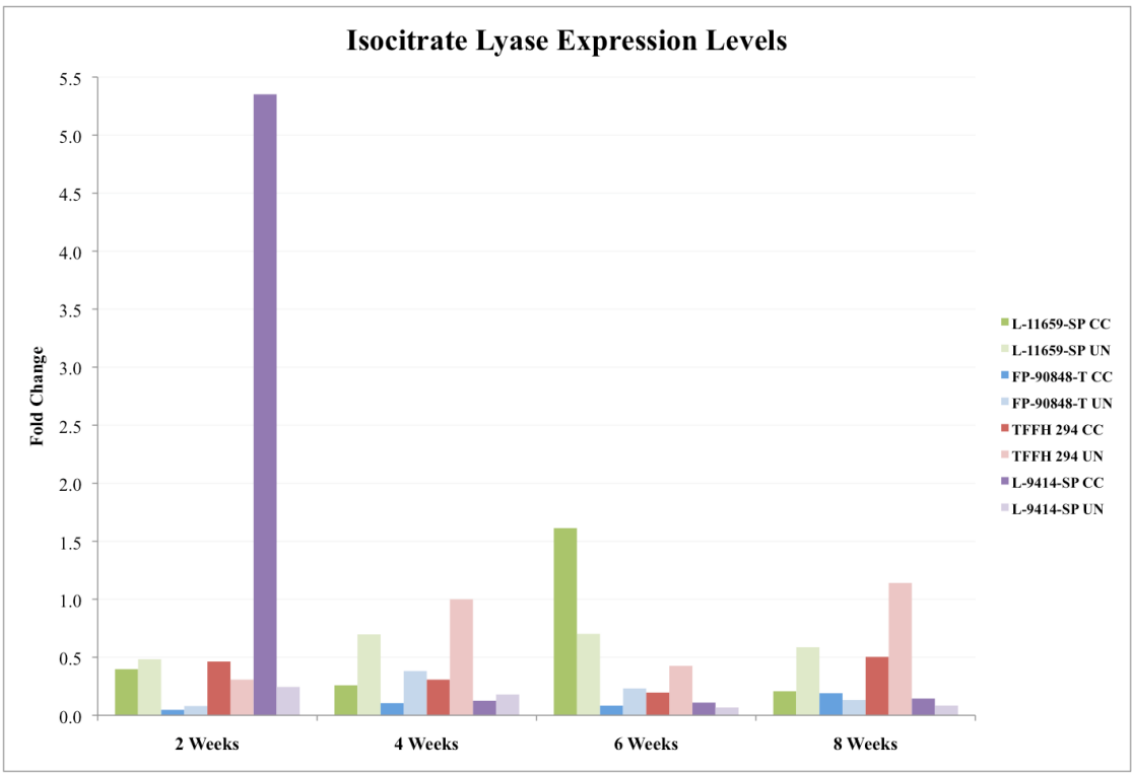

Figure 3.14 Isocitrate lyase expression levels of L-11659-SP (green), FP-90848-T (blue), TFFH 294 (red), and L-9414-SP (purple) exposed to copper citrate (CC) and untreated (UN) test wafers for 2, 4, 6, and 8 weeks.

Dark colors (green, blue, red, and purple) represent CC treatment and light colors represent UN treatment (Figure 3.15). L-11659-SP and TFFH 294 had the largest fold change difference in comparison to the other three isolates. Interestingly, FP-90848-T showed low expression levels at all time points when compared to the endogenous control. With the exception of the CC treatment at week 2, L-9414-SP also had lower expression levels when compared to the endogenous control. Nearly all of the isolates at the four time points showed higher expression levels in the UN controls when compared to the CC treatment.

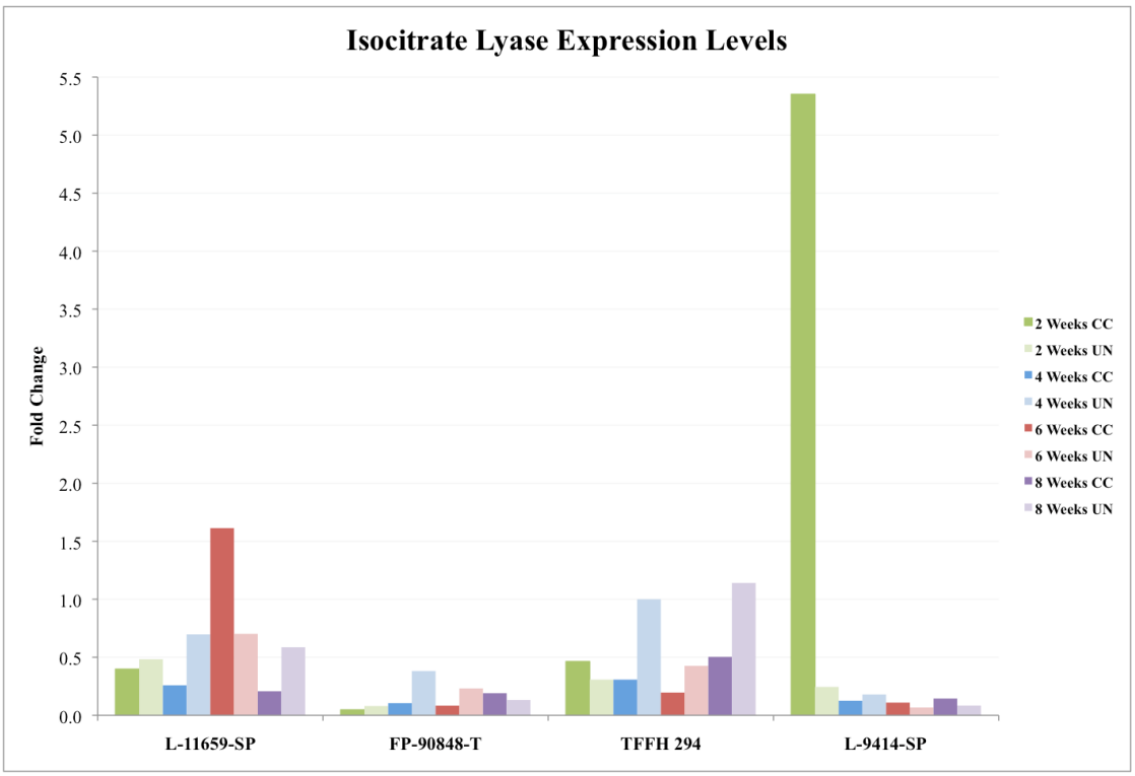

Figure 3.15 Isocitrate lyase expression levels for 2 weeks (green), 4 weeks (blue), 6 weeks (red) and 8 weeks (purple) for isolates L-11659-SP, FP-90848-T, TFFH 294, and L-9414-SP exposed to copper citrate (CC) and untreated (UN) test wafers.

Relative changes in GLOXDH expression for each isolate with respect to time can be seen in Figures 3.16 and 3.17. Dark colors (green, blue, red, and purple) represent CC treatment and light colors represent UN treatment (Figure 3.16). Like ICL expression levels, there was not a large variation in fold change values between treatment, isolate, and time for GLOXDH with respect to the endogenous control (TFFH 294 UN w4) with a few exceptions. L-9414-SP exposed to CC at week 2 had the highest fold change difference (5.657) when compared to the other three isolates. The CC treatment generated higher expression of GLOXDH for L-11659-SP, TFFH 294, and L-9414-SP when compared to the UN controls at week 2 but not at the other time points. L-11659-SP exposed to CC at week 6 also showed higher expression levels than UN controls.

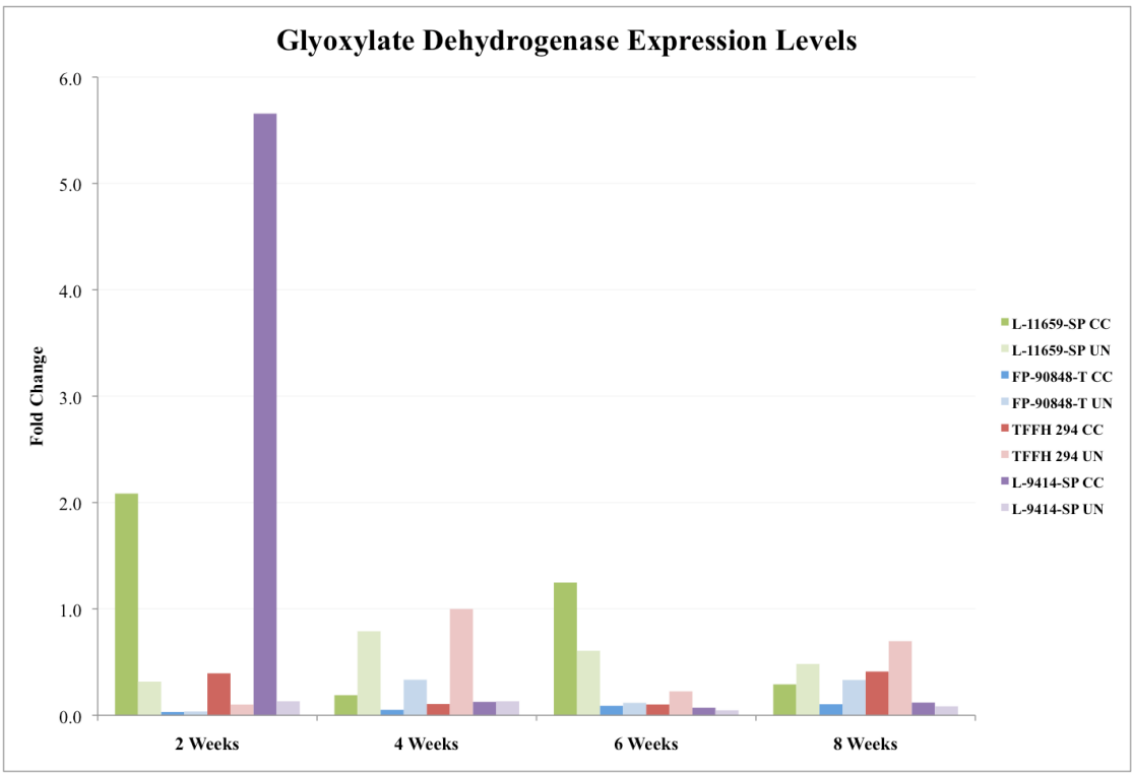

Figure 3.16 Glyoxylate dehydrogenase expression levels of L-11659-SP (green), FP-90848-T (blue), TFFH 294 (red), and L-9414-SP (purple) exposed to copper citrate (CC) and untreated (UN) test wafers for 2, 4, 6, and 8 weeks.

Dark colors (green, blue, red, and purple) represent CC treatment and light colors represent UN treatment (Figure 3.17). Overall, L-11659-SP had the largest fold change difference in comparison to the endogenous control and the other three isolates for the four time points. FP-90848-T had the lowest GLOXDH expression when compared to the other isolates. The CC treatment did not stimulate higher GLOXDH expression levels than the UN controls for FP-90848-T. The UN controls showed lower expression levels than the CC treatment for L-9414-SP at weeks 2, 6, and 8. TFFH 294 showed higher expression on CC treated wood at week 2 only, while L-11659-SP showed higher expression on CC treated wood at weeks 2 and 6.

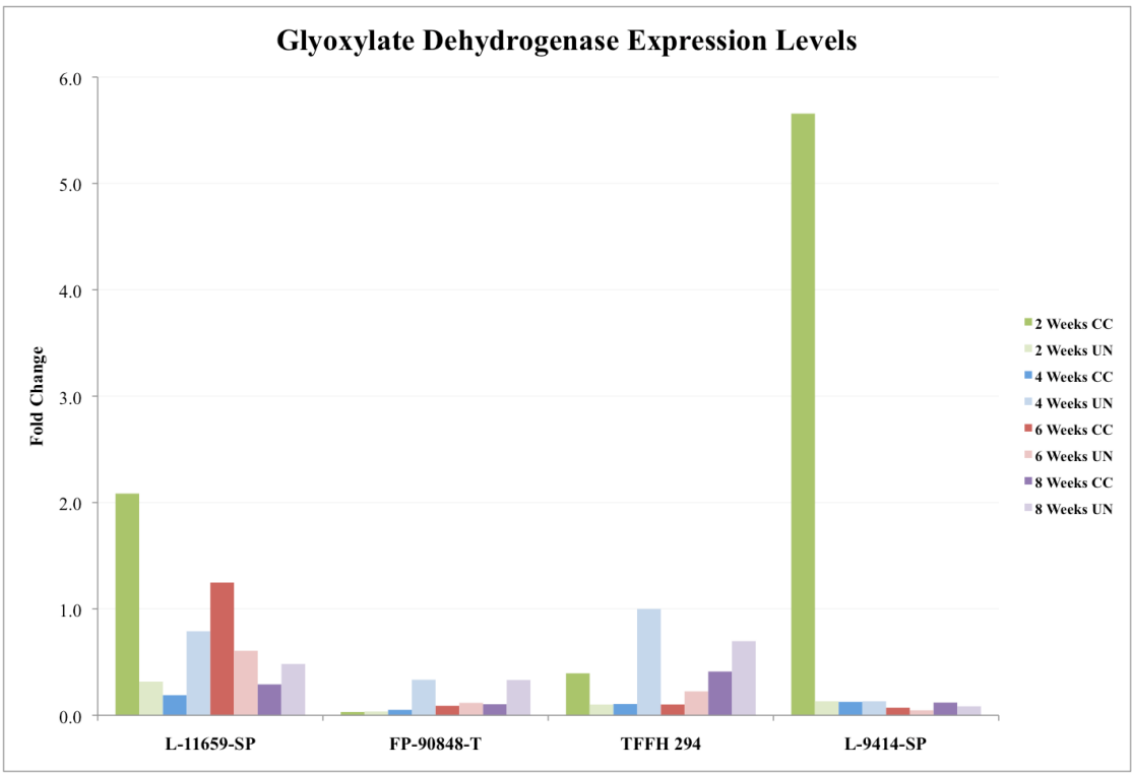

Figure 3.17 Glyoxylate dehydrogenase expression levels for 2 weeks (green), 4 weeks (blue), 6 weeks (red) and 8 weeks (purple) for isolates L-11659-SP, FP-90848-T, TFFH 294, and L-9414-SP exposed to copper citrate (CC) and untreated (UN) test wafers.

Relative changes in CS expression for each isolate with respect to time can be seen in Figures 3.18 and 3.19. Dark colors (green, blue, red, and purple) represent CC treatment and light colors represent UN treatment (Figure 3.18). Like ICL and GLOXDH expression levels, CS fold change differences do not largely vary between isolate, treatment, and time with respect to the endogenous control (TFFH 294 UN w4). Like GLOXDH, week 2 shows higher fold change differences for L-11659-SP, TFFH 294, and L-9414-SP for the CC treatment in comparison to the UN controls. L-9414-SP exposed to CC at week 2 had the highest fold change difference (4.724) when compared to the other three isolates. Week 6 for both CC and UN treatments showed lower fold change differences in comparison to all other time points.

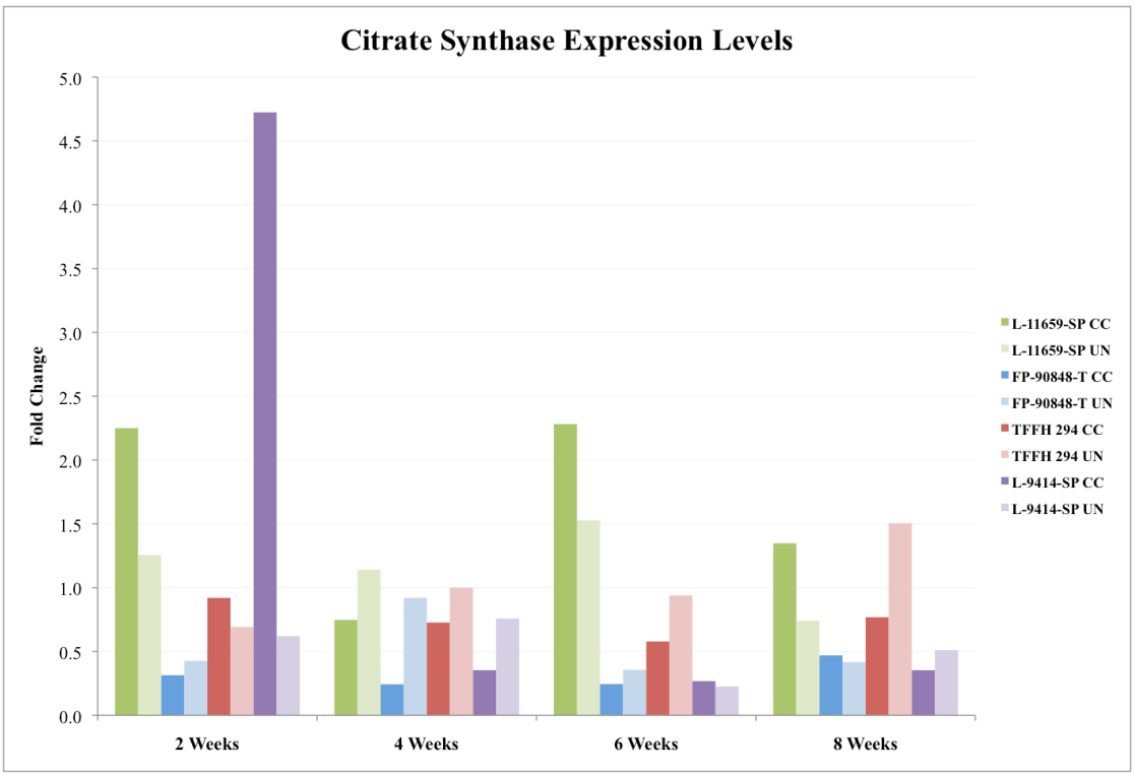

Figure 3.18 Citrate synthase expression levels of L-11659-SP (green), FP-90848-T (blue), TFFH 294 (red), and L-9414-SP (purple) exposed to copper citrate (CC) and untreated (UN) test wafers for 2, 4, 6, and 8 weeks.

Dark colors (green, blue, red, and purple) represent CC treatment and light colors represent UN treatment (Figure 3.19). Overall, L-11659-SP had the largest CS expression in comparison to the other isolates. Both FP-90848-T and L-9414-SP had the smallest overall CS expression levels. There was no variation in fold change differences between weeks and treatment when exposed to TFFH 294 until week 8. The CC treatment did not stimulate higher CS expression levels than the UN controls for FP-90848-T except for week 8 where the CC treatment was slightly higher than the UN controls. The UN controls showed lower expression levels than the CC treatment for L-11659-SP at weeks 2, 6, and 8. TFFH 294 showed higher expression on CC treated wood

at week 2 only. L-9414-SP showed a much higher expression on CC treated wood at weeks 2 than the UN controls.

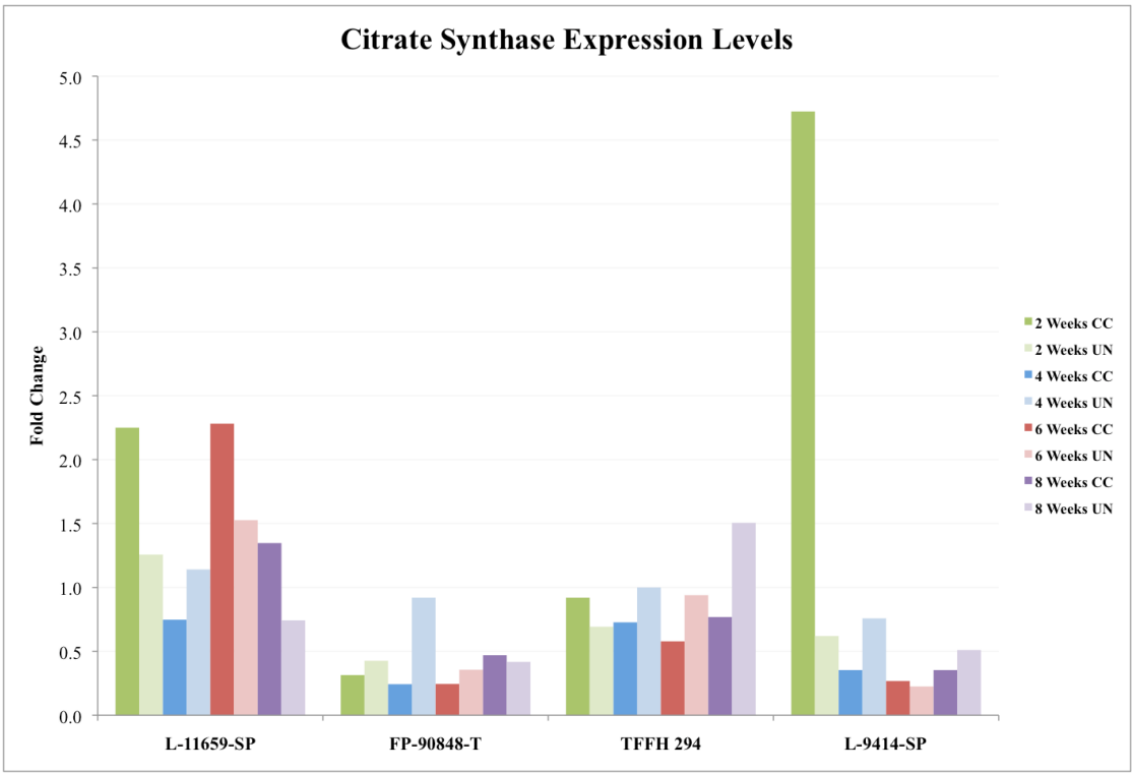

Figure 3.19 Citrate synthase expression levels for 2 weeks (green), 4 weeks (blue), 6 weeks (red) and 8 weeks (purple) for isolates L-11659-SP, FP-90848-T, TFFH 294, and L-9414-SP exposed to copper citrate (CC) and untreated (UN) test wafers.

Relative changes in ANTI expression for each isolate with respect to time can be seen in Figures 3.20 and 3.21. Dark colors (green, blue, red, and purple) represent CC treatment and light colors represent UN treatment (Figure 3.20). Again, there is an overall lower variability in ANTI expression with respect to the endogenous control (TFFH 294 UN w4). L-9414-SP exposed to CC at week 2 had the highest fold change difference (6.964) when compared to the other three isolates. UN controls had higher ANTI expression than the CC treatment at week 4 for all isolates.

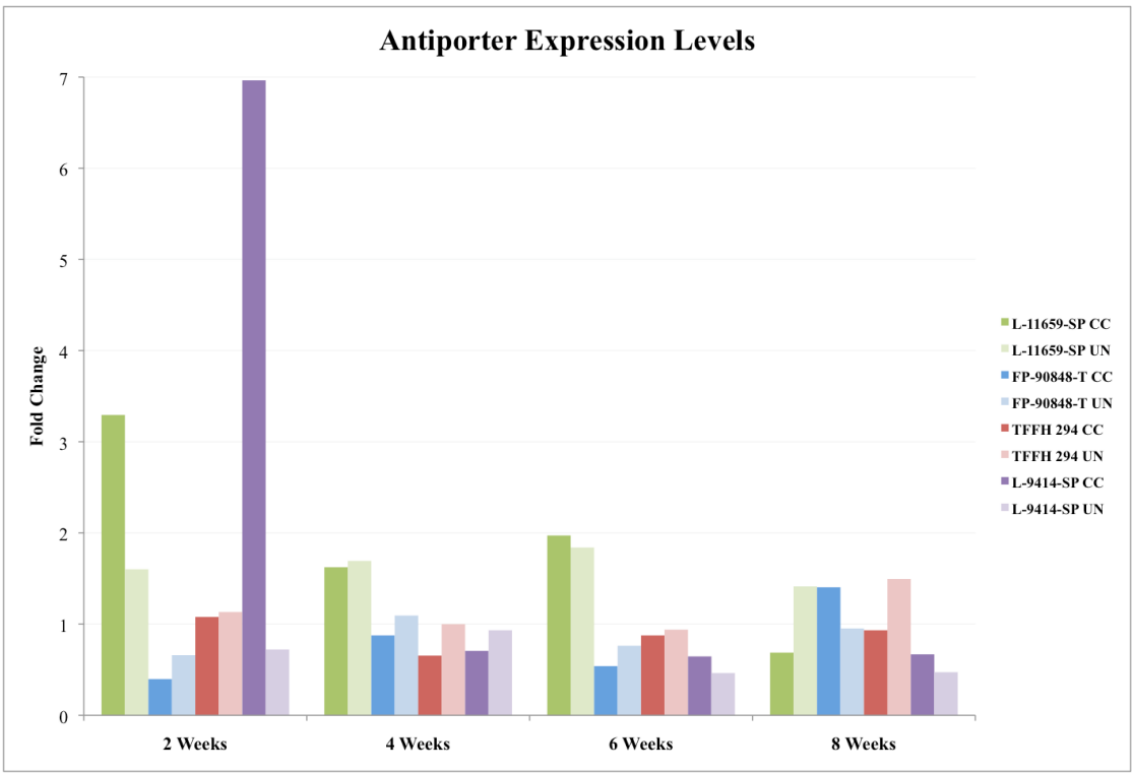

Figure 3.20 Antiporter expression levels of L-11659-SP (green), FP-90848-T (blue), TFFH 294 (red), and L-9414-SP (purple) exposed to copper citrate (CC) and untreated (UN) test wafers for 2, 4, 6, and 8 weeks.

Dark colors (green, blue, red, and purple) represent CC treatment and light colors represent UN treatment (Figure 3.21). L-11659-SP had the highest overall ANTI expression in comparison to the other isolates. Both FP-90848-T and L-9414-SP had lower ANTI expression than L-11659-SP and TFFH 294. Like CS, the CC treatment did not stimulate higher ANTI expression levels than the UN controls for FP-90848-T except for week 8 where the CC treatment was slightly higher than the UN controls. The UN controls showed lower expression levels than the CC treatment for L-9414-SP at weeks 2, 6, and 8. TFFH 294 only showed slightly higher expression on CC treated wood at week 2 and 4. L-11659-SP showed higher expression on CC treated wood at weeks 2 and 6.

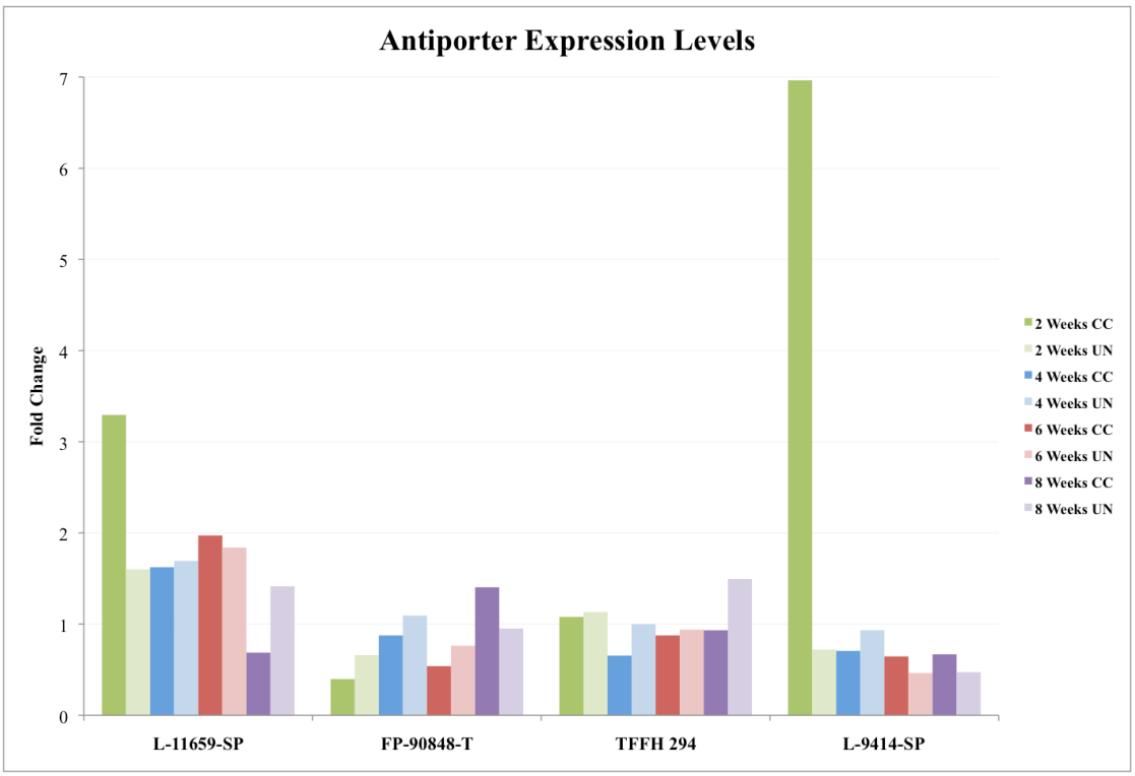

Figure 3.21 Antiporter expression levels for 2 weeks (green), 4 weeks (blue), 6 weeks (red) and 8 weeks (purple) for isolates L-11659-SP, FP-90848-T, TFFH 294, and L-9414-SP exposed to copper citrate (CC) and untreated (UN) test wafers.

Relative changes in ATPase expression for each isolate with respect to time can be seen in Figures 3.22 and 3.23. Dark colors (green, blue, red, and purple) represent CC treatment and light colors represent UN treatment (Figure 3.22). There were large fluctuations in ATPase expression levels between treatment, isolate, and time for ATPase with respect to the endogenous control (TFFH 294 UN w4). Nearly all of the samples had much higher expression levels when compared to the endogenous control. The largest fold change difference (15.455) was seen in L-11659-SP exposed to CC at week 4. Week 8 had much lower expression of ATPase with respect to the other three time points.

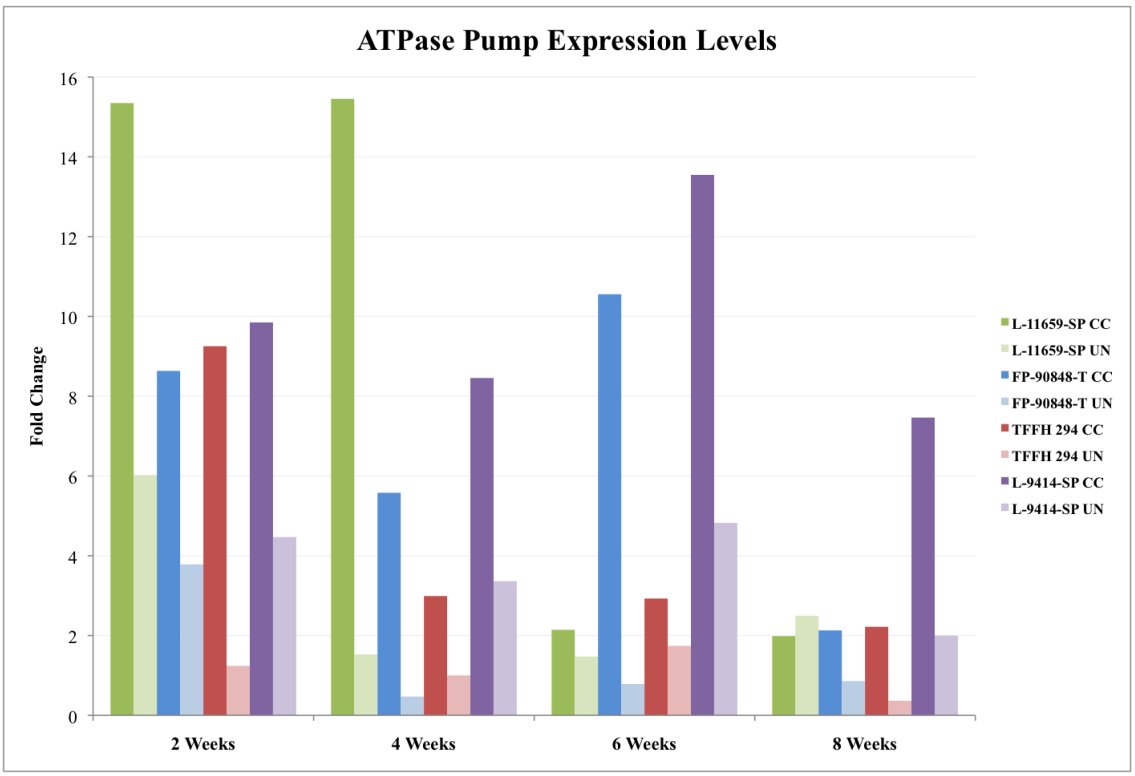

Figure 3.22 ATPase pump expression levels of L-11659-SP (green), FP-90848-T (blue), TFFH 294 (red), and L-9414-SP (purple) exposed to copper citrate (CC) and untreated (UN) test wafers for 2, 4, 6, and 8 weeks.

Dark colors (green, blue, red, and purple) represent CC treatment and light colors represent UN treatment (Figure 3.23). L-9414-SP had the largest fold change difference in comparison to the other three isolates. The CC treatment generated much higher expression levels than the UN controls for all isolates at weeks 2 and 4. FP-90848-T and L-9414-SP also show much higher expression levels for the CC treatment than the UN controls at week 6. Again, L-9414-SP showed a considerably higher ATPase expression in the CC treatment than the UN control at week 8.

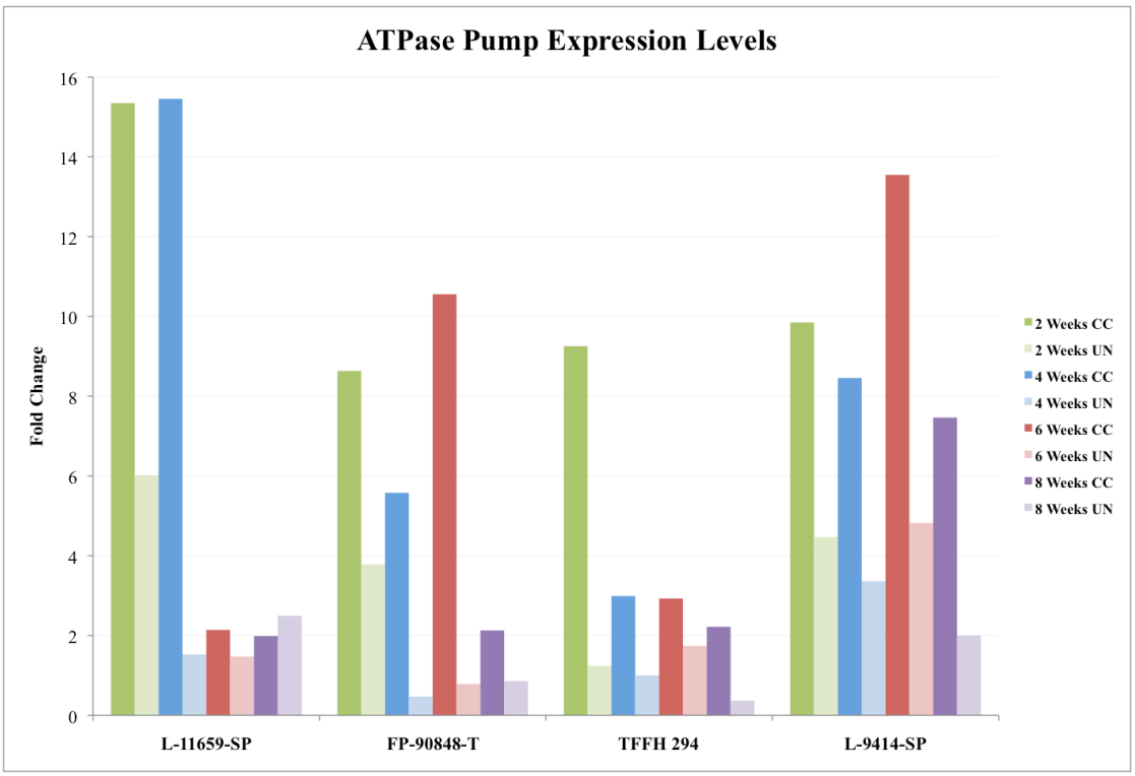

Figure 3.23 ATPase pump expression levels for 2 weeks (green), 4 weeks (blue), 6 weeks (red) and 8 weeks (purple) for isolates L-11659-SP, FP-90848-T, TFFH 294, and L-9414-SP exposed to copper citrate (CC) and untreated (UN) test wafers.

Evaluating gene expression is a more sensitive approach in determining the active participants in the biosynthesis of oxalate. Both ICL and GLOXDH were analyzed for expression because the crude-homogenate mixtures demonstrated quantifiable enzyme activity in the four isolates over the course of the study. FUM, MS, and OAA were not evaluated for expression because the crude-homogenate failed to demonstrate measurable enzyme activity in the same test samples. Based on the genome analysis of TFFH 294 by Tang (2011), three other genes were included and measured for expression levels. Tang (2011) found that citrate synthase (CS), a succinate-fumarate antiporter (ANTI), and a copper resistance ATPase pump (ATPase) were up-regulated in the early stages of decay.

It is important to note, that ICL and GLOXDH were also up-regulated in the early stages of decay (Tang 2011). Citrate synthase is found in the mitochondria as part of the TCA cycle and converts oxaloacetate to citrate (Figure 3.24). The succinate/fumarate antiporter, found in the cytoplasm, functions as the shunt from isocitrate in the TCA cycle to isocitrate in the GLOX cycle which is located in the glyoxysome (Figure 3.24). The ATPase pump is not associated with either the TCA or GLOX cycles; instead, it is found in the cytoplasm and functions to pump copper ions (Cu^{2+}) out of the cell (Figure 3.24). Because these five genes are up-regulated at the earlier stages of decay, it would be expected that expression levels should be observed in the samples used for this study.

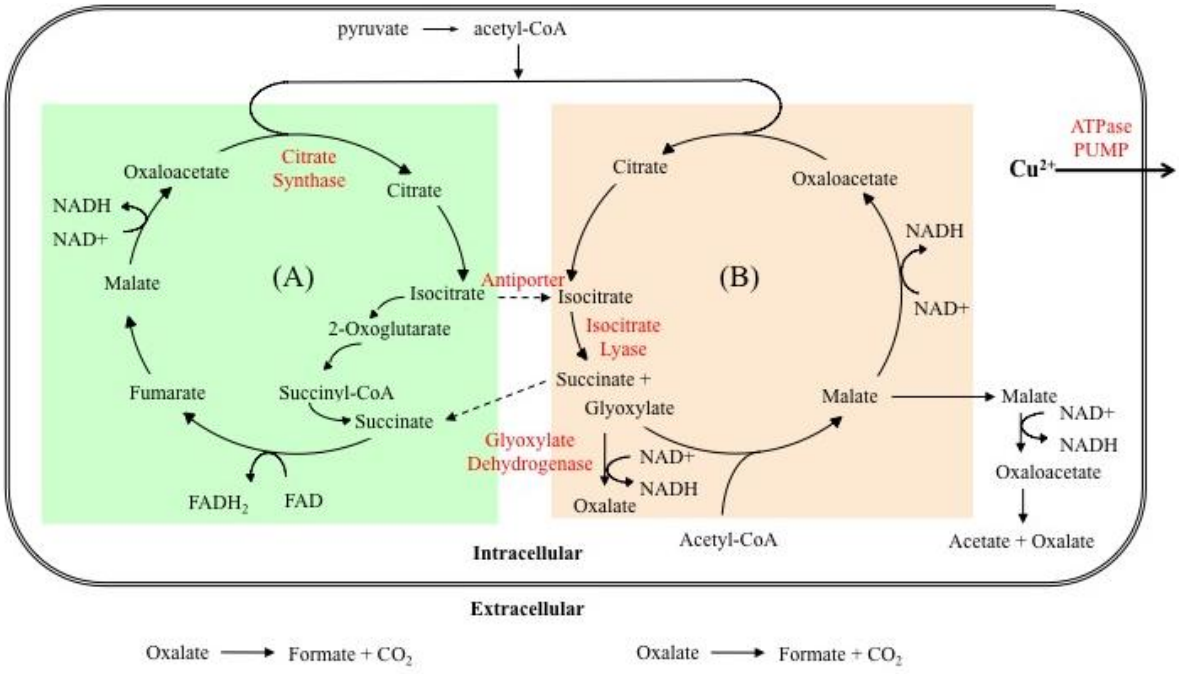

Figure 3.24 Genes up-regulated in early decay; genes are in red. (A) TCA cycle; (B) GLOX cycle. Green box indicates TCA cycle in the mitochondria; orange box indicates GLOX cycle in the glyoxysome (Tang 2011).

Expression levels of the five genes were seen in all isolates through the 8 week period; however, the expression patterns did not directly correlate to the patterns seen in

oxalate production (Figure 3.6). For ICL, GLOXDH, CS, and ANTI, expression levels were highest in L-9414-SP exposed to CC at week 2 when compared to the other isolates. Highest oxalate production for L-9414-SP was not seen until week 6 (Figure 3.6). It is possible that the genes are being expressed much sooner than the appearance of end product. For example, elevated ICL expression could occur after a few days, which may not be reflected in oxalate production until week 4 or 6. The same could hold true for GLOXDH expression. It would be expected that elevated ICL expression would occur before elevated GLOXDH expression since glyoxylate needs to be produced before oxalate can be produced (Figure 3.24). However, both of these enzymes could have been expressed much higher prior to the first time point evaluated in this study. Also, it would be expected that CS, ANTI, ICL, and GLOXDH expression levels would be connected based on their location in the TCA cycle (Figure 3.24).

If copper functions to initiate a response in elevated oxalate production, it should be reflected in the expression levels of all five genes. It is possible for levels of expression to fluctuate based on isolate and time, which could be dependent on the metabolism of the particular isolate. ATPase expression levels are higher for all isolates exposed to CC treatment when compared to the UN controls over the course of the study (Figure 3.22). It is probable that the presence of copper in the CC treatment causes the increase in expression of ATPase through week 8 for all isolates. Since the ATPase pumps copper out of the cell, it would be expected that in a copper-rich environment expression would be higher. The organism would need to efficiently pump the copper ions out to keep the copper from building to a toxic level in the cell. It can also be deduced that the organism would need to pump out the copper ions at the earliest stage

possible, which would show much higher ATPase expression in copper-rich environments when compared to untreated environments. The biggest difference between the CC and UN treatments were seen at week 2 in TFFH 294, week 4 in L-11659-SP, and week 6 in FP-90848-T and L-9414-SP (Figure 3.23). The elevated ATPase expression could reflect differences between the two treatments seen in oxalate production of these four isolates (Figure 3.6).

Evaluating the Role of Oxalate: The Effects of Copper Availability

The purpose of this study was to determine if alternating applications of copper citrate led to differences in the response of the isolates over time. Four variations of 1.2% ammoniacal copper citrate treatments as well as an untreated control were analyzed for oxalate concentration and % weight loss. SYP blocks tested for oxalate production were untreated blocks (UN), 1.2% ammoniacal copper citrate blocks (CC), untreated blocks stacked underneath 1.2% ammoniacal copper citrate blocks (ST), and 100µl of 1.2% ammoniacal copper citrate added to untreated blocks (LIQ); blocks from each test configuration were analyzed every two weeks over an eight week period. Oxalate production of untreated blocks replaced with 1.2% ammoniacal copper citrate blocks (RP) every two weeks was only analyzed every two weeks for a six week period. Concentration values shown in the figures are the average of six biological replicates.

Oxalate Assay

Differences in L-11659-SP oxalate concentration (mg/mL) between the five treatments with respect to time can be seen in Figure 3.25. Treatments are distinguished based on color: UN (green), CC (blue), ST (red), LIQ (purple), and RP (orange).

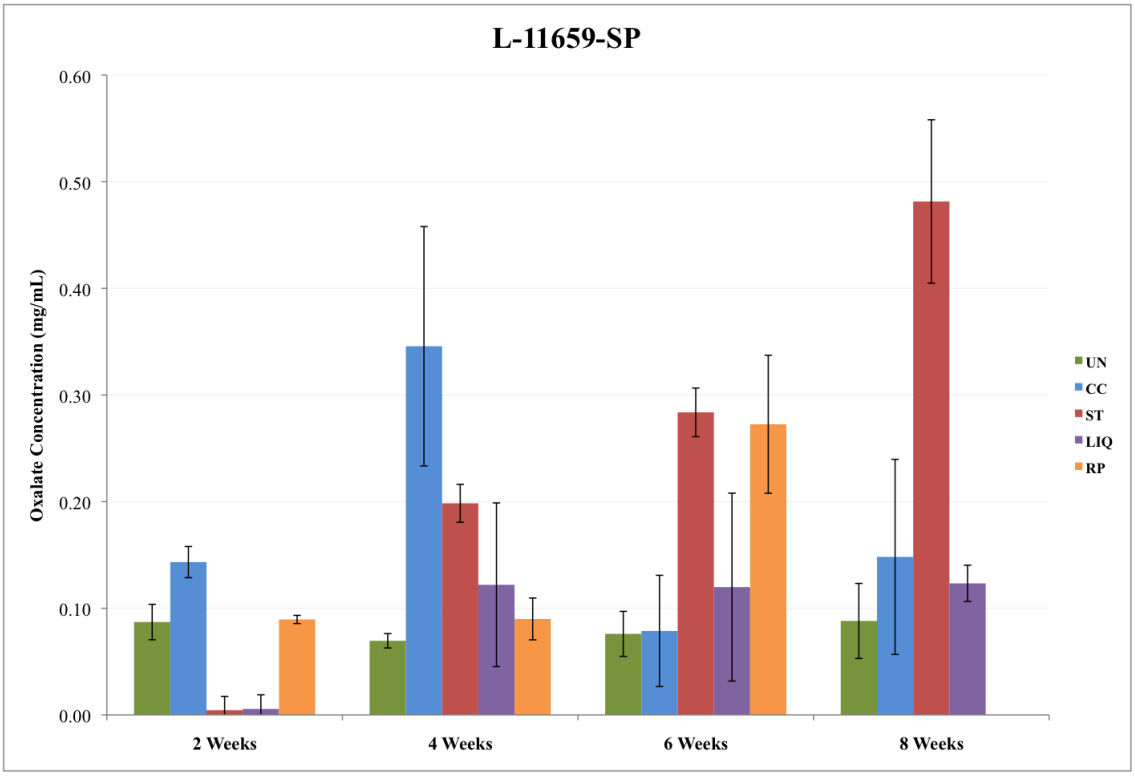

Figure 3.25 Oxalate concentration values (mg/mL) of L-11659-SP exposed to UN (green), CC (blue), ST (red), LIQ (purple), and RP (orange) SYP blocks with respect to time.

L-11659-SP exposed to the ST treatment stimulated highest oxalate production (0.481 mg/mL) at week 8. Lowest production of oxalate was at week 2 with ST, LIQ, and RP, week 4 with UN, and week 6 with CC treatments. Highest oxalate concentrations were at week 4 with CC, week 6 with RP, and week 8 with UN, ST, and LIQ. Minimal changes in oxalate concentration were observed when exposed to UN over the eight week period. Concentration values continually increased over time when exposed to ST. No change in

oxalate concentration was seen from week 4 through week 8 when exposed to LIQ. With the exception of ST and LIQ treatments at week 2, oxalate concentrations are higher for all copper variations with respect to time when compared to untreated controls.

Variations in oxalate concentration (mg/mL) for FP-90848-T between the five treatments with respect to time can been seen in Figure 3.26. Again, treatments are distinguished based on color: UN (green), CC (blue), ST (red), LIQ (purple), and RP (orange).

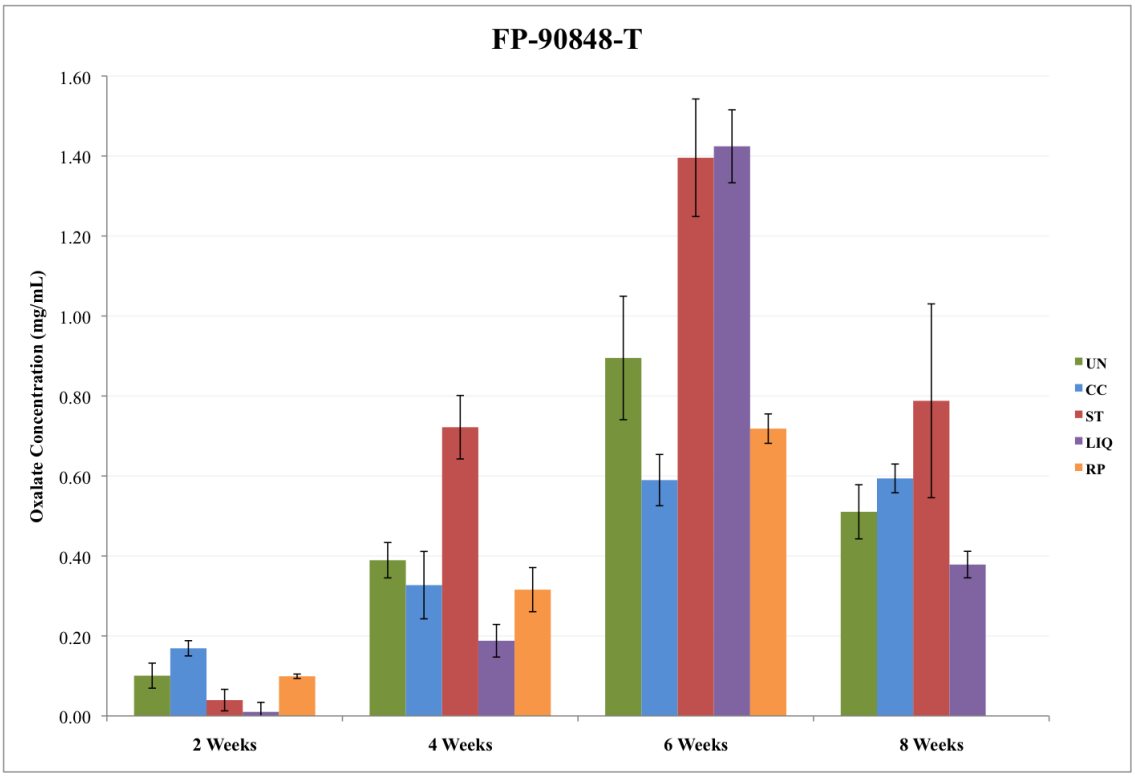

Figure 3.26 Oxalate concentration values (mg/mL) of FP-90848-T exposed to UN (green), CC (blue), ST (red), LIQ (purple), and RP (orange) SYP blocks with respect to time.

In FP-90848-T, the ST and LIQ treatments stimulated highest oxalate production (1.396 mg/mL and 1.424 mg/mL, respectively) at week 6. Overall, week 2 had the lowest oxalate production for all five treatments when exposed to this isolate. Highest oxalate

concentrations were seen at week 6 for all five treatments. Increasing oxalate concentration was observed from week 2 through week 6 and then decreased from week 6 to week 8 for most of the treatments (no change observed in CC from week 6 to week 8). Unlike L-11659-SP, oxalate concentration was not higher for all copper variations when compared to untreated controls.

For TFFH 294, variations in oxalate concentration (mg/mL) between the five treatments with respect to time can been seen in Figure 3.27. Following the same pattern above, treatments are distinguished based on color: UN (green), CC (blue), ST (red), LIQ (purple), and RP (orange).

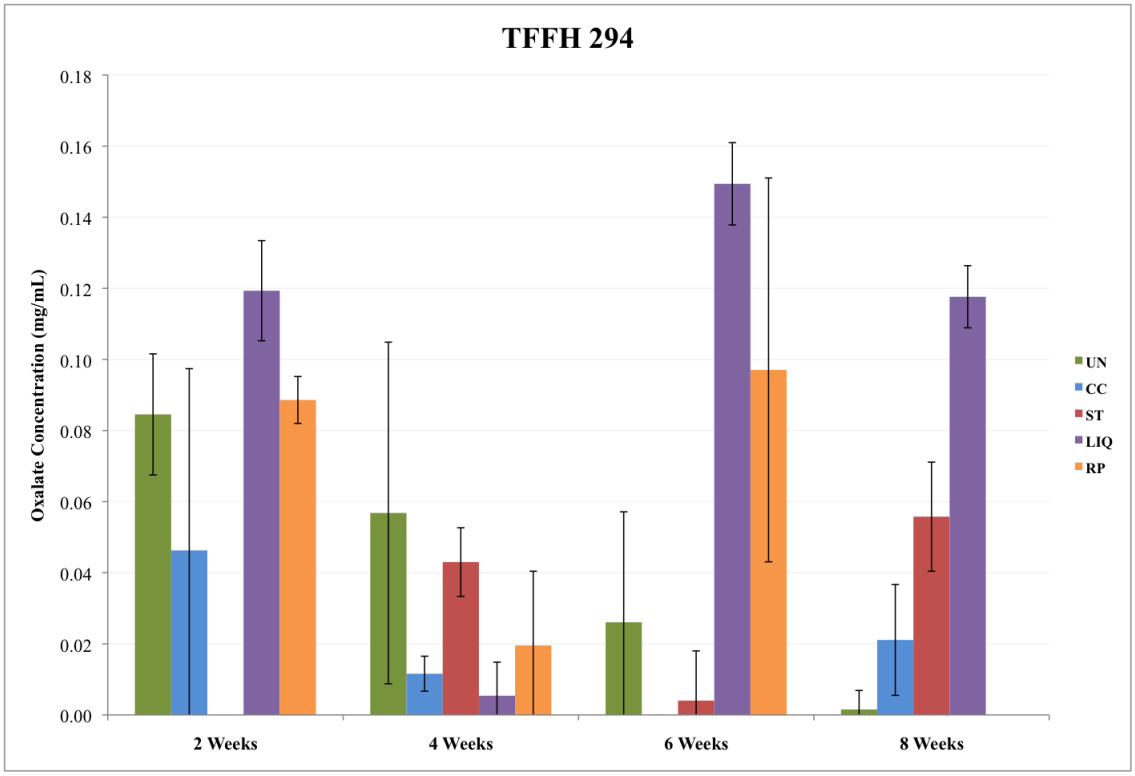

Figure 3.27 Oxalate concentration values (mg/mL) of TFFH 294 exposed to UN (green), CC (blue), ST (red), LIQ (purple), and RP (orange) SYP blocks with respect to time.

Overall, TFFH 294 did not grow well and oxalate values fluctuated over the course of the study with respect to both time and treatment. None of the treatments were able to produce oxalate values higher than 0.150 mg/mL over the eight week period. TFFH 294 produced highest oxalate values when exposed to LIQ and RP treatments. Because of the high variability of the data, it is hard to differentiate the time point that stimulated the highest and lowest production of oxalate with respect to treatment.

Differences in oxalate concentration (mg/mL) for L-9414-SP between the five treatments with respect to time can been seen in Figure 3.28. Again, all treatments are distinguished based on color: UN (green), CC (blue), ST (red), LIQ (purple), and RP (orange).

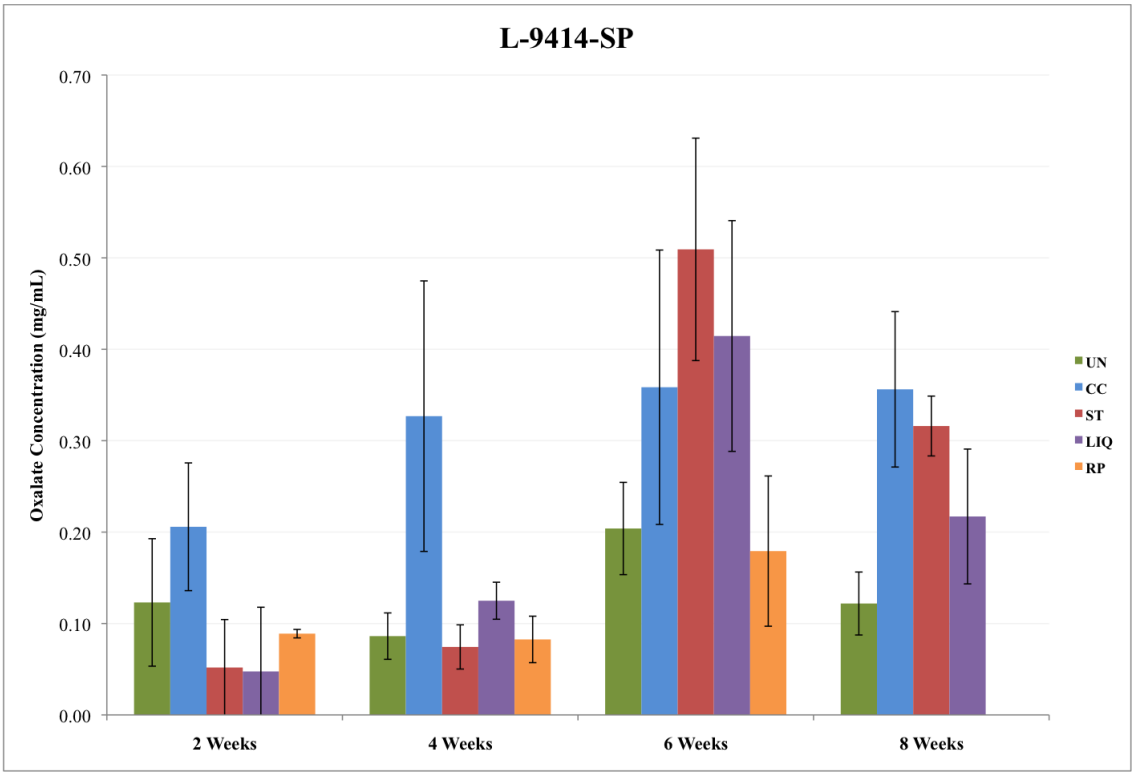

Figure 3.28 Oxalate concentration values (mg/mL) of L-9414-SP exposed to UN (green), CC (blue), ST (red), LIQ (purple), and RP (orange) SYP blocks with respect to time.

L-9414-SP exposed to the ST treatment stimulated the highest oxalate production (0.509 mg/mL) at week 6. The lowest oxalate production for the five treatments exposed to this isolate was at week 2. Highest oxalate concentrations were observed at week 6 for all treatments. Like FP-90848-T, increasing oxalate concentration was observed from week 2 through week 6 and then decreased from week 6 to week 8 for most of the treatments (no change observed in CC from week 6 to week 8). The copper treatments did not stimulate higher oxalate values when compared to untreated controls until weeks 6 and 8.

ANOVA analysis (P = 0.05) indicated that oxalate production in the ST treatment was significantly greater than the other four treatments. The UN, CC, LIQ, and RP treatments were not significantly different from each other. Table 3.13 details the variation between treatments; a difference of 0.0602 between mean values signifies the minimum significant difference.

Table 3.13 Statistical (ANOVA) analysis of significant variation in oxalate production with respect to treatment. A is significantly different than B.

Tukey's Grouping	Treatment	Mean
A	ST	0.31047
B	CC	0.23262
B	LIQ	0.22297
B	UN	0.18252
B	RP	0.17844

Statistical analysis also showed both isolates and time were significantly different from each other with respect to oxalate production. Table 3.14 and 3.15 detail variations between isolates and time, respectively.

Table 3.14 Statistical (ANOVA) analysis of significant variation in oxalate production with respect to isolate. A difference of 0.0488 between mean values indicates the minimum significant difference.

Tukey's Grouping	Isolate	Mean
A	FP-90848-T	0.31047
B	L-9414-SP	0.23262
C	L-11659-SP	0.22297
D	TFFH 294	0.18252

Table 3.15 Statistical (ANOVA) analysis of significant variation in oxalate production with respect to time. A difference of 0.0489 between mean values indicates the minimum significant difference.

Tukey's Grouping	Time	Mean
A	6 weeks	0.31047
B	8 weeks	0.23262
C	4 weeks	0.22297
D	2 weeks	0.18252

With the exception of RP, the copper treatments produced higher amounts of oxalate than the untreated controls (Table 3.13). However, based on the statistical analysis, only the ST treatment showed a significant difference in oxalate concentration. FP-90848-T generated the highest amount of oxalate with respect to treatment and time (Table 3.14). According to the statistical data, week 6 gave highest oxalate concentrations, while week 2 gave the lowest (Table 3.15).

Oxalate plays an important role in the ability of *F. radiculosa* to tolerate copper. This study was designed to evaluate changes in the response of the four isolates to different applications of copper citrate. Because TFFH 294 had difficulty growing, its validity in this study is in question. Any comparisons made between TFFH 294 and the other three isolates are likely not biologically relevant. Statistical analysis indicated the

ST treatment produced significantly higher oxalate amounts than the other treatments (Table 3.13). It is possible the increased oxalate production seen in the ST treatment could be a result of greater surface contact between the UN test block and the CC test block stacked above. Theoretically, the UN test block could be stimulated by contact with copper ions in the CC test block. In any case, it is evident that stacking the CC test block above the UN test block stimulated a higher production of oxalate for L-11659-SP, FP-90848-T, and L-9414-SP over the eight week time period.

In the RP treatment, UN test blocks were also in direct contact with CC test blocks; however, there was no significant difference in oxalate production when compared to the other treatments (Table 3.13). In fact, the RP treatment produced the lowest oxalate amounts in comparison to the other treatments. One difference between the RP and ST treatments was the orientation of the UN and CC test blocks. In the RP treatment, the CC test block was in direct contact with one side of the UN test block; because it was not stacked above the UN test block, the cross section face of neither block was in direct contact. The low oxalate production indicates that this type of contact did not facilitate the production of more oxalate in these isolates. The isolates were not able to obtain the copper ions as readily unless the cross section face of the treated block was in direct contact with the untreated block as was the case in the ST variation. Based on oxalate production in the ST and RP treatments, it is possible that the placement of the CC test blocks in relation to the UN test blocks has an effect on the organisms' accessibility in obtaining the copper ions from the CC test blocks.

There are similarities in oxalate production between this study and the previous study (Evaluating the Role of Oxalate: Enzyme Analysis Results). The amount of oxalate

produced by the isolates throughout the course of this study (Table 3.14) mirrors the amount of oxalate produced in the previous study (Table 3.2). However, for this study oxalate production is significantly different between each isolate (Table 3.14). Oxalate production based on weeks in this study (Table 3.15) also reflects the oxalate production seen in the previous study (Table 3.1). Based on the repeatable data in these two studies, it can be inferred that the oxalate production seen is a true representation for these particular isolates exposed to CC and UN wood.

Weight Loss

Decay capacity was determined by recording the weight of the test blocks pre-exposure and post-exposure for each sampling time point. The weights of the blocks were used to calculate % weight loss over time. Values seen in the graphs below are the average of six biological replicates. Differences in the % weight loss of L-11659-SP between the five treatments with respect to time can be seen in Figure 3.29. Treatments are distinguished based on color: UN (green), CC (blue), ST (red), LIQ (purple), and RP (orange).

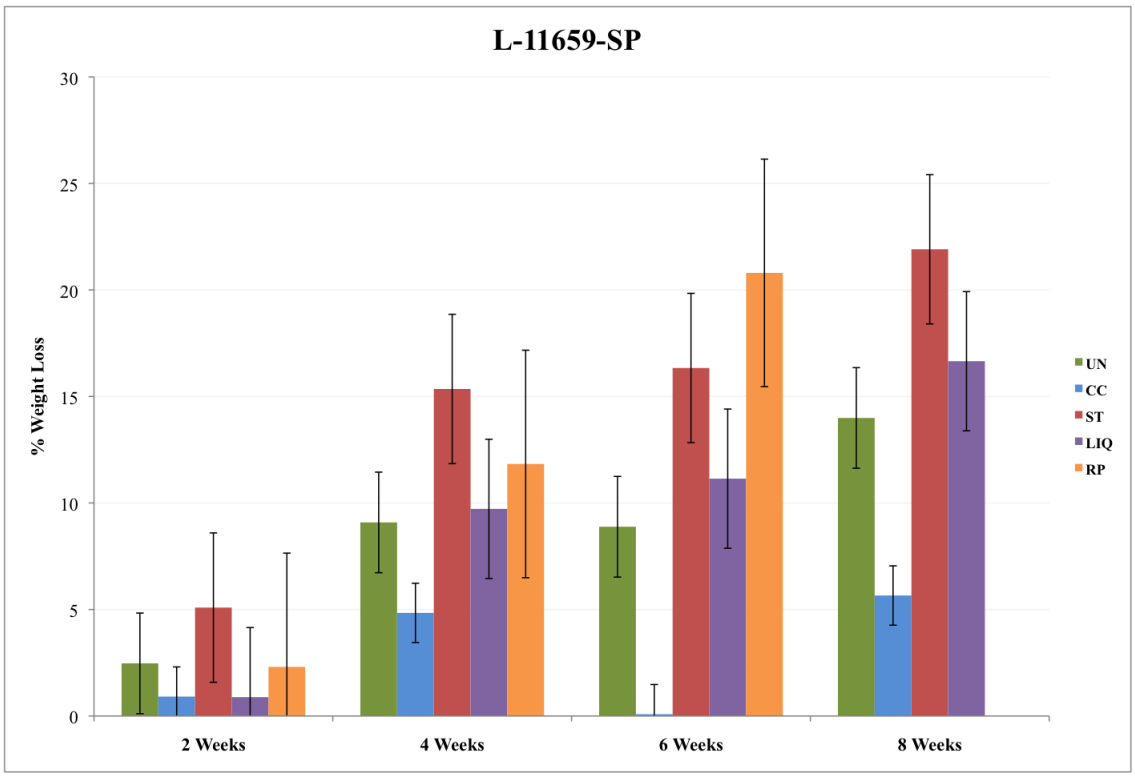

Figure 3.29 Weight loss percentages of L-11659-SP exposed to UN (green), CC (blue), ST (red), LIQ (purple), and RP (orange) SYP blocks with respect to time

When exposed to the ST treatment, L-11659-SP had the highest % weight loss at week 8 (23%). The CC treatment at week 6 had the lowest % weight loss when exposed to this organism. Smallest % weight loss was seen at week 2 for most of the treatments (CC week 6 was the only exception). Overall, the last sampling time point generated the largest % weight loss for all treatments. With the exception of the CC treatment, the UN controls had lower % weight loss when compared to the various copper treatments throughout the eight week period.

Differences in the % weight loss of FP-90848-T between the five treatments with respect to time can be seen in Figure 3.30. Again, treatments are distinguished based on color: UN (green), CC (blue), ST (red), LIQ (purple), and RP (orange).

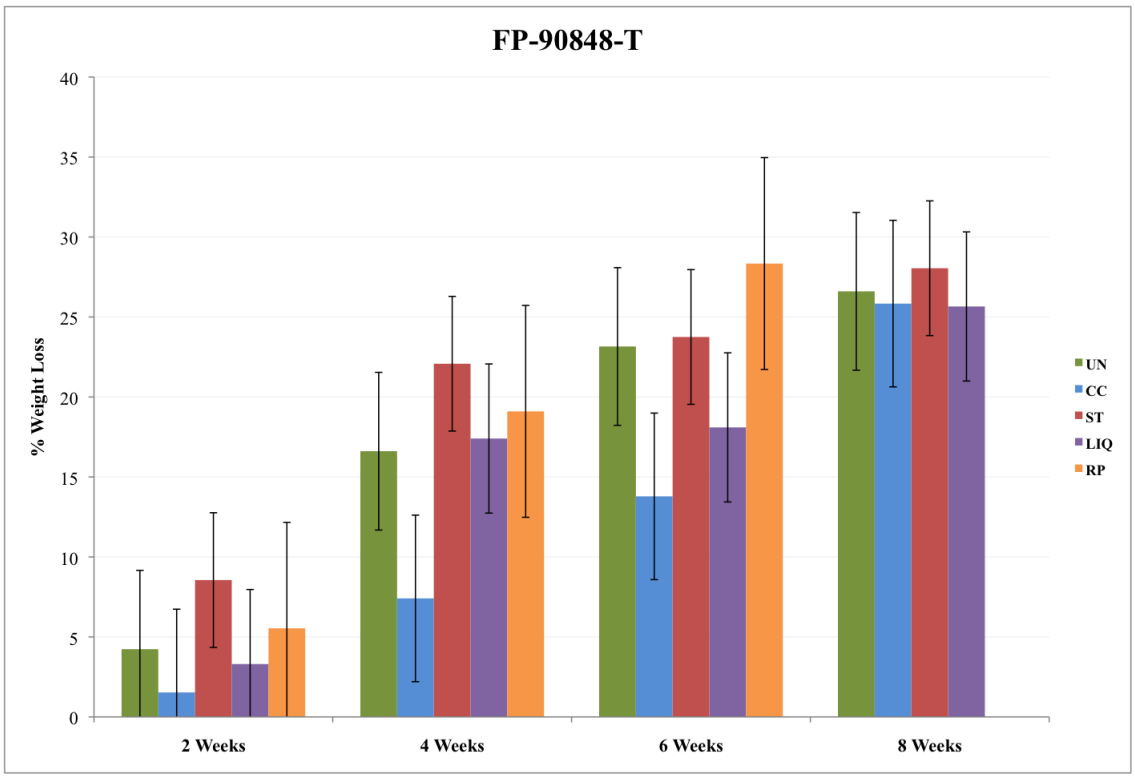

Figure 3.30 Weight loss percentages of FP-90848-T exposed to UN (green), CC (blue), ST (red), LIQ (purple), and RP (orange) SYP blocks with respect to time.

FP-90848-T had the highest % weight loss at week 6 (28%) when exposed to the RP treatment. The CC treatment at week 2 had the lowest % weight loss when exposed to this organism. Smallest % weight loss was seen at week 2 for all five treatments. Like L-11659-SP, the last sampling time point generated the largest % weight loss for all treatments. When compared to the UN controls, only the ST and RP treatments had higher % weight loss with respect to time. In this organism, % weight loss increases over time for all treatments.

Differences in the % weight loss of TFFH 294 between the five treatments with respect to time can be seen in Figure 3.31. Again, treatments are distinguished based on color: UN (green), CC (blue), ST (red), LIQ (purple), and RP (orange).

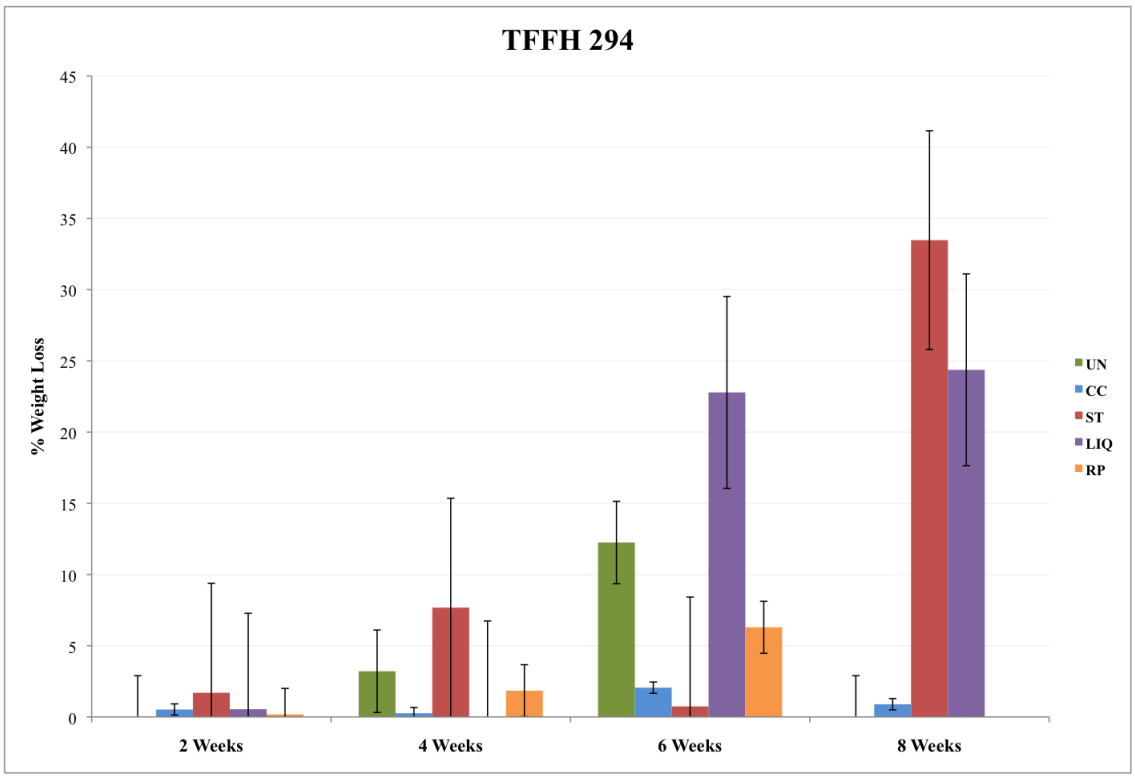

Figure 3.31 Weight loss percentages of TFFH 294 exposed to UN (green), CC (blue), ST (red), LIQ (purple), and RP (orange) SYP blocks with respect to time.

Because TFFH 294 did not grow well during this experiment, decay capacity is hard to establish based on the results shown in Figure 3.15. The highest % weight loss was seen at week 8 (33.5%) when exposed to the ST treatment. Smallest % weight loss was seen at week 2 for all five treatments. Again, because of the lack of data, it is hard to accurately pinpoint the time point and treatment that stimulated the highest and lowest % weight loss.

Differences in the % weight loss of L-9414-SP between the five treatments with respect to time can be seen in Figure 3.32. As before, treatments are distinguished based on color: UN (green), CC (blue), ST (red), LIQ (purple), and RP (orange).

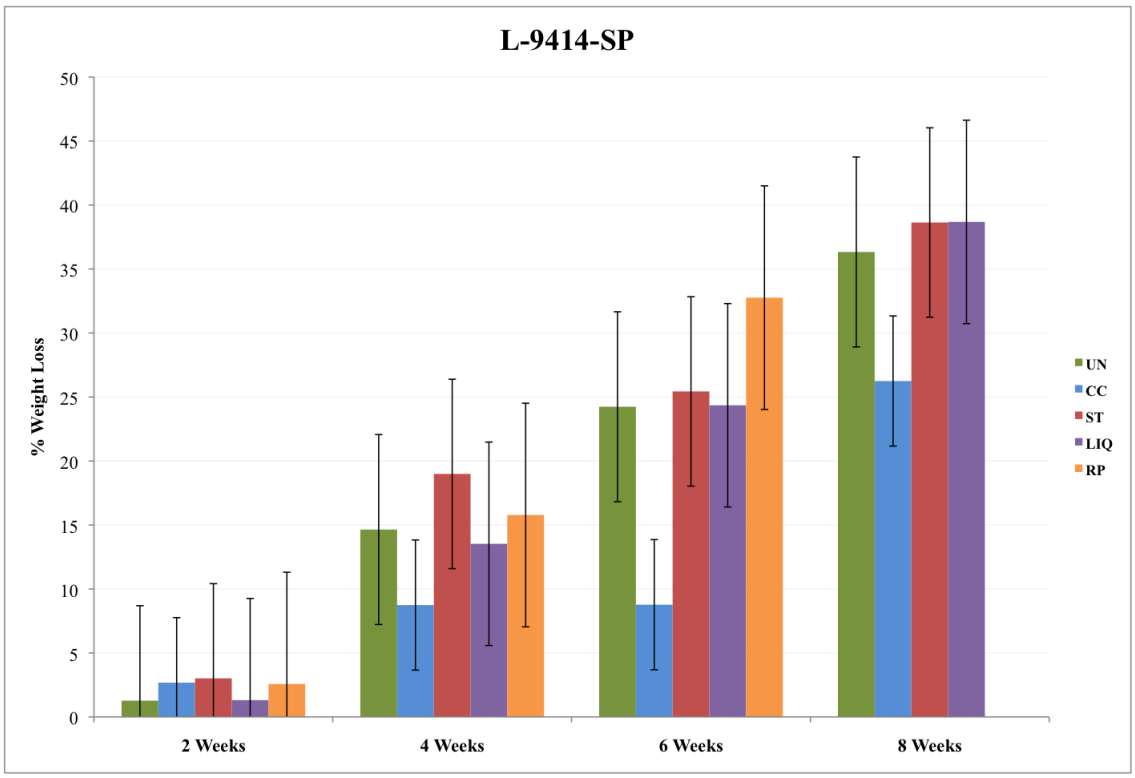

Figure 3.32 Weight loss percentages of L-9414-SP exposed to UN (green), CC (blue), ST (red), LIQ (purple), and RP (orange) SYP blocks with respect to time.

L-9414-SP had the highest % weight loss at week 8 (38.6%) when exposed to both the ST and LIQ treatments. The UN and LIQ treatments at week 2 had the lowest % weight loss when exposed to this organism. Like L-11659-SP and FP-90848-T, the smallest % weight loss was seen at week 2 for all five treatments. Again, the last sampling time point generated the largest % weight loss for all treatments. When compared to the UN controls, the ST, LIQ, and RP treatments had higher % weight loss with respect to time. Like FP-90848-T, % weight loss increased over time for all treatments.

ANOVA analysis (P = 0.05) indicated that the ST, LIQ, and CC treatment were significantly different with respect to % weight loss. The UN controls and RP treatment were not significantly different from each other, but were significantly different than the other three treatments with respect to % weight loss. Table 3.16 details the variation between treatments; a difference of 1.5678 between mean values signifies the minimum significant difference.

Table 3.16 Statistical (ANOVA) analysis of significant variation between treatments with respect to % weight loss.

Tukey's Grouping	Treatment	Mean
A	ST	16.9272
B	LIQ	14.2775
C	UN	12.3102
C	RP	12.2781
D	CC	6.8888

Statistical analysis also showed isolates L-9414-SP and FP-90848-T were not significantly different from each other. Table 3.17 shows the variation between isolates with respect to % weight loss.

Table 3.17 Statistical (ANOVA) analysis of significant variation in % weight loss with respect to isolate. A difference of 1.2703 between mean values indicates the minimum significant difference.

Tukey's Grouping	Isolate	Mean
A	L-9414-SP	17.8288
A	FP-90848-T	16.7435
B	L-11659-SP	9.2397

Each time point was significantly different from each other with respect to % weight loss. Table 3.18 details the variations between the four time points.

Table 3.18 Statistical (ANOVA) analysis of significant variation in % weight loss with respect to time. A difference of 1.2731 between mean values indicates the minimum significant difference.

Tukey's Grouping	Time	Mean
A	8 weeks	22.6865
B	6 weeks	15.7847
C	4 weeks	10.8201
D	2 weeks	2.4149

L-9414-SP generated the highest % weight loss with respect to treatment and time, while TFFH 294 produced the lowest amount (Table 3.16). According to the statistical data, week 8 gave the highest % weight loss, while week 2 gave the lowest (Table 3.17).

In comparison to the statistical data for oxalate production, it can be inferred that oxalate alone is not the only factor contributing to the decay capacity of the wood. This can hold true based on the fact that for oxalate production the ST treatment was the only significantly different treatment with respect to time and isolate (Table 3.13); however, in the % weight loss analysis multiple treatments are significantly different with respect to time and isolate (Table 3.18).

The purpose of measuring weight loss is to determine the decay capacity of the organisms in a given environment. In this study, decay capacity can be directly related to the isolate's ability to degrade wood treated with different variations of copper citrate availability. Again, comparisons are made excluding TFFH 294 because its validity in this study remains in question. Once the organism initiates decay, it would be expected that percent weight loss would continue to increase over time. In L-11659-SP, all treatments, with the exception of CC at week 6, continually increased in weight loss with

respect to time (Figure 3.29). Both FP-90848-T and L-9414-SP showed an increase in weight loss for all five treatments with respect to time (Figure 3.30 and 3.32, respectively). This indicates that L-11659-SP, FP-90848-T, and L-9414-SP efficiently degraded the wood regardless of the treatment. Statistical analysis showed significantly higher weight loss at week 8 (Table 3.18). The analysis also indicated a significant increase in weight loss for each time point (Table 3.18). This makes sense because it would be expected that the breakdown of wood components would continue to increase as time progresses unless the preservative treatment is toxic to the organism.

Interestingly, the statistical analysis showed a significant difference in all treatments except UN and RP, which were not significantly different (Table 3.16). This suggests that the isolates function differently metabolically when breaking down the treatments, depending on the delivery of copper to the wood. The CC treatment showed significantly lower weight loss than the other treatments (Table 3.16). This could be caused by the organisms' need to detoxify the copper ions before obtaining nutrients from the wood. It is also possible that the isolates take longer to adapt to the toxic properties of copper when the ions have been fixed into the wood, which would be reflected in a lower weight loss percentage. Therefore, a delay in the organism having to come in contact with copper is helpful in establishing the growth, especially across any copper gradient. The LIQ treatment showed the second highest weight loss indicating the copper ions did not affect the organisms' ability to efficiently degrade the wood (Table 3.16). This could be due to the fact that the copper ions were on the surface of the wood in the LIQ treatment. This could be an indication that adaptation is more favorable across a gradient from low to high copper.

CHAPTER IV

CONCLUSIONS

- The four isolates showed variability in oxalate production, protein production, enzyme activity, and gene expression when compared to each other over the course of this study. This could be credited to a number of factors: adaptability, environment, growth, metabolism, and exposure time.
- While the isolates were in the "adaptation" phase, protein production was relatively low. It is possible that this may have been a reflection of the organism acclimating to the surrounding environment. After adaptation, protein production increases over time, which could indicate the active breakdown of wood cell wall components by the organism and a start of growth metabolism.
- Enzyme activity was an indication of the amount of ICL and GLOXDH present in the crude-homogenate mixture for a particular isolate. ICL production was significantly higher than GLOXDH production for an individual isolate, which could imply the presence of both mitochondrial (TCA cycle) and glyoxysome (GLOX cycle) ICL activity. Because the crude-homogenate was used to measure enzyme activity, differentiating between mitochondrial ICL or glyoxysome ICL would be impossible.

- The lack of activity for FUM, MS, and OAA in individual isolates could have been caused by a number of factors:
    - inefficiency to break open the cell wall and release intracellular enzymes
    - interference of extracellular proteins in the crude-homogenate mixture
    - expression levels were undetectable because they are present in such low quantities
- The primers designed to measure ICL and GLOXDH expression (Table 2.1) targeted the ICL and GLOXDH present in the glyoxysome (Figure 3.24; based on Tang 2011 genome). Since the ICL enzyme activity does not reflect the measured ICL expression levels, it is highly likely that the enzyme activity measured represents both mitochondrial ICL and glyoxysome ICL. Both ICL and GLOXDH expression levels correlate to one another, which could also indicate that measured ICL enzyme activity was due to both mitochondrial and glyoxysome ICL.
- Metabolically, CS, ANTI, ICL, and GLOXDH feed into each other (Figure 3.24). Expression levels of these four genes are connected in the individual isolates. For example, in L-9414-SP, expression levels of the four genes, CS (4.72), ANTI (6.96), ICL (5.35), and GLOXDH (5.65), all increase proportionally when exposed to CC at week 2. Based on this connection, it is likely that these four genes play a key role in the synthesis of oxalate as an adaptive mechanism when exposed to copper.

- It can be suggested that the ATPase pump functions in the organism's ability to adapt to a copper-rich environment based on the elevated expression levels in all treated samples as seen in this study (Figure 3.22). In the presence of copper the expression of ATPase increased, which could be a response to an absence of oxalate. During this adaptation to copper phase, the fungus needs oxalate to tie up the copper. When initial oxalate levels are low, the ATPase pump would need to expel toxic levels of copper from the cell. As oxalate binds with copper making it inert, the ATPase pump should work less and expression levels decrease accordingly.
- If it is assumed that the ATPase pump indicates the adaptation phase in a copper-rich environment it can be inferred:
    - L-11659-SP seems to have adapted by week 6 (ATPase expression is much higher in CC than UN at weeks 2 and 4 then decreases by week 6).
    - FP-90848-T seems to have adapted by week 8 (ATPase expression is higher in CC than UN through week 6 and decreases by week 8).
    - TFFH 294 has not yet adapted (ATPase expression is higher in CC than UN through week 8).
    - L-9414-SP has not yet adapted (ATPase expression is higher in CC than UN through week 8).
- If oxalate is needed to detoxify copper, it would be expected that the individual isolates need to continue producing oxalate until the majority of the copper is bound. From this it can be inferred:

- L-11659-SP shows higher oxalate production in CC than UN at week 4. Both CC and UN treatments at week 6 and 8 have similar oxalate production. This could suggest that by week 6, L-11659-SP has bound up the excess copper and no longer needs to produce higher amounts of oxalate.
- FP-90848-T shows higher oxalate production in CC than UN at weeks 6 and 8 suggesting it requires oxalate through week 8.
- TFFH 294 shows higher oxalate production in CC than UN at week 6 but not at week 8. This could suggest that the organism has not fully adapted to the environment by week 8 and still requires oxalate to some degree.
- L-9414-SP shows higher oxalate production in CC than UN at week 8 which could also indicate that the organism has not fully adapted to the environment at this particular stage.

- Assuming that adaptation and oxalate production are related in these four isolates it can be inferred:
    - L-11659-SP has adapted by week 4. Expression indicated higher levels of CS, AN, and GLOXDH in CC than UN, which generated a jump in oxalate production at week 4. It is possible that the highest expression increase occurred before week 2, indicating the possibility that this isolate is metabolically ahead of the other three in relation to adapting to copper.

- FP-90848-T has adapted by week 8. Expression of the four metabolic genes did not increase in CC treated wood; however, there was an increase in GLOXDH enzyme activity at weeks 2, 4, and 8 in CC treated wood. This could indicate that FP-90848-T utilizes different isozymes of these genes to produce oxalate.
- TFFH 294 has not yet adapted. There is an increased GLOXDH expression at week 2, but not in the other metabolic genes. There is also a slight increase in GLOXDH enzyme activity for this isolate. However, it is unclear as to how oxalate is being produced in this isolate. It could be possible that TFFH 294 is more efficient in oxalate production, which could require less enzyme expression.
- L-9414-SP has not yet adapted. Expression of the four metabolic genes was highly increased at week 2 in CC treated wood. It is possible that the expression of genes in week 2 lead to the increased production of oxalate at week 8. This would suggest that in this isolate it takes approximately 4 weeks to detect increased oxalate production. Expression levels drop significantly by week 4, which could indicate that L-9414-SP assumed the increased expression of the four metabolic genes at week 2 will generate enough oxalate to adapt to the copper-rich environment.

- This research tracked the production of oxalate from expression of the four key genes to detection of oxalate outside the fungal cell walls in the four isolates.

- Two of the isolates followed similar paths to oxalate production, and interestingly, these same two isolates were most closely related with 99.1% identity (Appendix 1). All isolates varied with respect to oxalate levels, timing of production, enzyme activity, and gene expression.
- Further studies are need to "fine tune" these differences and similarities and should include earlier sampling times and compression tests to estimate stage of decay.

REFERENCES

Akamatsu, Y., Takahashi, M., and Shimada, M. 1992. Cell-free extraction and assay of oxaloacetase from the brown-rot fungus *Tyromyces palustris.* Mokuzai Gakkaishi. 38: 495-500.

American Wood Protection Association. 2009. E10-09 Standard method of testing wood preservatives by laboratory soil-block cultures.

American Wood Protection Association. 2010. E22-09 Standard accelerated laboratory method for testing the efficacy of preservatives against wood decay fungi using compression strength.

Arango, R., Lebow, P., and Green III, F. 2009. Correlation between oxalic acid production and tolerance of *Tyromyces palustris* strain TYP-6137 to N',N-naphthaloylhydroxamine. International Biodeterioration and Biodegradation. 63: 46-51.

Arantes, V., Qian, Y., Milagres, A., Jellison, J., and Goodell, B. 2009. Effect of pH and oxalic acid on the reduction of Fe^{3+} by a biomimetic chelator and on Fe^{3+} desorption/adsorption onto wood: Implications for brown-rot decay. International Biodeterioration and Biodegradation. 63: 478-483.

Clausen, C. 2010. Biodeterioration of wood. Pp. 14.1-14.16. *In*: Wood Handbook: Wood as an Engineering Material. General Technical Report FPL-GTR-190. Madison, WI: U.S. Department of Agriculture, Forest Service, Forest Products Laboratory. 508 pages.

Clausen, C. and Green, F. 2003. Oxalic acid overproduction by copper-tolerant brown-rot basidiomycetes on southern yellow pine treated with copper-based preservatives. International Biodeterioration and Biodegradation. 51: 139-144.

Clausen, C. and Jenkins, K. 2011. Chronicles of *Fibroporia radiculosa* (= *Antrodia radiculosa*) TFFH 294. General Technical Report FPL-GTR-204. Madison, WI: U.S. Department of Agriculture, Forest Service, Forest Products Laboratory. 7 pages.

Clausen, C., Green III, F., Woodward, B., Evans, J., and DeGroot, R. 2000. Correlation between oxalic acid production and copper tolerance in *Wolfiporia cocos*. International Biodeterioration and Biodegradation. 46: 69-76.

Collet, O. 1992. Comparative tolerance of the brown-rot fungus *Antrodia vaillantii* (DC:Fr) Ryv. isolates to copper. Holzforschung. 46: 293-298.

Daniel, G. 2003. Microview of wood under degradation by bacteria and fungi. Pp. 34-72. *In*: B. Goodell, D. Nicholas, and T. Schultz (eds.), Wood Deterioration and Preservation, Advances in Our Changing World. ACS Symposium Series 845. American Chemical Society, Washington, D.C.

DeGroot, R., and Woodward, B. 1999. Using copper-tolerant fungi to biodegrade wood treated with copper based preservatives. International Biodeterioration and Biodegradation. 44: 17-27.

Dutton, M., and Evans, C. 1996. Oxalate production by fungi: its role in pathogenicity and ecology in the soil environment. Canadian Journal of Microbiology. 42: 881-895.

Espejo, E., and Agosin, E. 1991. Production and degradation of oxalic acid by brown rot fungi. Applied and Environmental Microbiology. 57: 1980-1986.

Freeman, M., and McIntyre, C. 2008. A comprehensive review of copper-based wood preservatives with a focus on new micronized or dispersed copper systems. Forest Products Journal. 58: 6-27.

Gadd, G. 1993. Tansley review no. 47: interactions of fungi with toxic metals. New Phytologist. 124: 25-60.

Gardes, M. and Bruns, T. 1993. ITS primers with enhanced specificity basidiomycestes: application to the identification of mycorrhizae and rusts. Molecular Ecology. 2: 113-118.

Green III, F. and Clausen, C. 2003. Copper tolerance of brown-rot fungi: time course of oxalic acid production. International Biodeterioration and Biodegradation. 51: 145-149.

Green III, F. and Clausen, C. 2005. Copper tolerance of brown-rot fungi: oxalic acid production in southern pine treated with arsenic-free preservatives. International Biodeterioration and Biodegradation. 56: 75-79.

Green III, F. and Highley, T. 1997. Mechanism of brown-rot decay: paradigm or paradox. International Biodeterioration and Biodegradation. 39: 113-124.

Green III, F., Larsen, M., Winandy, J., and Highley, T. 1991. Role of oxalic acid in incipient brown-rot decay. Material und Organismen. 26: 191-209.

Goodell, B. 2003. Brown-rot fungal degradation of wood: our evolving view. Pp. 34-72. *In*: B. Goodell, D. Nicholas, and T. Schultz (eds.), Wood Deterioration and Preservation, Advances in Our Changing World. ACS Symposium Series 845. American Chemical Society, Washington, D.C.

Goodell, B., Qian, Y., and Jellison, J. 2008. Fungal decay of wood: soft rot - brown rot - white rot. Pp. 34-72. *In*: B. Goodell, D. Nicholas, and T. Schultz (eds.), Wood Deterioration and Preservation, Advances in Our Changing World. ACS Symposium Series 845. American Chemical Society, Washington, D.C.

Hall, J. 2002. Cellular mechanisms for heavy metal detoxification and tolerance. Journal of Experimental Botany. 53: 1-11.

Hastrup, A., Green III, F., Clausen, C., and Jensen, B. 2005. Tolerance of *Serpula lacrymans* to copper-based wood preservatives. International Biodeterioration and Biodegradation. 56: 173-177.

Hastrup, A., Jensen, B., Clausen, C., and Green III, F. 2006. The effect of $CaCl_2$ on growth rate, wood decay and oxalic acid accumulation in *Serpula lacrymans* and related brown-rot fungi. Holzforschung. 60: 339-345.

Henriksson, G. 2009. Lignin. Pp. 121-144. *In*: M. Ek, G. Gellerstedt, and G. Henriksson (eds.), Pulp and Paper Chemistry and Technology: Wood Chemistry and Wood Biotechnology. Vol. 1. Walter de Gruyter and Co.

Lebow, S. 2004. Alternatives to chromate copper arsenate for residential construction. Res. Pap. FPL-RP-618. Madison, WI: U.S. Department of Agriculture, Forest Service, Forest Products Laboratory. 9 pages.

Lebow, S. 2006. Preservative treatments for building components. Wood Protection - Session 1. 57-64.

Lebow, S., Winandy, J., and Bender, D. 2004. Treated wood in transition: a look at CCA and the candidates to replace it. Wood Design Focus. 3-8.

Lebow, S. 2010. Wood Preservation. Pp. 15.1-15.28. *In*: Wood Handbook: Wood as an Engineering Material. General Technical Report FPL-GTR-190. Madison, WI: U.S. Department of Agriculture, Forest Service, Forest Products Laboratory. 508 pages.

Li, K. 2003. The role of enzymes and mediators in white-rot fungal degradation of lignocellulose. Pp. 34-72. *In*: B. Goodell, D. Nicholas, and T. Schultz (eds.), Wood Deterioration and Preservation, Advances in Our Changing World. ACS Symposium Series 845. American Chemical Society, Washington, D.C.

Livak, K. and Schmittgen, T. 2001. Analysis of relative gene expression data using real-time quantitative PCR and the $2^{-\Delta\Delta C}{}_{T}$ method. Methods. 25:402-408.

Messner, K., Fackler, K., Lamaipis, P., Gindl, W., Srebotnik, E., and Watanabe, T. 2003. Overview of white-rot research: where we are today. Pp. 34-72. *In*: B. Goodell, D. Nicholas, and T. Schultz (eds.), Wood Deterioration and Preservation, Advances in Our Changing World. ACS Symposium Series 845. American Chemical Society, Washington, D.C.

Munir, E., Yoon, J., Tokimatsu, T., Hattori, T., and Shimada, M. 2000. New role for glyoxylate cycle enzymes in wood-rotting basidiomycetes in relation to biosynthesis of oxalic acid. Journal of Wood Science. 47: 368-373.

Munir, E., Yoon, J., Tokimatsu, T., Hattori, T., and Shimada, M. 2001. A physiological role for oxalic acid biosynthesis in the wood-rotting basidiomycetes *Fomitopsis palustris*. Proceedings of the National Academy of Sciences. 98: 11126-11130.

Nilsson, T. 2009. Biological wood degradation. Pp. 121-144. *In*: M. Ek, G. Gellerstedt, and G. Henriksson (eds.), Pulp and Paper Chemistry and Technology: Wood Chemistry and Wood Biotechnology. Vol. 1. Walter de Gruyter and Co.

Panshin, A.J. and C. de Zeeuw. 1980. Textbook of Wood Technology. 4th edition. McGraw-Hill Book Co., New York, NY.

Pereira, H., Graça, J., and Rodrigues, J. 2003. Wood chemistry in relation to quality. Pp. 53-86. *In*: J. Barnett and G. Jeronimidis (eds.), Wood Quality and its Biological Basis. Blackwell Publishing Ltd, Oxford UK.

Pérez, J., Muñoz-Dorado, J., Rubia, T., and Martínez, J. 2002. Biodegradation and biological treatments of cellulose, hemicellulose and lignin: an overview. International Microbiolgy. 5: 53-63.

Pohleven, H. and Humar, M. 2006. Addition of boron compounds and octanoic acid for improvement of biocidal properties and copper fixation at copper-ethanolamine based wood preservatives. IRG/WP/06-30408. Int. Res. Group on Wood Pres., IRG Secretariat, Stockholm.

Schilling, J. and Jellison, J. 2005. Oxalate regulation by two brown rot fungi decaying oxalate-amended and non-amended wood. Holzforschung. 59: 681-688.

Schilling, J. and Inda, J. 2011. Assessing the relative bioavailability of copper to fungi degrading treated wood. International Biodeterioration and Biodegradation. 65:18-22.

Schmidt, C., Whitten, B., and Nicholas, D. 1981. A proposed role for oxalic acid in non-enzymatic wood decay by brown-rot fungi. American Wood Preservers' Association. 77: 157-164.

Shmulsky, R. and Jones, P. 2011. Durability and Protection. Pp. 229-252. *In*: Forest Products and Wood Science: An Introduction, 6th ed.

Shupe, T., Lebow, S., and Ring, D. 2008. Causes and control of wood decay, degradation and stain. Louisiana State University Agriculture Center, Baton Rouge, LA. Publication 2703. 27 pages.

Sigma-Aldrich Technical Document, 1998. *Enzymatic Assay of Fumarase (EC 4.2.1.2).*

Sigma-Aldrich Technical Document, 1996a. *Enzymatic Assay of Isocitrate Lyase (EC 4.1.3.1).*

Sigma-Aldrich Technical Document, 1996b. *Enzymatic Assay of Malate Synthase (EC 4.1.3.2).*

Sjöström, E. 1993. Wood Chemistry: Fundamentals and Applications. 2nd ed. Academic Press, Boston. 293 pages.

Somers, E. 1963. The uptake of copper by fungal cells. Annuals of Applied Biology 51: 425-437.

Sutter, H., Jones, G., and Walchli, O. 1983. The mechanism of copper tolerance in *Poria placenta* (Fr.) Cke. and *Poria vaillanti* (Fr.) Cke. Material und Organismen. 18: 241-262.

Tang, Juliet Dao-May. 2011. A genomic and transcriptomics analysis of wood decay and copper tolerance in the brown rot fungus *Fibroporia radiculosa*. Ph.D. Dissertation, Mississippi State University. 122 Pages.

Teleman, A. 2009. Hemicellulose and Pectin. Pp. 121-144. *In*: M. Ek, G. Gellerstedt, and G. Henriksson (eds.), Pulp and Paper Chemistry and Technology: Wood Chemistry and Wood Biotechnology. Vol. 1.

Tokimatsu, T., Nagai, Y., Hattori, T., and Shimada, M. 1998. Purification and characteristics of a novel cytochrome *c* dependent glyoxylate dehydrogenase from a wood-destroying fungus *Tyromyces palustris*. FEBS Letters. 437: 117-121.

Vesentini, D., Dickinson, D., and Murphy, R. 2006. Fungicides affect the production of extracellular mucilaginous material (ECMM) and the peripheral growth unit (PGU) in two wood-rotting basidiomycetes. Mycological Research. 110: 1207-1213.

Wiedenhoeft, A. 2010. Structure and function of wood. Pp. 3.1-3.18. *In*: Wood Handbook: Wood as an Engineering Material. General Technical Report FPL-GTR-190. Madison, WI: U.S. Department of Agriculture, Forest Service, Forest Products Laboratory. 508 pages.

Xu, G. and Goodell, B. 2001. Mechanisms of wood degradation by brown-rot fungi: chelator-mediated cellulose degradation and binding of iron by cellulose. Journal of Biotechnology. 87: 43-57.

Yoon, J., Hattori, T., and Shimada, M. 2002. A metabolic role of the glyoxylate and tricarboxylic acid cycles for development of the copper-tolerant brown-rot fungus *Fomitopsis palustris*. FEMS Microbiology Letters. 217: 9-14.

APPENDIX A

Percent Identity

	1	2	3	4		
1		98.8	96.7	81.7	1	TFFH 294.seq
2	1.3		99.1	96.9	2	FP-90848-T.seq
3	3.4	0.9		92.1	3	L-9414-SP.seq
4	21.1	3.2	8.3		4	L-11659-SP.seq
	1	2	3	4		

Divergence

Figure A.1 Sequence distances based on percent identity and divergence of four *F. radiculosa* isolates.

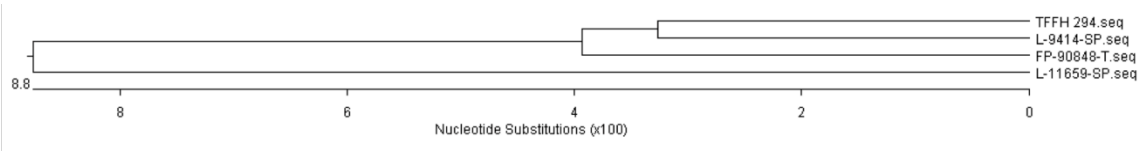

Figure A.2 Phylogenetic tree of four *F. radiculosa* isolates based on sequence distances (nucleotide substitutions).

Table A.1 Analysis of gene expression for ICL. Data analyzed by the comparative C_T method (Livak and Schmittgen 2001).

Isolate	Treatment	Time Point	Fold Change ($2^{-\Delta\Delta CT}$)
L-11659-SP	CC	2 Weeks	0.398
L-11659-SP	CC	4 Weeks	0.259
L-11659-SP	CC	6 Weeks	1.613
L-11659-SP	CC	8 Weeks	0.207
L-11659-SP	UN	Week 2	0.483
L-11659-SP	UN	Week 4	0.697
L-11659-SP	UN	Week 6	0.702
L-11659-SP	UN	Week 8	0.586
FP-90848-T	CC	Week 2	0.047
FP-90848-T	CC	Week 4	0.105
FP-90848-T	CC	Week 6	0.084
FP-90848-T	CC	Week 8	0.191
FP-90848-T	UN	Week 2	0.080
FP-90848-T	UN	Week 4	0.382
FP-90848-T	UN	Week 6	0.232
FP-90848-T	UN	Week 8	0.132
TFFH 294	CC	Week 2	0.463
TFFH 294	CC	Week 4	0.308
TFFH 294	CC	Week 6	0.196
TFFH 294	CC	Week 8	0.503
TFFH 294	UN	Week 2	0.308
TFFH 294	**UN**	**Week 4**	**1.000**
TFFH 294	UN	Week 6	0.426
TFFH 294	UN	Week 8	1.141
L-9414-SP	CC	Week 2	5.352
L-9414-SP	CC	Week 4	0.126
L-9414-SP	CC	Week 6	0.110
L-9414-SP	CC	Week 8	0.145
L-9414-SP	UN	Week 2	0.245
L-9414-SP	UN	Week 4	0.179
L-9414-SP	UN	Week 6	0.067
L-9414-SP	UN	Week 8	0.084

Table A.2 Analysis of gene expression for GLOXDH. Data analyzed by the comparative C_T method (Livak and Schmittgen 2001).

Isolate	Treatment	Time Point	Fold Change ($2^{-\Delta\Delta CT}$)
L-11659-SP	CC	2 Weeks	2.085
L-11659-SP	CC	4 Weeks	0.189
L-11659-SP	CC	6 Weeks	1.248
L-11659-SP	CC	8 Weeks	0.291
L-11659-SP	UN	Week 2	0.316
L-11659-SP	UN	Week 4	0.790
L-11659-SP	UN	Week 6	0.607
L-11659-SP	UN	Week 8	0.483
FP-90848-T	CC	Week 2	0.032
FP-90848-T	CC	Week 4	0.052
FP-90848-T	CC	Week 6	0.090
FP-90848-T	CC	Week 8	0.104
FP-90848-T	UN	Week 2	0.036
FP-90848-T	UN	Week 4	0.334
FP-90848-T	UN	Week 6	0.117
FP-90848-T	UN	Week 8	0.332
TFFH 294	CC	Week 2	0.395
TFFH 294	CC	Week 4	0.107
TFFH 294	CC	Week 6	0.102
TFFH 294	CC	Week 8	0.412
TFFH 294	UN	Week 2	0.102
TFFH 294	**UN**	**Week 4**	**1.000**
TFFH 294	UN	Week 6	0.225
TFFH 294	UN	Week 8	0.697
L-9414-SP	CC	Week 2	5.657
L-9414-SP	CC	Week 4	0.127
L-9414-SP	CC	Week 6	0.072
L-9414-SP	CC	Week 8	0.120
L-9414-SP	UN	Week 2	0.132
L-9414-SP	UN	Week 4	0.132
L-9414-SP	UN	Week 6	0.048
L-9414-SP	UN	Week 8	0.085

Table A.3 Analysis of gene expression for CS. Data analyzed by the comparative C_T method (Livak and Schmittgen 2001).

Isolate	Treatment	Time Point	Fold Change ($2^{-\Delta\Delta CT}$)
L-11659-SP	CC	2 Weeks	2.250
L-11659-SP	CC	4 Weeks	0.747
L-11659-SP	CC	6 Weeks	2.282
L-11659-SP	CC	8 Weeks	1.347
L-11659-SP	UN	Week 2	1.257
L-11659-SP	UN	Week 4	1.141
L-11659-SP	UN	Week 6	1.526
L-11659-SP	UN	Week 8	0.742
FP-90848-T	CC	Week 2	0.314
FP-90848-T	CC	Week 4	0.243
FP-90848-T	CC	Week 6	0.245
FP-90848-T	CC	Week 8	0.470
FP-90848-T	UN	Week 2	0.426
FP-90848-T	UN	Week 4	0.920
FP-90848-T	UN	Week 6	0.356
FP-90848-T	UN	Week 8	0.418
TFFH 294	CC	Week 2	0.920
TFFH 294	CC	Week 4	0.727
TFFH 294	CC	Week 6	0.578
TFFH 294	CC	Week 8	0.768
TFFH 294	UN	Week 2	0.693
TFFH 294	**UN**	**Week 4**	**1.000**
TFFH 294	UN	Week 6	0.940
TFFH 294	UN	Week 8	1.505
L-9414-SP	CC	Week 2	4.724
L-9414-SP	CC	Week 4	0.354
L-9414-SP	CC	Week 6	0.268
L-9414-SP	CC	Week 8	0.354
L-9414-SP	UN	Week 2	0.620
L-9414-SP	UN	Week 4	0.758
L-9414-SP	UN	Week 6	0.225
L-9414-SP	UN	Week 8	0.511

Table A.4 Analysis of gene expression for ANTI. Data analyzed by the comparative C_T method (Livak and Schmittgen 2001).

Isolate	Treatment	Time Point	Fold Change ($2^{-\Delta\Delta CT}$)
L-11659-SP	CC	2 Weeks	3.294
L-11659-SP	CC	4 Weeks	1.625
L-11659-SP	CC	6 Weeks	1.972
L-11659-SP	CC	8 Weeks	0.688
L-11659-SP	UN	Week 2	1.602
L-11659-SP	UN	Week 4	1.693
L-11659-SP	UN	Week 6	1.840
L-11659-SP	UN	Week 8	1.414
FP-90848-T	CC	Week 2	0.398
FP-90848-T	CC	Week 4	0.877
FP-90848-T	CC	Week 6	0.540
FP-90848-T	CC	Week 8	1.404
FP-90848-T	UN	Week 2	0.660
FP-90848-T	UN	Week 4	1.094
FP-90848-T	UN	Week 6	0.763
FP-90848-T	UN	Week 8	0.953
TFFH 294	CC	Week 2	1.079
TFFH 294	CC	Week 4	0.655
TFFH 294	CC	Week 6	0.877
TFFH 294	CC	Week 8	0.933
TFFH 294	UN	Week 2	1.133
TFFH 294	**UN**	**Week 4**	**1.000**
TFFH 294	UN	Week 6	0.940
TFFH 294	UN	Week 8	1.495
L-9414-SP	CC	Week 2	6.964
L-9414-SP	CC	Week 4	0.707
L-9414-SP	CC	Week 6	0.646
L-9414-SP	CC	Week 8	0.669
L-9414-SP	UN	Week 2	0.722
L-9414-SP	UN	Week 4	0.933
L-9414-SP	UN	Week 6	0.463
L-9414-SP	UN	Week 8	0.473

Table A.5 Analysis of gene expression for ATPase. Data analyzed by the comparative C_T method (Livak and Schmittgen 2001).

Isolate	Treatment	Time Point	Fold Change ($2^{-\Delta\Delta CT}$)
L-11659-SP	CC	2 Weeks	15.348
L-11659-SP	CC	4 Weeks	15.455
L-11659-SP	CC	6 Weeks	2.144
L-11659-SP	CC	8 Weeks	1.986
L-11659-SP	UN	Week 2	6.021
L-11659-SP	UN	Week 4	1.526
L-11659-SP	UN	Week 6	1.474
L-11659-SP	UN	Week 8	2.497
FP-90848-T	CC	Week 2	8.634
FP-90848-T	CC	Week 4	5.579
FP-90848-T	CC	Week 6	10.556
FP-90848-T	CC	Week 8	2.129
FP-90848-T	UN	Week 2	3.784
FP-90848-T	UN	Week 4	0.470
FP-90848-T	UN	Week 6	0.785
FP-90848-T	UN	Week 8	0.859
TFFH 294	CC	Week 2	9.254
TFFH 294	CC	Week 4	2.990
TFFH 294	CC	Week 6	2.928
TFFH 294	CC	Week 8	2.219
TFFH 294	UN	Week 2	1.240
TFFH 294	**UN**	**Week 4**	**1.000**
TFFH 294	UN	Week 6	1.741
TFFH 294	UN	Week 8	0.366
L-9414-SP	CC	Week 2	9.849
L-9414-SP	CC	Week 4	8.456
L-9414-SP	CC	Week 6	13.548
L-9414-SP	CC	Week 8	7.464
L-9414-SP	UN	Week 2	4.469
L-9414-SP	UN	Week 4	3.364
L-9414-SP	UN	Week 6	4.823
L-9414-SP	UN	Week 8	2.000